Systems Toxicology – Oxidative Stress

TABLE OF CONTENTS

1. INTRODUCTION 8

2. CELLULAR STRESS RESPONSES 9

2.1 Heat Shock Response 9

2.2 Unfolded Protein Response 9

2.3 Hypoxic Stress Response 10

2.4 Osmotic Stress Response 10

2.5 DNA Damage Response 10

2.6 Autophagic Response 11

2.7 Sirtuin Response 11

2.8 Inflammatory Response 12

2.9 Oxidative Stress Response 12

3. CIGARETTE SMOKING-RELATED CELLULAR STRESS RESPONSES IN CVD, COPD AND LUNG CANCER 13

3.1 Cardiovascular Disease 13

3.2 Chronic Obstructive Pulmonary Disease 14

3.3 Lung Cancer 15

4. QUANTIFYING THE IMPACT OF CIGARETTE SMOKE ON CELLULAR STRESS RESPONSES IN EXPERIMENTAL MODELS USING A SYSTEMS BIOLOGY APPROACH 17

4.1 Tools for Assessment of Cellular Stress *In Vitro* and *In Vivo* 17

4.1.1 *In Vitro* Systems to Study Cigarette Smoke-Related Cellular Stress 17

4.1.2 Assays and Markers to Determine Oxidative Burden *In Vitro* 18

4.1.3 *In Vivo* Systems to Study Cigarette Smoke-Related Cellular Stress 21

4.1.4 Systems Biology Tools 23

4.2 Assessment of Cellular Stress *In Vitro* and *In Vivo* - Results 25

4.2.1 Results from *In Vitro* Studies 26

4.2.1.1 Adhesion Assay 26
4.2.1.2 THS2.2 Aerosol Fraction Impact Assessment Study 32
4.2.1.3 Oral Organotypic Study 38
4.2.1.4 Nasal Organotypic Study 44
4.2.1.5 Bronchial Organotypic Study 48
4.2.2 Results from *In Vivo* Studies 52
4.2.2.1 Rat OECD Studies 52
4.2.2.1.1 Rat OECD THS2.2 Study 52
4.2.2.1.2 Rat OECD THS2.2 Menthol Study 61
4.2.2.2 *Apoe*$^{-/-}$ THS Switching Study 68
4.2.2.3 A/J Lung Cancer Study 76
5. CONCLUSIONS 83
6. REFERENCES 84

LIST OF TABLES

Table 1. Nonclinical Studies with Measures of Oxidative Stress 26

LIST OF FIGURES

Figure 1. Cellular stress model overview 24
Figure 2. Network perturbations in human coronary arterial endothelial cells treated with 3R4F cigarette smoke or THS2.2 aerosol aqueous extracts. 28
Figure 3. Relative network perturbation amplitude (NPA) of specific cell stress subnetworks in human coronary arterial endothelial cells treated with 3R4F cigarette smoke or THS2.2 aerosol aqueous extracts. 29
Figure 4. Network perturbations in MM6 cells treated with 3R4F cigarette smoke or THS2.2 aerosol aqueous extracts. 31
Figure 5. Oxidative stress in normal human bronchial epithelial cells exposed to 3R4F cigarette smoke or THS2.2 aerosol fractions. 33
Figure 6. Genotoxic stress in normal human bronchial epithelial cells exposed to 3R4F cigarette smoke or THS2.2 aerosol fractions. 34

Figure 7. Network model-based analysis of the biological impact factor (BIF) in normal human bronchial epithelial cells exposed to 3R4F cigarette smoke or THS2.2 aerosol fractions. 35
Figure 8. Network perturbations in normal human bronchial epithelial cells exposed to 3R4F cigarette smoke or THS 2.2 aerosol fractions. 37
Figure 9. Network model-based analysis of the biological impact factor (BIF) in EpiOral™ cultures exposed to 3R4F cigarette smoke or THS2.2 aerosol, compared with air controls. 39
Figure 10. Network perturbations in EpiOral™ cultures exposed to 3R4F cigarette smoke or THS2.2 aerosol, compared with air controls. 40
Figure 11. Relative Network Perturbation Amplitude (NPA) scores of specific CST subnetworks in EpiOral™ cultures exposed to 3R4F cigarette smoke or THS2.2 aerosol, compared with air controls. 42
Figure 12. Altered expression levels of genes linked to the oxidative stress response in EpiOral™ cultures exposed to 3R4F cigarette smoke or THS2.2 aerosol, compared with air controls. 43
Figure 13. Network model-based analysis of the biological impact factor (BIF) in nasal MucilAir™ cultures exposed to 3R4F cigarette smoke or THS2.2 aerosol, compared with air controls. 45
Figure 14. Network perturbations in nasal MucilAir™ cultures exposed to 3R4F cigarette smoke or THS2.2 aerosol, compared with air controls. 46
Figure 15. Altered expression levels of genes linked to the oxidative stress response in nasal MucilAir™ cultures following exposure to 3R4F cigarette smoke or THS2.2 aerosol, compared with air controls. 47
Figure 16. Network model-based analysis of the biological impact factor (BIF) in bronchial MucilAir™ cultures exposed to 3R4F cigarette smoke or THS2.2 aerosol, compared with air controls. 49
Figure 17. Network perturbations in bronchial MucilAir™ cultures exposed to 3R4F cigarette smoke or THS2.2 aerosol, compared with air controls. 50
Figure 18. Altered expression levels of genes linked to the oxidative stress response in bronchial organotypic cultures exposed to 3R4F cigarette smoke or THS2.2 aerosol, compared with air controls. 51
Figure 19. Network perturbations in rat nasal epithelial tissues following exposure to 3R4F cigarette smoke or THS2.2 aerosol, compared with air-exposed controls. 54

Figure 20. Relative network perturbation amplitude (NPA) of specific cell stress subnetworks in nasal epithelial tissues following exposure of male rats to 3R4F cigarette smoke or THS2.2 aerosol, compared with air-exposed controls. 56
Figure 21. Altered expression levels of genes linked to the oxidative stress response in nasal epithelial tissues of male rats following exposure to 3R4F cigarette smoke or THS2.2 aerosol, compared with air-exposed controls. 57
Figure 22. Network perturbations in rat lung tissues following exposure to 3R4F cigarette smoke or THS2.2 aerosol, compared with air-exposed controls. 58
Figure 23. Relative network perturbation amplitude (NPA) of the oxidative stress subnetwork in lung tissues of male rats following exposure to 3R4F cigarette smoke or THS2.2 aerosol, compared with air-exposed controls. 59
Figure 24. Altered expression levels of genes linked to the oxidative stress response in rat lung tissues following exposure to 3R4F cigarette smoke or THS2.2 aerosol, compared with air-exposed controls. 60
Figure 25. Network perturbations in rat nasal epithelial tissues following exposure to 3R4F cigarette smoke or THS2.2M aerosol, compared with air-exposed controls. 63
Figure 26. Relative network perturbation amplitude (NPA) of the oxidative stress subnetworks in nasal epithelial tissues of female rats following exposure to 3R4F cigarette smoke or THS2.2 aerosol, compared with air-exposed controls. 64
Figure 27. Altered expression levels of genes linked to the oxidative stress response in rat nasal epithelial tissues following exposure to 3R4F cigarette smoke or THS2.2 aerosol, compared with air-exposed controls. 65
Figure 28. Network perturbations in rat lung tissues following exposure to 3R4F cigarette smoke or THS2.2 aerosol, compared with air-exposed controls. 67
Figure 29. Altered expression levels of genes linked to the oxidative stress response in rat lung tissues following exposure to 3R4F cigarette smoke or THS2.2 aerosol, compared with air-exposed controls. 68
Figure 30. Network model-based analysis of the biological impact factor (BIF) in nasal epithelia from *Apoe*$^{-/-}$ mice exposed to 3R4F cigarette smoke or THS2.2 aerosol, compared with air-exposed controls. 70
Figure 31. Network perturbations in *Apoe*$^{-/-}$ mouse nasal tissues following exposure to 3R4F cigarette smoke or THS2.2M aerosol, compared with air-exposed controls. 71

Figure 32. Relative network perturbation amplitude (NPA) of the Oxidative Stress subnetwork in *Apoe*$^{-/-}$ mouse nasal tissues following exposure to 3R4F cigarette smoke or THS2.2 aerosol, compared with air-exposed controls. 72
Figure 33. Network model-based analysis of the biological impact factor (BIF) in lungs from *Apoe*$^{-/-}$ mice exposed to 3R4F cigarette smoke or THS2.2 aerosol, compared with air-exposed controls. 73
Figure 34. Network perturbations in *Apoe*$^{-/-}$ mouse lung tissues following exposure to 3R4F cigarette smoke or THS2.2M aerosol, compared with air-exposed controls. 74
Figure 35. Relative network perturbation amplitude (NPA) of the Oxidative Stress subnetwork in *Apoe*$^{-/-}$ mouse lung tissues following exposure to 3R4F cigarette smoke or THS2.2 aerosol, compared with air-exposed controls. 75
Figure 36. Network model-based analysis of the biological impact factor (BIF) in nasal tissues from A/J mice exposed to 3R4F cigarette smoke or THS2.2 aerosol, compared with air-exposed controls. 77
Figure 37. Network perturbations in A/J mouse nasal tissues following exposure to 3R4F cigarette smoke or THS2.2M aerosol, compared with air-exposed controls. 78
Figure 38. Relative network perturbation amplitude (NPA) of the Oxidative Stress subnetwork in A/J mouse nasal tissues exposed to 3R4F cigarette smoke or THS2.2 aerosol. 79
Figure 39. Network model-based analysis of the biological impact factor (BIF) in tracheal tissues from A/J mice exposed to 3R4F cigarette smoke or THS2.2 aerosol, compared with air-exposed controls. 80
Figure 40. Network perturbations in A/J mouse tracheal tissues following exposure to 3R4F cigarette smoke or THS2.2M aerosol, compared with air-exposed controls. 81
Figure 41. Relative network perturbation amplitude (NPA) of the Oxidative Stress subnetwork in A/J mouse tracheal tissues following exposure to 3R4F cigarette smoke or THS2.2 aerosol. 82

ABBREVIATIONS

8-iso-PGF2$_\alpha$	8-iso-Prostaglandin 2 alpha
8-OHdG	8-Hydroxy-2′-deoxyguanosine
AE	Aerosol extract
ALI	Air-liquid interface
BIF	Biological impact factor
CAM	Cell adhesion molecule
CCL	Chemokine (C-C motif) ligand
CFA	Cell Fate
COPD	Chronic obstructive pulmonary disease
CPR	Cell Proliferation
CS	Cigarette smoke
CSC	Cigarette smoke condensate
CSE	Cigarette smoke extract
CST	Cell Stress
CVD	Cardiovascular disease
CXCL	Chemokine (C-X-C motif) ligand
DDR	DNA damage response
DEG	Differentially expressed gene
DNA	Deoxyribonucleic acid
DSB	Double-strand break
eIF2α	Eukaryotic initiation factor 2 alpha
eNOS	Endothelial nitric oxide synthase
EPO	Erythropoeitin
ER	Endoplasmic reticulum
GSH	Glutathione
GSSG	Glutathione disulfide
HCAEC	Human coronary artery endothelial cell
HCS	High-content screening
HPHC	Harmful and potentially harmful constituents
HSR	Heat shock response
HUVEC	Human umbilical vein endothelial cell
IL	Interleukin

IPN	Inflammatory Process Network
mRNA	Messenger ribonucleic acid
NHBEC	Normal human bronchial epithelial cell
NO	Nitric oxide
NPA	Network perturbation amplitude
OECD	Organisation for Economic Co-operation and Development
RBIF	Relative biological impact factor
RC	Reference cigarette
REF	Reference
RNS	Reactive nitrogen species
ROS	Reactive oxygen species
THS	Tobacco heating system
TNFα	Tumor necrosis factor alpha
TPM	Total particulate matter
TRA	Tissue Repair and Angiogenesis
UPR	Unfolded protein response

1. INTRODUCTION

The 2013 U.S. Surgeon General's Report "How Tobacco Smoke Causes Diseases" identifies inflammation and oxidative stress, among others, as key mechanisms underlying all major smoking-related diseases (Services, 2010).

Cigarette smoking is causally linked to the development of cardiovascular disease (CVD) contributing to endothelial injury and dysfunction, a pro-atherogenic lipid profile, chronic inflammation and an abnormally increased tendency toward coagulation. Evidence gathered in *in vitro* and *in vivo* studies as well as in population-based observational studies, has led to the recognition of vascular inflammatory processes as central to all stages of atherogenesis, from local endothelial dysfunction to plaque development and rupture (Libby et al, 2002; Ross, 1999). In addition, multiple lines of evidence suggest that reactive oxygen species (ROS) are key contributors to molecular signaling pathways underlying the development of atherosclerosis (Harrison et al, 2003; Madamanchi et al, 2005) and playing a central role in modifying most known main risk factors for CVD, including hypertension, hypercholesterolemia, obesity and diabetes (Asmat et al, 2015; Ceriello & Motz, 2004; Keaney et al, 2003; Rodriguez-Porcel et al, 2001).

Chronic obstructive pulmonary disease (COPD) is a respiratory disease characterized by progressive airflow limitation and is associated with an abnormal inflammatory response of the lung to noxious particles and gases ((GOLD), 2013). Development of COPD in smokers has been linked to a number of sustained cellular stress responses, including endoplasmic reticulum (ER), hypoxic and autophagic stresses (Chen et al, 2008b; Hengstermann & Müller, 2008; Hwang et al, 2010; Malhotra et al, 2009; Vasilios & Ioannis, 2008). Most, if not all, of these stress responses result from oxidative insults arising from direct exposure to cigarette smoke (CS), causing tissue injury through oxidative stress. At the same time, CS-related oxidative stress also leads to immune cell recruitment, their activation and release of proinflammatory mediators from immune cells which, in turn, produce a number of endogenous oxidative stressors that perpetuate the inflammatory response. Importantly, there is ample evidence that these same cellular stress responses are also linked to the initiation and progression of lung cancer in smokers (Durham & Adcock, 2015; Federico et al, 2007; Halliwell, 2007; Yang et al, 2011).

The following section of this dossier provides a brief overview of cellular stress responses as well as the *in vitro* and *in vivo* models and systems biological tools with which these stress responses can be assessed. It also describes results employing these tools to evaluate cellular stress responses exerted by CS exposure and those caused by exposure to tobacco heating system v2.2 (THS2.2), the potential modified risk tobacco product (MRTP) from Philip Morris International (PMI).

2. CELLULAR STRESS RESPONSES

A fundamental characteristic of all living systems is the ability to respond to, counteract and adapt to internal and external disturbances (Demirovic & Rattan, 2013). This ability is typically exhibited at the cellular level as cellular stress responses, universal mechanisms mobilizing defense reactions to prevent damage to cellular macromolecules, including DNA, proteins and lipids. Such responses are induced by a wide range of endogenous and exogenous stressors (Kültz, 2005). In general, an attempt to regain homeostasis by adapting to the changed environmental conditions is the first step in the cellular response to stress. Various cellular stress responses can be triggered, including heat shock response (HSR), unfolded protein response (UPR), hypoxic stress response, osmotic stress response, DNA damage response (DDR), autophagic response, sirtuin response, oxidative stress and antioxidant response and inflammatory response pathways (Kültz, 2005; Milisav, 2011a; Simmons et al, 2009). Which responses are initiated primarily depends on the nature of the stressor or the damage it elicits. Some cellular stress responses are stressor-specific while others are solely directed at counteracting the effects of macromolecular damage, independent of the stressor (Demirovic & Rattan, 2013; Fulda et al, 2010). In addition, it is now known that multiple cellular stress responses can be elicited in parallel or in sequence and that these very likely interact with one another to promote survival under adverse conditions (Simmons et al, 2009).

2.1 Heat Shock Response

The HSR is a universal cell stress response to stressors eliciting protein damage and is characterized by activation of heat shock transcription factors (HSFs) which, in turn, initiate production of heat shock proteins (HSPs). HSPs are represented by a number of molecular chaperone protein families, each designated by molecular weight (e.g., HSP90, HSP70 and HSP60), present in the cytosol, mitochondria, ER or nucleus (Kregel, 2002; Pirkkala et al, 2001). Following stressors such as heat shock, hypoxia, ischemia or energy depletion, HSPs are readily induced to establish thermotolerance and counteract protein denaturation by promoting protein (re)folding, preventing protein aggregation and degrading damaged proteins (Kregel, 2002).

2.2 Unfolded Protein Response

Prior to being transported to their ultimate destination or released into the extracellular space, membrane-targeted and secreted proteins are folded in the ER lumen (Walter & Ron, 2011). This process is governed by tightly controlled quality control measures, allowing only correctly folded proteins to exit the ER, while retaining unfolded or misfolded proteins for ultimate degradation (Shen et al, 2004b). Any stressor interfering with ER homeostasis causes ER stress which then leads to activation of the UPR. UPR pathways facilitate adaptation to the increased demand for ER-resident molecular chaperones and foldases by rapidly inducing their transcription and translation via the activating transcription factor 6 (ATF6) pathway. In parallel, protein kinase R (PKR)-like ER kinase (PERK)- and inositol-requiring enzyme 1 (IRE1)-mediated signaling leads to an overall decrease in ER load by, respectively, indirect inactivation of the eukaryotic

initiation factor 2 alpha (eIF2α) and accelerated mRNA decay (Schröder & Kaufman, 2005).

2.3 Hypoxic Stress Response

Oxygen deprivation can lead to significant stress responses aimed at adaptation of metabolic, bioenergetic and redox demands to the low oxygen levels (Majmundar et al, 2010). These responses generally result in suppression of energy-consuming cellular activities. For example, hypoxia was reported to interfere with mRNA translation by modulating PERK-mediated eIF2α phosphorylation and the 5′ adenosine monophosphate-activated protein kinase (AMPK)/ tuberous sclerosis complex 2 (TSC2) signaling pathway, thus restricting availability of eIF4E protein and preventing cap-dependent translation (Gardner & Corn, 2008; Liu et al, 2006; Liu et al, 2008a). However, most hypoxic stress responses are regulated by evolutionarily conserved mechanisms involving transcriptional regulation, by hypoxia-inducible factors (HIFs), of downstream effectors such as vascular endothelial growth factor (VEGF), solute carrier family 2, facilitated glucose transporter member 1 (SLC2A1) and erythropoeitin (EPO) (Greer et al, 2012; Majmundar et al, 2010; Semenza, 2007; Stockmann & Fandrey, 2006). Therefore, the hypoxic stress response is associated with HIF-1α-dependent processes, including transcription, translation and crosstalk with pathways related to oxidative stress, UPR (ER stress) and osmotic stress.

2.4 Osmotic Stress Response

Sudden changes in the external solute concentration, or osmolarity, of a cell can cause osmotic stress leading to water rapidly effluxing from or influxing into the cell. This interferes with cell volume and intracellular inorganic ion homeostasis (Finan & Guilak, 2010; Kültz & Burg, 1998). These negative effects are generally counteracted by both short- and long-term adaptive responses involving accumulation of small molecules such as glycerol to re-establish osmotic balance as well as regulation of genes associated with mitochondrial function, antioxidation and detoxification by transcription factor nuclear factors of activated T cells 5 (NFAT5) (Aramburu et al, 2006; Burg et al, 2007; de Nadal et al, 2002; Ortells et al, 2012; Saito & Posas, 2012). Aquaporin and cystic fibrosis transmembrane receptor (CFTR) pathways are also affected by osmotic stress (Schlage et al, 2011).

2.5 DNA Damage Response

DNA damage can arise spontaneously, caused by endogenous ROS produced by the mitochondrial electron transport chain during normal cellular respiration, by replication errors or through the action of environmental stressors such as ionizing radiation and genotoxic agents. To maintain genomic integrity, DNA damage is met by the DDR, a complex signal transduction pathway specialized in sensing damage and initiating DNA repair or inducing apoptosis via signal transducer proteins that control the response through phosphorylation of various effector proteins (Barzilai & Yamamoto, 2004; Ciccia & Elledge, 2010; Kastan, 2008).

DNA strand breaks are considered the key lesions that induce DDR-mediated repair (Fulda et al, 2010). DNA double strand break (DSB) repair is carried out by either homologous recombination or non-homologous end joining, during which progress through the cell cycle is slowed or halted (Jackson, 2002). DNA single strand breaks (SSB) can be repaired by different pathways, each involving a number of key factors: The nucleotide excision repair (NER) pathway repairs bulky lesions such as pyrimidine dimers, other products of photochemical reactions, large chemical adducts and DNA cross-links. The base excision repair (BER) pathway operates on small lesions, such as oxidized/reduced bases, fragmented or non-bulky adducts and adducts produced by methylating agents. Mismatch repair (MMR) corrects replication errors (base–base or insertion–deletion mismatches) caused by DNA polymerase. Finally, alkylated bases can also be directly removed by the suicide enzyme O^6-methylguanine-DNA methyltransferase (MGMT). Each of these repair pathways utilizes a specific set of enzymes that recognize the type and extent of damage and recruit appropriate repair enzymes to re-establish DNA duplex continuity. If it cannot be repaired, however, the DNA damage will be transduced to effector molecules that then activate and execute cell death pathways (Fulda et al, 2010).

2.6 Autophagic Response

Autophagy is a tightly regulated cellular mechanism for degrading cytoplasmic organelles and components. It is activated by a variety of cellular stressors, including nutrient or growth factor deprivation, hypoxia, ROS, DNA damage, protein aggregates, damaged organelles and intracellular pathogens (Kroemer et al, 2010). The three known types of autophagy are macroautophagy, microautophagy and chaperone-mediated autophagy (Glick et al, 2010). Macroautophagy, the major autophagic stress response, involves delivery of cytoplasmic cargo to the lysosome via formation of double- or multimembrane vesicles called autophagosomes. Fusion of autophagosomes with lysosomes generates autolysosomes, in which sequestered material is degraded and the endproducts diverted to recycling or elimination (Mizushima & Komatsu, 2011). Autophagy proceeds through a series of steps that are highly regulated by a genetic program involving at least five molecular components, including 1) the autophagy related 1 (Atg1)/unc-51-like kinase (ULK) complex; 2) the Beclin 1/class III phosphatidylinositol 3-kinase (PI3K) complex; 3) two transmembrane proteins, Atg9 and vacuole membrane protein 1 (VMP1); 4) two ubiquitin-like protein (Atg12 and Atg8/microtubule-associated protein 1A light chain 3A (LC3)) conjugation systems; and 5) proteins that mediate fusion between autophagosomes and lysosomes (Kroemer et al, 2010; Ryter & Choi, 2013).

2.7 Sirtuin Response

Sirtuins are a family of 7 nicotinamide adenine dinucleotide (NAD^+)-dependent protein deacetylases originally implicated in regulating organismal life span. In the context of cellular stress responses, sirtuins are considered effectors of stresses associated with calorie restriction or energy depletion (Guarente, 2007; Sauve et al, 2006). Experimental evidence suggested that sirtuin-mediated resistance to metabolic stress results from deacetylation and, hence, activation of peroxisome proliferator-activated receptor gamma

coactivator 1-alpha (PGC-1α), a transcriptional coactivator involved in gluconeogenesis. This, in turn, leads to increased hepatic glucose output (Rodgers et al, 2005). Other lines of evidence also point to deacetylation of forkhead (FOXO) transcription factors, an interaction that appears to occur during energy deprivation or oxidative stress and that was shown to induce cell cycle arrest and DNA repair, while attenuating apoptosis (Brunet et al, 2004; Giannakou & Partridge, 2004; Kobayashi et al, 2005). However, sirtuin 1 (SIRT1), the best characterized member of the family, also fulfills a broad range of other physiological roles due to its multitude of substrates and ability to move freely between cellular compartments (Liu & McCall, 2013) as highlighted in three recent reviews (McBurney et al, 2013; Morris, 2013; Raynes et al, 2013). Therefore, SIRT1 is very likely to encounter cellular stressors through other pathways that are not yet fully characterized.

2.8 Inflammatory Response

The complex series of cellular interactions accomplished by the innate immune system in response to pathogens, allergens or cellular damage is commonly referred to as the inflammatory stress response. This first-line defense mechanism rapidly triggers the release of proinflammatory substances, including cytokines, free radicals, hormones and other small molecules, to combat the stressor by initiating inflammation-resolving processes like the adaptive immune response (Berridge, 2012). However, a number of additional cell types also participate in the concerted effort to limit and repair tissue injury. For example, damage to endothelial cells can result in activation of the complement system and the release of thrombin, leading to subsequent initiation of the coagulation factor cascade, platelet aggregation and clot formation, thus contributing to injury repair and tissue remodeling (Berridge, 2012; Deng et al, 2009; Shen et al, 2004a). Various transcription factors, including nuclear factor kappa-light-chain-enhancer of activated B cells (NF-κB), activator protein 1 (AP-1) and early growth response 1 (EGR-1), induce expression of gene products integral to the inflammatory response. Thus, they control production of inflammatory mediators while also indirectly contributing to activation of the cells involved (Deng et al, 2009).

2.9 Oxidative Stress Response

Oxidative stress results from an imbalance between levels of ROS and antioxidants. ROS and other reactive species act directly on cellular macromolecules, damaging lipids, proteins and DNA. Key players of the oxidative stress response include the transcription factors AP-1, NF-κB and Nrf2 (Schlage et al, 2011). In general, cells respond to oxidative stress by activation of Nrf2 (encoded by the *NFE2L2* gene), a key regulator of detoxification and antioxidant genes (Ishii et al, 2002). When expressed, the products of these genes then either act as quenchers to eliminate the oxidative insult or contribute to regulation of downstream effectors, determining cell fate based on the extent of damage. However, oxidative damage is also known to elicit a number of other cellular responses, triggering various protein kinase signaling cascades, most notably those of the mitogen-activated protein kinase (MAPK) family. This results in proliferation, growth arrest, senescence or cell death, typically depending on the type of stressor and duration and extent of stress (Martindale & Holbrook, 2002).

3. CIGARETTE SMOKING-RELATED CELLULAR STRESS RESPONSES IN CVD, COPD AND LUNG CANCER

CS is a complex and dynamic mixture consisting of more than 8,000 unique chemical compounds (Perfetti & Rodgman, 2011). It is very likely that the biological effects of cigarette smoking are related to complex interactions of these compounds and their metabolites with one another and with various cells, including those of the respiratory tract and the cardiovascular system, in which smoke exposure elicits a series of adaptive cellular stress responses (Müller & Gebel, 2006). For example, acute exposure of rodent and human cells to CS or its fractions resulted in rapid upregulation of genes and protein involved in HSR and antioxidant responses (Bosio et al, 2002; Gál et al, 2011; Gebel et al, 2004; Henderson et al, 2008; Kreutmayer et al, 2011; Lu et al, 2007; Müller & Gebel, 1998). CS exposure also initiated the UPR (Csordas et al, 2011; Hengstermann & Müller, 2008; Jorgensen et al, 2008; Somborac-Bačura et al, 2013) and the sirtuin response (Hwang et al, 2010; Hwang et al, 2013; Yang et al, 2007). Furthermore, autophagic and DNA damage responses were reported to result from exposure of mammalian cells to CS (Jorgensen et al, 2010a; Kim et al, 2008; Messner et al, 2012; Salem et al, 2013; Yauk et al, 2012; Zhao et al, 2009). Finally, a vast amount of literature supports the link between smoking and the inflammatory stress response. Importantly, there is ample evidence that most, if not all, of these cellular stress responses interact with one another to counteract the deleterious effects of CS on cellular homeostasis and that, if resolution is not achieved, chronic exposure or ongoing stress can lead to the development of smoking-related diseases (Demirovic & Rattan, 2013; Glover-Cutter et al, 2013).

3.1 Cardiovascular Disease

Cigarette smoking is causally linked to the development of CVD by contributing to endothelial injury and dysfunction, a pro-atherogenic lipid profile, chronic inflammation and an abnormally increased tendency toward coagulation. While sustained UPR, ER and hypoxic stress were reported to contribute to all these disease-related processes, most of the evidence to date is focused on the roles of oxidative stress and inflammation in development and progression of CVD (Austin, 2009; Kaufman, 2002; Minamino & Kitakaze, 2010; Minamino et al, 2010; Tabas, 2010; Wang & Kaufman, 2012). Both gas and particulate (tar) phases of CS contain high levels of oxidants, with an estimated 10^{15} radicals per puff and 10^{17} radicals per gram of tar (Pryor, 1992; Pryor, 1997). Many of these free radicals, along with endogenously generated ROS and reactive nitrogen species (RNS), are the prime mediators of endothelial dysfunction in smokers, a key event in the development of atherosclerosis (Salahuddin et al, 2012).

The healthy endothelium produces a wide range of factors that regulate vascular tone, cellular adhesion, thromboresistance, smooth muscle cell proliferation and vessel wall inflammation in response to various inflammatory and oxidative stimuli (Münzel et al, 2008). The endothelium is maintained in a quiescent state through the inhibitory signaling of nitric oxide (NO), an important vasodilator (Deanfield et al, 2007). When the endothelium is injured, a host response is evoked, involving a switch from NO-mediated silencing of cellular processes to redox signaling, ultimately resulting in the activation of transcription factors such as NF-κB and subsequent production of inflammatory mediators including interleukin (IL)-1, IL-8 and tumor

necrosis factor alpha (TNFα) (Mudau et al, 2012; Yang et al, 2006). Endothelial nitric oxide synthase (eNOS), the source of NO under physiological conditions, becomes uncoupled and produces superoxide O_2^-, which can interact with NO, thus reducing its bioavailability and forming the highly reactive peroxynitrite ($ONOO^-$), adding to the overall oxidant burden (Nedeljkovic et al, 2003; Versari et al, 2009). The activated endothelium expresses surface molecules, such as P-selectin and integrins, that attract platelets and mediate platelet rolling and adhesion. The process of adhesion leads to platelet activation and the subsequent release of growth factors (e.g., platelet-derived growth factor (PDGF), transforming growth factor beta (TGF-β), epidermal growth factor (EGF) and basic fibroblast growth factor (bFGF)), chemokines (e.g., chemokine (C-C Motif) ligand 5 (CCL5), chemokine (C-X-C Motif) ligand 4 (CXCL4) and CXCL5), cytokines (e.g., IL-1β), chemoattractants (e.g., macrophage inflammatory protein-1 alpha (MIP-1α)) and coagulation factors (e.g., factor V, factor IX, plasminogen and plasminogen activator inhibitor (PAI-1)). These, in turn, promote monocyte recruitment to the site of inflammation, platelet aggregation, coagulation, cell survival and proliferation (Gawaz et al, 2005). Monocytes attracted to the sites of endothelial damage attach to the endothelial surface, transmigrate to the subendothelial space and differentiate into macrophages which begin to secrete proinflammatory mediators, supporting establishment of chronic inflammation (Facchinetti et al, 2007; Libby, 2012). Moreover, these macrophages also phagocytose oxidized lipids, present at elevated levels in smokers (Bloomer, 2007; Yamaguchi et al, 2005), and develop into lipid-laden foam cells, eventually forming the fatty streaks that are the first visible signs of atherosclerosis (Fearon et al, 2011). Activated endothelial cells and monocytes/macrophages release cytokines that attract vascular smooth muscle cells that migrate into the vessel just beneath the endothelial cell layer where they proliferate and contribute to the growth of the developing plaque. Oxidative stress was identified as a contributing factor to each of the steps in this complex cascade of events, as further detailed in several review articles (Cai & Harrison, 2000; Förstermann, 2010; Schulz et al, 2004; Thomas et al, 2008).

3.2 Chronic Obstructive Pulmonary Disease

COPD is a respiratory disease characterized by progressive airflow limitation and is associated with an abnormal inflammatory response of the lung to noxious particles and gases. Pathological changes characteristic of COPD are found in the proximal airways, peripheral airway, lung parenchyma and pulmonary vasculature. These changes include chronic inflammation, with increased numbers of specific inflammatory cell types in different parts of the lung, and structural abnormalities resulting from repeated injury and repair. Development of COPD in smokers has been linked to a number of sustained cellular stress responses. For example, exposure of lung epithelial cells *in vitro* causes an increase in intracellular levels of ubiquitin-protein conjugates, suggesting extensive protein damage. Concomitantly, and despite decreased nascent protein synthesis, a decrease in proteosomal activities leads to accumulation of proteins in the ER and ER stress ensues (Malhotra et al, 2009; Somborac-Bačura et al, 2013). Moreover, unresolved ER stress triggers several components of the UPR and results in activation of eIF2α which, in turn, initiates anti-apoptotic signaling via PERK and ATF6 UPR effector pathways (Hengstermann & Müller, 2008; Jorgensen et al, 2008). In addition, activation of the ER stress protein eIF2α also initiates ATF4-mediated transcriptional control of

oxidative stress response genes and genes involved in cellular metabolism and apoptosis (Harding et al, 2000; Harding et al, 2003; Jiang & Wek, 2005; Teske et al, 2011). However, the fate of lung epithelial cells exposed to CS can be determined, also, by DDRs, occurring as a consequence of increased oxidative DNA and RNA lesions in lung tissues. Repair of these lesions is accompanied by increased histone 2A family member X (H2AX) phosphorylation, p53 expression and phosphorylation, ataxia telangiectasia mutated kinase (ATM) phosphorylation, expression of 8-oxoguanine-DNA glycosylase (OGG1) and increased tissue and plasma levels of 8-hydroxy-2′-deoxyguanosine (8-OHdG) (Aoshiba et al, 2012; Caramori et al, 2011; Deslee et al, 2010; Deslee et al, 2009; Neofytou et al, 2012; Pastukh et al, 2011; Shi et al, 2012). If DNA damage is too severe, programmed cell death mechanisms such as apoptosis are induced, as evidenced by increased caspase 3 activity and elevated B-cell lymphoma 2 (BCL2)-associated X (BAX) and BCL2-associated death promoter (BAD) protein levels in lung epithelial and endothelial cells of COPD smokers (Aoshiba et al, 2012; Hu et al, 2009; Zeng et al, 2012). More recent studies suggested that autophagic cell death also plays an important role in COPD. For example, the number of autophagosomes was higher in lungs of COPD patients than in lungs of control subjects and CS exposure induced autophagosome formation and upregulated LC3-phosphatidylethanolamine conjugate (LC3B-II) expression *in vitro* and *in vivo* (Chen et al, 2008b; Hwang et al, 2010; Kim et al, 2008). Moreover, cellular senescence induced by exposure to oxidants from CS may contribute to the enhancement of COPD by augmenting inflammatory processes and alveolar tissue degradation (Nyunoya et al, 2013; Nyunoya et al, 2006; Tsuji et al, 2006). Not surprisingly, most, if not all, of these stress responses are executed as an answer to oxidative insults arising from direct exposure to CS, causing tissue injury through oxidative stress. At the same time, CS-related oxidative stress also leads to immune cell attraction, their activation and subsequent release of proinflammatory mediators from immune cells which, in turn, produce a number of endogenous oxidative stressors, perpetuating the inflammatory response.

3.3 Lung Cancer

There is overwhelming evidence that cigarette smoking is the major cause of lung cancer in most human populations and an increased risk of lung cancer in smokers was demonstrated in a number of epidemiological studies (Doll & Peto, 1981; Doll et al, 2004; Harris et al, 2004; Wakai et al, 2006; Zhang & Cai, 2003).

Direct damage to DNA by ROS and RNS is accepted as an explanation for the initiation of events that ultimately lead to lung cancer (Halliwell, 2007). It is well known that the interaction of DNA with hydroxyl radicals leads to formation of mutagenic purines and pyrimidines such as 8-OHdG, one of the most abundant and readily-formed oxidized DNA bases (Valavanidis et al, 2009). 8-OHdG can induce G:T transversions, among the most frequent mutations in human cancers (Pilger & Rüdiger, 2006). Similarly, attack on DNA by RNS can result in deamination of nucleobases and the formation of oxidative lesions with pro-mutagenic characteristics (Ohshima et al, 2006). Oxidative damage to proteins can also promote mutagenesis, in particular when proteins involved in DNA replication or repair such as proliferating cell nuclear antigen (PCNA) and growth arrest and DNA-damage-inducible protein 45 (Gadd45) are affected (Fayolle et al, 2007; Kinoshita et al, 2007). Furthermore, oxidative modification of signal transducers such as

protein kinases can lead to their constitutive activation, accelerating transition through the cell cycle and promoting proliferation (Matés et al, 2008). Finally, ROS also act on lipids, causing their peroxidation and, in the process, generating a number of highly reactive intermediary carbonyl compounds that can form DNA-adducts and hence give rise to mutagenic lesions (Fearon et al, 2011). Malondialdehyde (MDA) is a well-studied example of such damaging lipid peroxidation products and was shown to be elevated in blood and urine of smokers (Fahn et al, 1998; Lykkesfeldt, 2007; Tanriverdi et al, 2006). Moreover, increased levels of MDA-adducts were found in bronchial and laryngeal tissues and buccal cells from smokers (Barreiro et al, 2013; Munnia et al, 2006; Munnia et al, 2004; Zhang et al, 2002).

In addition to their deleterious effects on cellular macromolecules, ROS can also act as second messengers and mediate proliferation and programmed cell death through regulation of transcription factors such as NF-κB and AP-1, which have been shown to induce early response genes involved in cell proliferation, angiogenesis and cell transformation (Burdon, 1995; Federico et al, 2007; Naugler & Karin, 2008; Storz, 2005). Furthermore, ROS and RNS can trigger a variety of cell stress signaling cascades by activating members of the MAPK family such as p38, c-Jun N-terminal kinase (JNK) and extracellular signal-regulated kinases (ERKs), thus modulating responses to apoptotic cues (Benhar et al, 2001; Benhar et al, 2002; Cuda et al, 2002; Shen & Liu, 2006; Siebel et al, 2013). Finally, the oxidative stress induced by exposure to CS, either directly or indirectly, elicits a strong Nrf-2-mediated antioxidant response, activating transcription of phase II detoxifying and antioxidant enzymes (Müller & Gebel, 2006; Müller & Hengstermann, 2012).

Of note, once a tumor has developed, similar cell stress responses may be mounted to counter the effects of rapid tumor growth, such as insufficient oxygen and glucose supply, and to prevent cell death (Kim et al, 2007; Kim et al, 2010; Lee et al, 2010; Matthew et al, 2009) or promote neo-angiogenesis and metastasis (Brahimi-Horn & Pouysségur, 2006; Dewhirst, 2009; Erler et al, 2006). In addition, proteins that were oxidatively damaged or arose from mutated genes might cause ER stress in tumor cells and trigger one or more UPR effector pathways to avoid apoptosis (Boelens et al, 2007; Wang et al, 2010). It has now also become clear that a change in extracellular osmolarity serves as a potent pro-inflammatory stimulus in itself. Hyperosmotic stress led to release of TNFα, IL-1β, IL-6 and IL-8 in various cell types (Brocker et al, 2012; Neuhofer, 2010; Schwartz et al, 2009). Experimental evidence further suggests that hyperosmotic stress results in ROS production, oxidative stress and subsequent NF-κB activation which evokes an apoptotic response, thus adding to the overall cellular stress level (Eisner et al, 2006).

4. QUANTIFYING THE IMPACT OF CIGARETTE SMOKE ON CELLULAR STRESS RESPONSES IN EXPERIMENTAL MODELS USING A SYSTEMS BIOLOGY APPROACH

4.1 Tools for Assessment of Cellular Stress *In Vitro* and *In Vivo*

4.1.1 *In Vitro* Systems to Study Cigarette Smoke-Related Cellular Stress

While the complexity of respiratory diseases in the context of cigarette smoking makes a direct translation to *in vitro* models difficult, many aspects of the disease processes, including ROS production and DNA damage following exposure, can be modelled adequately to obtain useful supporting information. Continuous lung epithelial cell lines, either immortalized or tumor-derived, provide suitable cellular model systems for testing chemical compounds and mixtures including CS. However, the functionality of immortal cells and their observed biological responses to various stimuli are known to differ considerably from those of primary cells derived from human airways (Ghio et al, 2013; Ioannidis et al, 2013; Koning et al, 2012; Lopez-Souza et al, 2004). Moreover, some of the early effects of CS exposure appear to be more adequately reflected in primary, versus immortalized, lung epithelial cells grown under submerged conditions *in vitro* when compared to the phenotype(s) of epithelial cells obtained by bronchial brushing of smokers (Dvorak et al, 2011; Martinez-Anton et al, 2013). Nevertheless, use of classical submerged cultures of primary normal bronchial epithelial cells (NHBECs) permits only limited conclusions because several structural properties, such as cell polarization, are lost *in vitro* (Paquette et al, 2003). However, there is a suitable alternative increasingly used to test inhalation toxins. Raising a confluent layer of primary bronchial or nasal epithelial cells grown on a porous membrane in the presence of essential growth factors, hormones and micronutrients to the air-liquid interface (ALI) induces terminal differentiation, ultimately leading to formation of a pseudostratified airway epithelium closely resembling that seen in human airways (Gray et al, 1996; Jetten, 1989; Paquette et al, 2003). Well-differentiated cultures created in this fashion consist of columnar epithelial, goblet, ciliated and basal cells. They exhibit tight junctions, display functional cilia and are capable of mucus production which accumulates at the apical surface, atop a thin layer of airway surface liquid (Adamson et al, 2011; Prytherch et al, 2011). The functional and morphological similarities of these cultures to human airway epithelium, for this reason also called organotypic cultures, make them prime candidates for evaluating CS and its fractions *in vitro*.

While similar complex cell cultures to model the cardiovascular system are not yet available, modelling defined processes underlying the pathogenesis of atherosclerosis is still possible *in vitro*. As seen with airway epithelial cells in submerged cultures, simple cell culture systems exemplifying the cardiovascular system do, however, have various drawbacks which have been expertly reviewed (Fearon et al, 2013). Nevertheless, these cell cultures provided meaningful insights into the mechanisms underlying CS-induced perturbations of the cardiovascular system. For example, CS-induced damage to endothelial cells was assessed in primary vascular endothelial cells, such as human umbilical vein endothelial cells (HUVECs) or human coronary artery endothelial cells (HCAECs), demonstrating exposure-related changes of various endpoints, including cell viability, production of ROS, cell migration, inflammatory mediator release and expression of cell adhesion molecules (CAMs) (Chen et al, 2004; McKarns et al, 2000; Orosz et al, 2007; Peluffo et al, 2009; Snajdar et al, 2001; Suzuki et al, 2006). Primary

human endothelial cells were also useful to investigate how exposure to CS changes the adhesive properties of primary blood-derived monocytes and neutrophils or immortalized monocyte-like cells such as THP1 or MM6 cells (Adams et al, 1997; Dovgan et al, 1994; Stone et al, 2002; Suzuki et al, 2006). Moreover, a series of studies highlighted the utility of human vascular smooth muscle cell cultures for studying the effects of CS exposure on cell viability, proliferation and vascular contractility (McKarns et al, 2000; Starke et al, 2013; Xiang et al, 2010; Xu et al, 2008; Xu et al, 2010; Zhou et al, 2015).

For PMI's *in* vitro studies of acute cell stress responses following a single exposure for a duration ranging from 28 minutes to 24 hours, with or without post-exposure, both NHBECs grown in submerged cultures and commercially available, ready-to-use bronchial and nasal MucilAir™ organotypic cultures (Epithelix SàRL, Geneva, Switzerland) were employed. In addition, vascular and immune cell crosstalk was mimicked with *in vitro* adhesion and transendothelial migration assays consisting of HCAECs and activated THP-1 or MM6 cells. These models and assays were subsequently shown to be useful for testing effects of CS exposure on adhesive and migratory properties of these cell types and for characterizing the resulting cellular stress response profiles (Poussin et al, 2014; Poussin et al, 2015; van der Toorn et al, 2015).

4.1.2 Assays and Markers to Determine Oxidative Burden *In Vitro*

While ROS can be directly and reliably measured by electron spin resonance or radical trapping, *in vitro* assays traditionally rely on their ability to readily bind to or react with a reporter molecule, yielding stable, often chromogenic, chemiluminescent or fluorescent products to determine the presence and extent of oxidative stress (Fearon & Faux, 2009; Kohen & Nyska, 2002). Alternatively, formation of oxidative DNA lesions, lipid peroxidation products or protein modifications resulting from interaction of ROS with intracellular macromolecules can be detected to assess oxidative stress *in vitro* and *in vivo*. There are several toxicity assays measuring various endpoints, including the differential regulation of specific cellular pathways. Rapid development, in particular in the course of drug discovery and testing, has made these assays amenable to high-throughput platforms, and it is anticipated that availability of a number of these assays, together with sophisticated computational tools, will shape the future of toxicity testing (NRC, 2007). Discussing this concept in the context of the cellular stress response, Simmons and colleagues proposed an ensemble approach, that could provide useful information about pathway activation patterns and give insights into specific stress signatures linked to cell fate and mechanisms of toxicity (Simmons et al, 2009).

There have been many *in vitro* studies utilizing fluorescing indicator dyes such as dihydroethidium (DHE), dichlorofluorescin diacetate (DCFDA) and dihydrorhodamine (DHR) to assess oxidative stress in live cells. These assays are based on interaction of the probes with ROS, resulting in their oxidation to yield bright fluorescent products that can be measured by flow cytometry, fluorometry or fluorescence microscopy. Using DCDFA with fluorescence microscopy or flow cytometry, oxidative stress was shown to increase in human bronchial epithelial cells (Kode et al, 2008; Lin et al, 2014; Pace et al, 2013; Tagawa et al, 2008; Tan et al, 2014; Wu et al, 2014), nasal epithelial cells (Pace et al, 2014), lung fibroblasts (Carnevali et al, 2003), cardiac myocytes (Yamada et al, 2009) and vascular endothelial cells (Edirisinghe et al, 2008; Michaud et al, 2006; Milara et al,

2010) following acute (short-term) treatment with cigarette smoke extract (CSE). Oxidative stress also increased in a dose- and time-dependent manner in lung epithelial cells treated with CS total particulate matter (TPM), as determined by DCFDA fluorometry (Faux et al, 2009), and in bronchial epithelial cells cultured at the ALI and exposed to whole smoke using a chemiluminescent probe (Scheffler et al, 2015). Recent technical advances have made high-throughput screening with indicator probes easy, fast and cost-effective, allowing for intracellular ROS loads to be examined in simple monolayer cell cultures under various conditions. Well-defined protocols for evaluating oxidative stress using, for example, DCFDA or DHE on (semi-) automated high-content screening (HCS) platforms, exist and were previously employed as part of the toxicological assessment of a number of chemicals, environmental toxicants and drugs, in particular in hepatocytes (Anguissola et al, 2014; Di Pietro et al, 2009; Garside et al, 2014; O'Brien, 2014). However, there are not many reports on similar approaches to assess oxidative stress in the context of CS exposure. In one study examining effects of several compounds listed as harmful or potentially harmful constituents (HPHC) of CS, there was no increase in ROS loads in primary human bronchial epithelial cells treated for 4, 8 or 24 hours (Gonzalez-Suarez et al, 2014).

It is worth noting here that many of the cited studies aimed at directly addressing the extent of intracellular ROS loads following exposure to CS or its fractions utilized indicator dyes and there is evidence that such assays have limitations. For example, loading live cells with these dyes produced oxidative stress by inducing ROS production and caused cytotoxicity (Halliwell & Whiteman, 2004), suggesting that the extent of treatment-related oxidative stress may be overestimated in such applications. It is, therefore, not surprising that there are ongoing efforts to improve the existing ROS probes or develop new, more specific ones (Fearon & Faux, 2009). Similarly, there is a drive to employ complementary measures that determine how well a system can cope with oxidative insults by assessing specific antioxidant levels, profiling antioxidant enzyme activities or measuring total antioxidant capacity (TAC). In *in vitro* assays and animal models, measuring glutathione (GSH) levels is a simple and fast means of assessing cellular redox potential. GSH is an essential intracellular tripeptide with potent free radical scavenging and detoxifying capabilities deriving from its cysteine thiol moeity. GSH exists in cells primarily in its reduced form, making up more than 95% of the total GSH pool. Interactions with ROS oxidize GSH to GSH disulfide (GSSG), which can be recycled to GSH by the action of glutathione reductase in the presence of nicotinamide adenine dinucleotide phosphate (NADPH). Therefore, the ratio of GSH to GSSG is regarded as a good indicator of oxidative stress (Owen & Butterfield, 2010). Measurement of the GSH:GSSG ratio by reduction of Ellman's reagent (5,5′-dithiobis-(2-nitrobenzoic acid) or DTNB) (Tietze, 1969) and subsequent spectrophotometry showed that treatment of human lung epithelial cells, alveolar macrophages and lung fibroblasts with CSE or cigarette smoke condensate (CSC) decreased cellular GSH content and the GSH:GSSG ratio in a dose-dependent manner (Carnevali et al, 2003; Hodge et al, 2011; Lau et al, 2011; Luppi et al, 2005; Rahman et al, 1995; van der Toorn et al, 2007), indicating a strong oxidative stress response. GSH measurements are also amenable to modern high-throughput methodologies, such as high-content imaging, and increasing numbers of studies have described their utility in the context of toxicological assessment. However, to date, there are very few studies using this technology for *in vitro* testing of CS and CS fractions. In a study examining

effects of several compounds from the FDA HPHC list (Food & Administration, 2012), GSH levels decreased in primary human bronchial epithelial cells exposed to acrolein for 4, 8 or 24 hours or to formaldehyde for 24 hours (Gonzalez-Suarez et al, 2014).

There are also various biomarkers that can be used to assess oxidative damage to DNA, proteins or lipids in experimental models, providing an indirect means for evaluating prior oxidative stress. Some of these markers, including F2-isoprostanes and 8-OHdG, were proposed as being valuable to assess oxidative burden in *in vitro* and *in vivo* models.

Peroxidation of arachidonic acid gives rise to isoprostanes, prostaglandin-like compounds produced in tissues by non-enzymatic free radical-catalyzed reactions. Oxidative damage *in vivo* generates a wide variety of isoprostane molecules and these exhibit widely differing biological activities (Janssen, 2001). The most widely studied group of isoprostanes is the family of F2-isoprostanes whose most well-known member is 8-iso-PGF2α, a potent pulmonary and renal vasoconstrictor (Jourdan et al, 1997; Takahashi et al, 1992) and mediator of platelet aggregation (Minuz et al, 1998; Morrow et al, 1992). Numerous studies demonstrated that quantification of F2-isoprostanes by mass spectrometry is the most accurate way to measure oxidative stress *in vitro* and in animal models of oxidant injury (Basu, 2008; Milne et al, 2005; Roberts & Morrow, 2000; Visioli et al, 2000). In smokers, free and esterified F2-isoprostanes in plasma and urine were elevated relative to in nonsmokers (Helmersson et al, 2005; Morrow et al, 1995; Reilly et al, 1996) and rapidly declined upon smoking cessation (Chehne et al, 2001; Pilz et al, 2000; Reilly et al, 1996). Another study reported that murine and human macrophages treated with fly ash particles readily released 8-isoprostane, as determined by immunoassay (Fritsch-Decker et al, 2011), and human lung epithelial cells produced increased amounts in response to hyperoxia with or without high concentrations of inorganic phosphates (Ravikumar et al, 2014). However, to our knowledge, there are no reports on changes of isoprostane levels in *in vitro* systems following exposure to CS, its fractions or its components. There are, in addition, only a limited number of studies reporting on the presence and quantity of lipid peroxidation products *in vitro* and most of these focus on MDA production under conditions of oxidative stress. The literature is equally sparse with respect to reports on oxidative DNA damage markers *in vitro*. Neonatal rat alveolar epithelial type II (AEII) cells produced increased amounts of 8-OHdG in response to hyperoxia (Jin et al, 2015) and elevated 8-OHdG levels were noted in supernatants of human neutrophils stimulated with phorbol myristate acetate (PMA) (Leanderson & Tagesson, 1992), in PMA-differentiated human promyelocytic leukemia (HL60) cells following exposure to asbestos fibers (Takeuchi & Morimoto, 1994), in human vascular endothelial cells due to hyperglycemia (Piconi et al, 2006) and in Jurkat T cells exposed to to silver nanoparticles (Chatterjee et al, 2014). To date, there are no cell culture studies investigating effects of CS exposure on formation of 8-OHdG. However, increasingly, many researchers are using alternative markers, for example, to indicate oxidative DNA damage. Common examples are the *in vitro* comet and γH2AX assays. The comet assay is based on single cell gel electrophoresis in which damaged DNA is separated according to fragment size, forming a "comet tail" and the tail measurements are an indicator of the extent of DNA damage. In a study using this assay, CSE treatment induced DNA damage in human lymphoblast-like Raji and MCL-5 cells (Wolz et al, 2001; Yang et al, 1999), lung fibroblasts (Carnevali et al, 2003), vascular endothelial cells (Chen et al, 2004) and lung epithelial cells (Cavallo et al, 2013; Liu et al, 2008b). Similarly, CSC treatment induced DNA

damage as evidenced by increased tail lengths, or moments, in L5178Y/Tk$^{+/-}$ 3.7.2C mouse lymphoma cells (DeMarini et al, 2008), human B lymphoblastoid cells (Lou et al, 2010) and primary human bronchial epithelial cells (Chen et al, 2008a). Most of these studies indicated that DNA damage was linked to CS exposure-induced oxidative stress by showing that pre- or co-incubation of cells with antioxidants such as vitamin C, α-tocopherol (vitamin E) or N-acetyl-cysteine (NAC) abolished most comet tails. In addition, in a modified comet assay with formamidopyrimidine N-glycosylase (FPG), a base excision repair enzyme capable of recognizing and removing oxidized purines, exposure of human lung epithelial cells to mainstream CS was reported to induce both reparable DNA strand-breaks and irreparable oxidative DNA lesions (Thorne et al, 2009). While the comet assay is easy, versatile and sensitive, it is susceptible to various physical factors such as pH and temperature and is not yet truly amenable to high throughput platforms (Lynch et al, 2011; Zainol et al, 2009). Therefore, the γH2AX assay, using flow cytometry or high-content analysis, was proposed as an alternative to assess DNA damage *in vitro*, in particular in the context of assessing CS genotoxicity (Garcia-Canton et al, 2012).

In response to DNA damage, the DDR becomes activated. Its function is to arrest cell cycle progression and division to prevent transfer of DNA damage to progeny cells, engage DNA damage repair mechanisms and activate the apoptotic pathway to eliminate cells with excessive DNA damage that cannot be repaired (Zhao et al, 2009). One of the earliest DDR events is the activation of H2AX as a result of DNA DSBs. Once key molecules of the DDR, such as ATM, ataxia telangiectasia and Rad3 related (ATR) and DNA-dependent protein kinase (DNA-PK), are recruited to the site of damage, H2AX is rapidly phosphorylated at serine residue 139, forming γH2AX (Rogakou et al, 1998). This is quickly followed by establishment of a signal amplification loop to ensure that DDR is executed efficiently at the appropriate location (Nakamura et al, 2010; Paull et al, 2000). Since the formation of γH2AX is rapid and its amount correlates with that of DSBs (Nakamura et al, 2010), it has become increasingly attractive as an indicator of DNA damage. Various methods can be employed to determine the extent of γH2AX foci formation, with flow cytometry and high-content screening with phospho-specific antibodies directed against γH2AX the most frequently used. Many studies using the assay on a high-content platform showed that exposure of human lung epithelial cells to CS caused increased γH2AX in a dose- and time-dependent manner (Albino et al, 2004; Albino et al, 2006; Garcia-Canton et al, 2014; Jorgensen et al, 2010b; Tanaka et al, 2007). Results were similar for select CS constituents when tested individually in NHBECs (Garcia-Canton et al, 2013; Gonzalez-Suarez et al, 2014), adding to the value of this assay in non-clinical product assessment.

4.1.3 *In Vivo* Systems to Study Cigarette Smoke-Related Cellular Stress

While providing significant new insights into mechanisms underlying CS-related diseases in men, *in vitro* models can never fully reproduce the interplay between the different cell types in an organism and the spectrum of biological processes occurring during the development of atherosclerosis, COPD or lung cancer in smokers. However, many gaps in our understanding of these processes can be filled by knowledge gained from animal models and a multitude of model organisms have been employed for this purpose. For example, CVD research has utilized animal models since the early 1900s (Leong et al,

2015). While atherosclerosis can be observed in many species fed a high-fat diet including hamsters, guinea pigs, rabbits, dogs and pigs, the mouse remains the most frequently used animal model owing to its easy maintenance and low cost (Getz & Reardon, 2012). However, mice are relatively resistant to diet-induced atherogenesis. Unlike in humans, in mice high-density lipoprotein (HDL) cholesterol is the main lipoprotein and cholesteryl ester transfer protein (CETP), a plasma protein facilitating exchange of esterified cholesterol and triglycerides from lipoproteins, is not expressed (Getz & Reardon, 2012). In addition, atherosclerotic lesions in mouse models also differ from those in human disease in other aspects. They preferentially form in the aortic root and typically do not develop a fibrous cap, so unstable plaques are uncharacteristic (Getz & Reardon, 2012). Most of these differences, however, are addressed by generating genetically modified mice, with *Apoe* knockout (*Apoe*$^{-/-}$) mice as the most widely studied murine atherosclerosis model. Developed in the early 1990s, these mice were shown to be hypercholesterolemic, even on normal chow, and to exhibit the full spectrum of lesions associated with atherosclerosis development in humans (Nakashima et al, 1994; Plump et al, 1992; Zhang et al, 1992). Moreover, studies using the *Apoe*$^{-/-}$ mouse with additional genetic modifications (knockout of *Rag2* or P-selectin or overexpression of *Crp*) confirmed that chronic inflammation plays a major role in the development of atherosclerotic lesions (Daugherty et al, 1997; Dong et al, 2000; Paul et al, 2004). Notably, CS exposure accelerated atherosclerosis in *Apoe*$^{-/-}$ mice, with increased intimal thickness, plaque size and plaque area in exposed compared with control animals (Catanzaro et al, 2007; Gairola et al, 2001; Gairola et al, 2010; Kunitomo et al, 2009; Schroeter et al, 2008; Tani et al, 2004; Von Holt et al, 2009). Importantly, we and others also observed a distinct oxidative stress response to CS in the *Apoe*$^{-/-}$ mouse, characterized by elevated tissue and serum levels of oxidative stress markers such as thiobarbituric acid-reactive substances (TBARS), oxidatively modified low-density lipoproteins (oxLDLs) and the protein oxidation marker 3-nitrotyrosine (3-NT) (Arunachalam et al, 2010; Knight-Lozano et al, 2002; Kunitomo et al, 2009). This suggested that the *Apoe*$^{-/-}$ mouse model may provide useful insights into the role of cellular stress responses as drivers of the development and progression of atherosclerosis, in particular when addressing questions regarding CS-related morbidities.

Similar to animal models of CVD, many cellular and molecular mechanisms involved in the pathogenesis of COPD in humans, including those related to cellular stress responses, are also observed in murine pulmonary emphysema models (Brusselle et al, 2006). In these, several features are shared between human early stage disease and mouse disease development, with the mice primarily recapitulating the emphysema component (Churg et al, 2011). Lesions in mice caused by chronic CS exposure resemble centrilobular human emphysema, both morphologically and physiologically (Churg et al, 2008). Small airway remodeling, an important cause of airflow obstruction in cigarette smokers with COPD (Hogg et al, 2004), was also observed in CS-exposed mice (Churg et al, 2008). In addition, exposure activated the innate immune response cascade in mice, leading to protease/anti-protease imbalances in lung tissue and eventual alveolar wall degradation, suggesting that murine models can also recapitulate these features of human COPD (Yoshida & Tuder, 2007). Finally, as observed in humans, the small airways from smoke-exposed C57Bl/6 mice exhibited persistent upregulation of type I pro-collagen and pro-fibrotic cytokine gene expression, which would be expected to contribute to airway remodeling (Churg et al, 2006). However, murine models of COPD/emphysema

have several limitations. First, these models display only a subset of disease phenotypes and do not fully recapitulate airflow limitation from chronic small airway obstruction, which defines COPD (Hogg et al, 2004). Second, there are considerable differences in respiratory physiology and anatomy between mice and humans, making disease modeling difficult. In contrast to humans, mice are obligate nose breathers and filter tobacco smoke differently. In addition, the submucosal glands in mice are limited to the trachea and mice lack a cough reflex, which further distinguishes the pulmonary physiologies of the two species from one another (Groneberg & Chung, 2004). Importantly, pulmonary emphysema in humans is classified according to the distribution of the airspace enlargement within the acini in centriacinar emphysema and, in cigarette smokers with COPD, significant airspace enlargement occurs primarily across the three generations of respiratory bronchioles (Hogg et al, 2004). However, rodents lack clearly defined respiratory bronchioles and distinct lobular architecture, further obscuring anatomically equivalent comparisons of disease development (March et al, 2000). Third, there are key species differences in the innate and adaptive immune responses, which are thought to be critical to the initiation and maintenance of disease. These include differences in the expression of defensins, toll-like receptors (TLRs) and chemokine receptors, as well as a unique repertoire of active chemokines in each species. Differences in adaptive immunity include immunoglobulin subtypes, Th1/Th2 differentiation dynamics and the roles and ratios of $CD4^+$ and $CD8^+$ T cell populations, together with co-stimulatory molecule expression and function (Mestas & Hughes, 2004). The theory of an autoimmune component to advanced COPD contributing to the self-perpetuating nature of the disease in men could not be corroborated in mice (Taraseviciene-Stewart et al, 2005). Fourth, unlike in humans, emphysema in mice induced by CS does not progress after smoking cessation and mice never develop spontaneous exacerbations. Finally, mice do not develop more severe COPD symptoms characteristic of the human GOLD stages III and IV. Despite these differences, the observed features of major cell stress responses, such as oxidative stress, leading to CS-related lung disease suggest that mouse models can aid our understanding of key mechanisms underlying human COPD pathophysiology. In previous studies at PMI aimed at elucidating these mechanisms, both C57Bl/6 and the *Apoe*$^{-/-}$ mouse strains were used (Boué et al, 2013; Cabanski et al, 2015; Phillips et al, 2015b). Furthermore, there is an opportunity to examine the role of oxidative stress and its interplay with other cell stress responses in the context of lung cancer progression in the A/J mouse study that is currently ongoing. More recently, in an effort to reduce the number of animals, studies of cell stress responses following exposure to conventional and modified tobacco products were combined with safety toxicology studies in Sprague-Dawley rats (Kogel et al, 2014; Phillips et al, 2015a), a practice PMI intends to continue in the future.

4.1.4 Systems Biology Tools

Owing to the complexity of cellular stress responses and their intricate cross-talk, we further pursued a systems biology view and developed a molecular causal network model combining available knowledge and large scale datasets of physiological responses to endogenous and exogenous stressors in non-diseased mammalian respiratory and cardiovascular cells (Schlage et al, 2011). The resulting Cell Stress (CST) Network, constructed in a computable framework, is a fully referenced mechanistic representation

of multiple physiological stress responses and consists of several building blocks, including xenobiotic stress, ER stress, hypoxic stress, osmotic stress, *NFE2L2* (Nrf-2) signaling and oxidative stress (Figure 1).

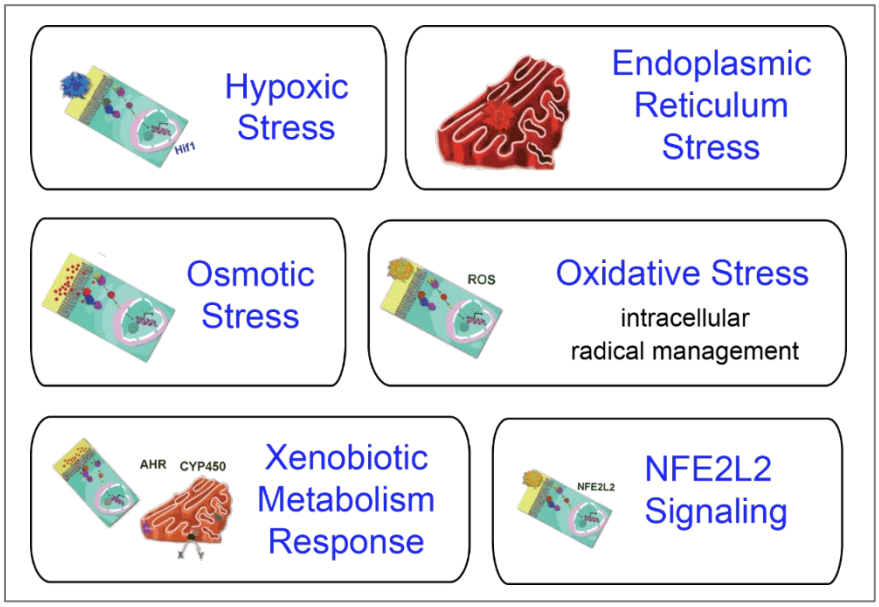


Figure 1. Cellular stress model overview

Extensive literature review enabled extraction of the relevant network nodes and their connections (edges) with a high degree of mechanistic detail. Then, a number of select transcriptomic data sets from experiments involving exposure to various stressors were employed to confirm and supplement model nodes from the literature-derived model components. This was done using reverse causal reasoning (RCR) to identify significant predictions or hypotheses (HYPs) of the activity states of biological mechanisms (such as protein abundance, activity and biological process) based on the gene expression datasets (Selventa, 2010). The resulting network model was subsequently verified through the application of a publicly available transcriptomic data set, demonstrating its ability to predict CS-induced state changes in *Nfe2l2*-deficient compared with wild-type mice. The results of this analysis highlighted a robust increase in the oxidative stress response and demonstrated that the model has utility in the identification of mechanistic details for complex cellular systems (Schlage et al, 2011). In addition, a highly sophisticated algorithm was developed to obtain, for a given network model, the network perturbation amplitude (NPA) as a quantitative measure of the impact a stressor exerts on a given biological system (Martin et al, 2012). Combining the NPAs of several network models then allows for the computation of the biological impact factor (BIF) that provides a measure of the overall biological impact across all network models (Thomson et al, 2013). The BIF was recently proposed as a systems-wide and pan-mechanistic biological impact measure for a given active substance or mixture (Hoeng et al, 2012).

4.2 Assessment of Cellular Stress *In Vitro* and *In Vivo* - Results

A number of nonclinical studies were performed in laboratory animals to identify potential hazards and characterize mechanisms underlying tobacco-related diseases associated with the use of THS2.2 (Table 1). Among these studies, the 90-day inhalation rat studies, as described in the Organisation for Economic Co-operation and Development (OECD) guideline 413 (OECD 2009a), aimed to characterize adverse effects caused by repeated daily inhalation exposure to aerosols generated from THS2.2 or THS2.2 Menthol (THS2.2M) for 90 days. An additional post-exposure period of 42 days was included in both studies to assess reversibility or delayed effects. Lung inflammation, histology of respiratory and non-respiratory organs, and various blood-based parameters were evaluated at the end of the 90-day inhalation and 42-day recovery periods. To obtain an understanding of the toxicity pathways, including oxidative stress, involved in the response to exposures, additional molecular endpoints including multi-analyte profiling in bronchoalveolar lavage fluid (BALF), transcriptomics and proteomics analysis of lung and nasal epithelium were examined at 90 days of exposure and after the 42-day recovery period. Furthermore, hallmarks of COPD and CVD and general exposure effects were investigated over an 8-month period in apolipoprotein E-deficient (*Apoe*$^{-/-}$) mice exposed to conventional CS or to the aerosol of THS2.2. These experiments also assessed the consequences of cessation or switching to THS2.2 after 2 months of CS exposure. Engaging a systems toxicology approach, exposure effects including cellular stress responses were investigated using the conventional toxicology parameters, such as physiology and histopathology of respiratory and non-respiratory organs, combined with transcriptomics, lipidomics, and proteomics measurements.

These rodent studies were further complemented by a series of *in vitro* studies to assess the impact of exposure to 3R4F CS and THS2.2 aerosol on oral, nasal and bronchial organotypic tissues cultured at the ALI. Various endpoints, including cytotoxicity, cytochrome P450 (CYP) 1A1/1B1 activity, histopathology and transcriptomics, were assessed at different time points following an acute 28-minute exposure. In addition, *in vitro* studies were performed in human coronary artery endothelial cells to study changes in their adhesive properties towards monocytes following treatment with aqueous extracts from 3R4F CS and THS2.2 aerosol. In other experiments, samples of conditioned medium from monocytes preincubated with these aqueous extracts were applied to challenge the endothelial cells. In both approaches, a functional adhesion assay was combined with transcriptomics and inflammatory protein marker measurements to investigate changes in this model system at the molecular level (Table 1).

Table 1. Nonclinical Studies with Measures of Oxidative Stress

Study	Type	Design	Reference
Adhesion assay	*In vitro*	Parallel-group (air (sham), RC[a] and THS2.2 aerosol extracts)	(Poussin et al, 2016)
Fraction Impact	*In vitro*	Parallel-group (air (sham), RC and THS2.2 aerosol fractions)	(Gonzalez-Suarez et al, 2016)
Organotypic buccal	*In vitro*	Parallel-group (air (sham), RC and THS2.2 aerosols)	1743_Organotypic_Buccal_SR (Zanetti et al, 2016)
Organotypic nasal	*In vitro*	Parallel-group (air (sham), RC and THS2.2 aerosols)	1722_Organotypic_Nasal_SR (Iskandar et al, 2016)
Organotypic bronchial	*In vitro*	Parallel-group (air (sham), RC and THS2.2 aerosols)	1709_Organotypic_Bronch_SR
Rat OECD THS2.2	*In vivo*	TG413 (air (sham), RC, THS2.2)	15006_150082_150083 THS SR
Rat OECD THS2.2M	*In vivo*	TG413 (air (sham), RC, THS2.2M)	15025_176500 THS SR
Apoe$^{-/-}$ THS2.2	*In vivo*	Parallel-group, switching (air (sham), RC, THS2.2, cessation, switching)	15015_CVD_SR (Lo Sasso et al, 2016a; Lo Sasso et al, 2016b; Phillips et al, 2016)
A/J Lung Cancer	*In vivo*	Parallel-group (air (sham), RC, THS2.2)	15020_AJ LC_QA-checked Interim Report

(a): 3R4F reference cigarette

The following part of this section summarizes the results from assessments of oxidative stress parameters in these nonclinical studies.

4.2.1 Results from *In Vitro* Studies

4.2.1.1 Adhesion Assay

Using the previously established adhesion assay together with a systems toxicology approach (Poussin et al, 2014; Poussin et al, 2015), the indirect and direct effects of extracts derived from 3R4F CS (CSE) and THS2.2 aerosol (AE) on the adhesion of monocytes to endothelial cells were investigated. First, using the indirect approach, monocytic MonoMac 6 (MM6) cells were exposed to CSE or AE for 2 hours and their resulting culture supernatants used to treat monolayers of serum-starved HCAECs for 4 hours prior to addition of untreated DRAQ5™-labeled MM6 cells. Adhesion of these MM6 cells was then evaluated using a high-content screening platform. Alternatively, HCAECs were treated with freshly prepared extracts (fresh direct approach) or with extracts that were aged for 2 hours at 37°C and then stored frozen (direct approach).

Following exposure of endothelial cells to conditioned media from treated MM6 cells in the indirect approach, monocyte-endothelial cell adhesion was promoted by exposure to low concentrations of 3R4F CSE or THS2.2 AE. Compared with CSE, 10 and 20 times higher concentrations of THS AE were necessary for indirect and fresh direct treatments, respectively, to induce comparable adhesion rates of MM6 cells to HCAECs. In addition, the highest concentrations of both 3R4F CSE and THS2.2 AE, using the fresh direct approach, significantly decreased the number of HCAEs. The other experimental conditions did not affect HCAEC numbers. In contrast, when HCAECs were exposed to a high concentration of previously frozen (direct approach) or freshly prepared (fresh direct approach) CSE, MM6 cell–HCAEC adhesion was not observed (Poussin et al, 2016). Transcriptomics profiling was performed on HCAEC samples following treatment with conditioned media, unconditioned media or fresh aqueous smoke/aerosol extracts for 4 hours to investigate the underlying mechanisms of the observed treatment effects as previously described (Poussin et al, 2014; Poussin et al, 2015). The HCAEC systems response profiles (SRPs) showed a concentration-dependent increase in the number of differentially expressed genes (DEGs) with all 3R4F CSE treatments. Following treatment with equivalent concentrations of THS2.2 AE, far fewer genes were significantly altered than with CSE exposure. Even treatment with THS2.2 AE at concentrations that were 10 to 20 times higher than those of 3R4F CSE did not lead to as many significantly DEGs as did treatment with CSE, regardless of exposure mode (Poussin et al, 2016). The mechanistic network analysis indicated maximum biological impact (Relative biological impact factor (RBIF) = 100%; reference (REF)) following indirect treatment with 3R4F CSE at the lowest concentration, affecting a broad spectrum of perturbed networks, while perturbations elicited with the higher 3R4F CSE concentration, although of the same nature, were of a lower amplitude. At the same concentrations, the overall magnitude of perturbations elicited by treatment with THS2.2 AE represented only 1% and 3% of the total perturbation of the reference, respectively, while it was 78% at the highest concentration with highly and similarly perturbed biology. The pattern and magnitude of network perturbations following direct and fresh direct treatments differed from those seen with the indirect treatment (Figure 2).

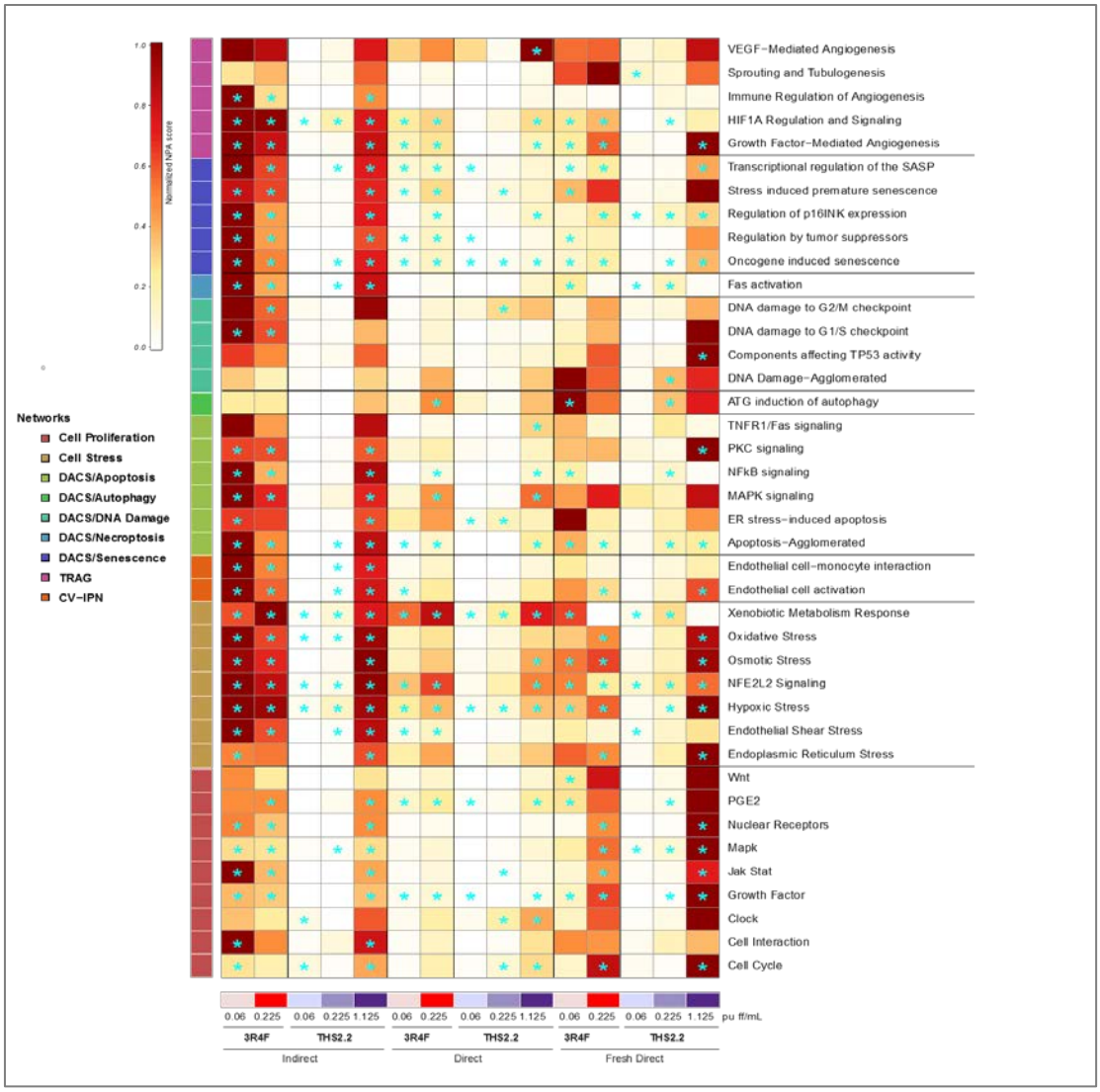


Figure 2. Network perturbations in human coronary arterial endothelial cells treated with 3R4F cigarette smoke or THS2.2 aerosol aqueous extracts.

Heatmap of Network Perturbation Amplitude scores summarizing subnetworks that were significantly perturbed with at least one treatment. A network is considered as perturbed if, in addition to the significance of the NPA score with respect to the experimental variation, the two companion statistics (O and K), derived to inform on the specificity of the NPA score with respect to the biology described in the network, are significant. Significantly perturbed networks are indicated by * (*i.e.*, O and K statistics *p*-values <0.05 and significant with respect to the experimental variation).

A deeper analysis of CST network perturbations revealed perturbations of the Xenobiotic Metabolism Response subnetwork which increased in a concentration-dependent manner, independent of the treatment mode. These perturbations were of considerably lower amplitudes at low and intermediate concentrations of THS2.2 AE, when compared with matching 3R4F CSE concentrations. The Oxidative Stress subnetwork was also significantly perturbed following indirect treatment, while fresh direct treatment elicited a strong impact only at the highest concentrations of either 3R4F CSE or THS2.2 AE

(Figure 3A). In addition, treatment with aqueous extracts resulted in significant perturbations of the NFE2L2 Signaling subnetwork. Treating HCAECs indirectly with 3R4F CSE had the strongest impact, and this extent of perturbation was seen only with THS2.2 AE concentrations exceeding those of 3R4F CSE by approx. 20-fold. This was also true for the direct and fresh direct treatment modes (Figure 3B).

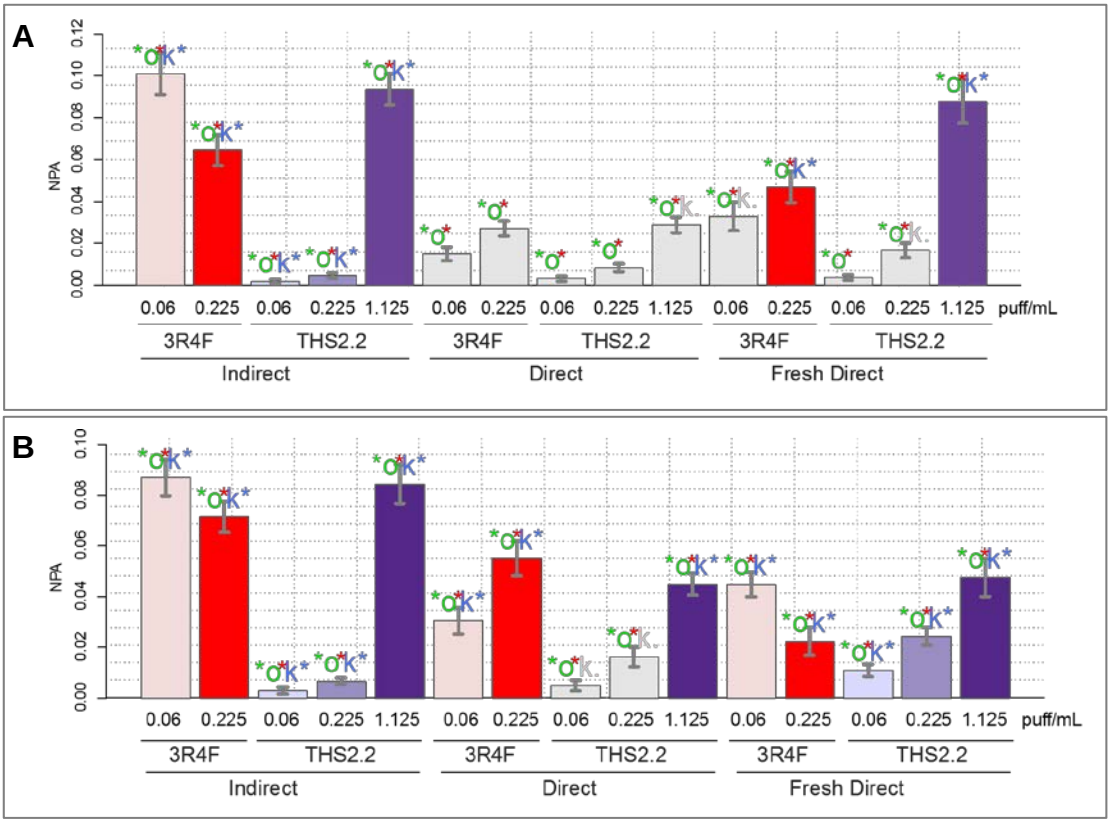


Figure 3. Relative network perturbation amplitude (NPA) of specific cell stress subnetworks in human coronary arterial endothelial cells treated with 3R4F cigarette smoke or THS2.2 aerosol aqueous extracts.

The relative NPA scores for the Oxidative Stress (A) and NFE2L2 Signaling (B) subnetwork models are shown with their confidence intervals accounting for experimental variation. The percentages are the relative NPA scores for the subnetworks, compared with the reference. The reference is the treatment comparison showing the highest perturbation. In addition, companion statistics, derived to inform on the specificity of the NPA score with respect to the biology described in the respective subnetwork models, are shown as *O and K*, respectively, if their p-values were below the significance level. Symbol legend:*, O and K statistic p-values <0.05; O and K, p-values between 0.05 and 0.1.

In the transcriptomics results from the MM6 cells, a concentration-dependent increase in DEGs with both THS2.2 AE and 3R4F CSE was observed. While a substantial number of DEGs were identified in MM6 cells treated with 3R4F CSE, with low and intermediate THS2.2 AE treatments there were, instead, no genes and a few genes significantly deregulated, respectively. Only treatment with THS2.2 AE at a concentration approximately 20 times greater resulted in a similar number of DEGs as was observed

with the lower concentration of 3R4F CSE. Of note, MM6 cell viability decreased by approximately 25%-30% at the high concentrations of both CSE and THS2.2 AE, indicating cytotoxicity.

The strongest biological impact was elicited by a low concentration of 3R4F CSE (RBIF =100%), while the highest concentration of 3R4F CSE resulted in a RBIF of 17% with little similarity in the underlying perturbed biology compared with the lower concentration. The network perturbations observed with THS2.2 AE showed a consistent concentration-dependent increase in RBIF values. However, even at the highest concentration used, the impact was less severe than that observed with the low 3R4F CSE concentration.

Nearly all networks were affected by treatment of MM6 cells with 3R4F CSE, with significant perturbations seen in the Cell Fate (CFA), Cell Proliferation (CPR), CST and Inflammatory Process networks (IPN). Among the CST subnetworks, only the Hypoxic Sstress and NFE2L2 Signaling subnetworks were significantly perturbed following 3R4F CSE treatment. In MM6 cells treated with THS2.2 AE at low and intermediate concentrations, significant perturbations were noted in the Senescence, Necroptosis, CST and CPR networks, and these had a noticeably lower amplitude than those seen with the matching 3R4F CSE concentrations. Treatment of MM6 cells with an approximately 20 times higher concentration of THS2.2 AE than the higher CSE caused more widespread network perturbations, also leading to significant perturbations in the IPN (Figure 4).

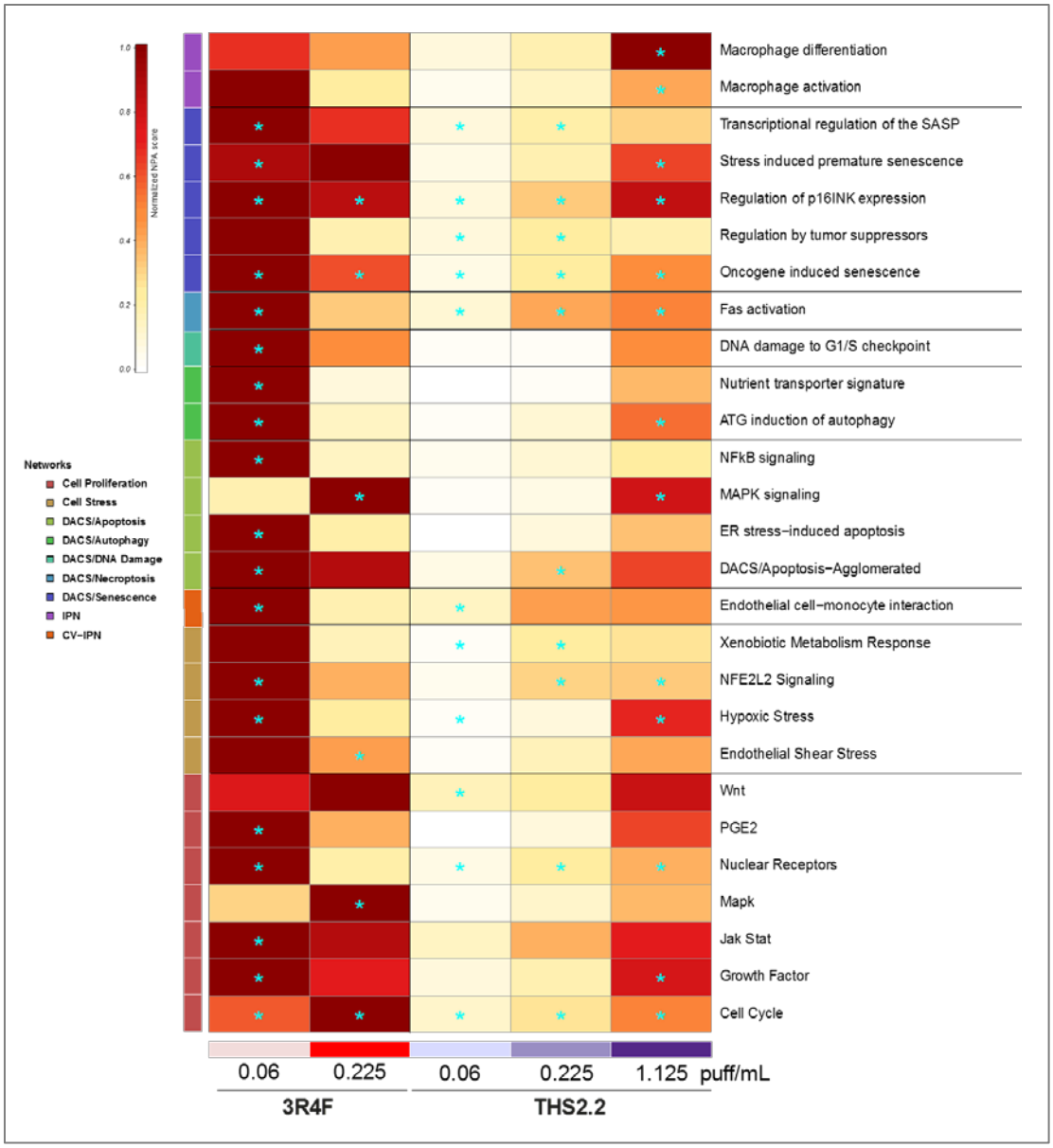


Figure 4. Network perturbations in MM6 cells treated with 3R4F cigarette smoke or THS2.2 aerosol aqueous extracts.

Heatmap of Network Perturbation Amplitude scores summarizing subnetworks that were significantly perturbed with at least one treatment. A network is considered as perturbed if, in addition to the significance of the NPA score with respect to the experimental variation, the two companion statistics (O and K), derived to inform on the specificity of the NPA score with respect to the biology described in the network, are significant. Significantly perturbed networks are indicated by * (*i.e.*, O and K statistics *p*-values <0.05 and significant with respect to the experimental variation).

In summary, 3R4F CSE promoted the adhesion of monocytic to endothelial cells *via* distinct indirect and direct mechanisms. At matching concentrations, THS2.2 AE did not trigger MM6 cell–HCAEC adhesion and clearly showed a lower impact than CSE, at the molecular level, on HCAECs and MM6 cells. MM6 cell–HCAEC adhesion, accompanied

by molecular changes in both cell types, reached similar magnitude increases as those induced by 3R4F CSE only when concentrations of THS2.2 AE were 10 and 20 times higher for fresh direct and indirect exposure modes, respectively.

4.2.1.2 THS2.2 Aerosol Fraction Impact Assessment Study

Multiple parameters indicating cell health, genotoxicity and cell stress were tested in NHBECs grown in submerged culture and treated with various doses of aqueous extract, TPM or gas-vapor phase (GVP) from 3R4F reference cigarettes and THS2.2 heat sticks, using real-time impedance and HCS.

When NHBECs were exposed to extract from 3R4F, a marked reduction in cell viability was noted after treatment for 4 hours, with viability further decreasing by 24 hours. However, THS2.2 AE exposure had no effect at 4 hours and, at the highest concentration, caused a much smaller decrease in cell viability at 24 hours than did 3R4F CSE treatment. Exposure to 3R4F GVP for 4 hours resulted in a dose-dependent decrease in NHBEC viability, with an even stronger effect after 24 hours treatment. In contrast, there was no effect on cell viability in cells exposed to THS2.2 GVP. Cell viability was also decreased when NHBECs were exposed to 3R4F TPM in a similar fashion to the effects of GVP. Again, THS2.2 TPM was not cytotoxic for the NHBECs.

ROS formation increased, as indicated by increased DHE fluorescence, in NHBECs treated with high doses of 3R4F CSE for 24, but not 4, hours (Figure 5A). As this effect was accompanied by significant cell death, it is very likely that the data did not reflect actual oxidative stress. ROS loads were also increased in cells treated with high doses of 3R4F CSE for 24 hours, again coinciding with increased cell death (Figure 5A). However, extracts derived from both items caused a dose-dependent decrease in GSH content at both time points, with noticeably larger decreases in cells treated with 3R4F than with THS2.2 extract, at comparable doses (Figure 5B). A 24 hour treatment with high doses of GVP derived from 3R4F cigarettes resulted in increased ROS load, coinciding with a significant increase in NHBEC death (Figure 5C). In addition, a dose-dependent decrease in GSH, indicative of increased oxidative stress, was noted following treatment with 3R4F GVP for 4 or 24 hours (Figure 5D). In comparison, exposure to THS2.2 GVP caused a dose-dependent decrease in GSH at 4 hours and this effect was no longer present at the later time point, suggesting that cellular GSH pools were replenished after the initial insult (Figure 5D). Oxidative stress following 3R4F TPM exposure could not be assessed because of a marked interference by this fraction with the DHE fluorescence signal, but a dose-dependent decrease in GSH levels could be detected following treatment for 4 or 24 hours (Figure 5E). Treatment of NHBECs with THS2.2 TPM also resulted in decreased GSH content at these time points, but increased ROS loads were noted following only a 24-hour treatment (Figure 5F).

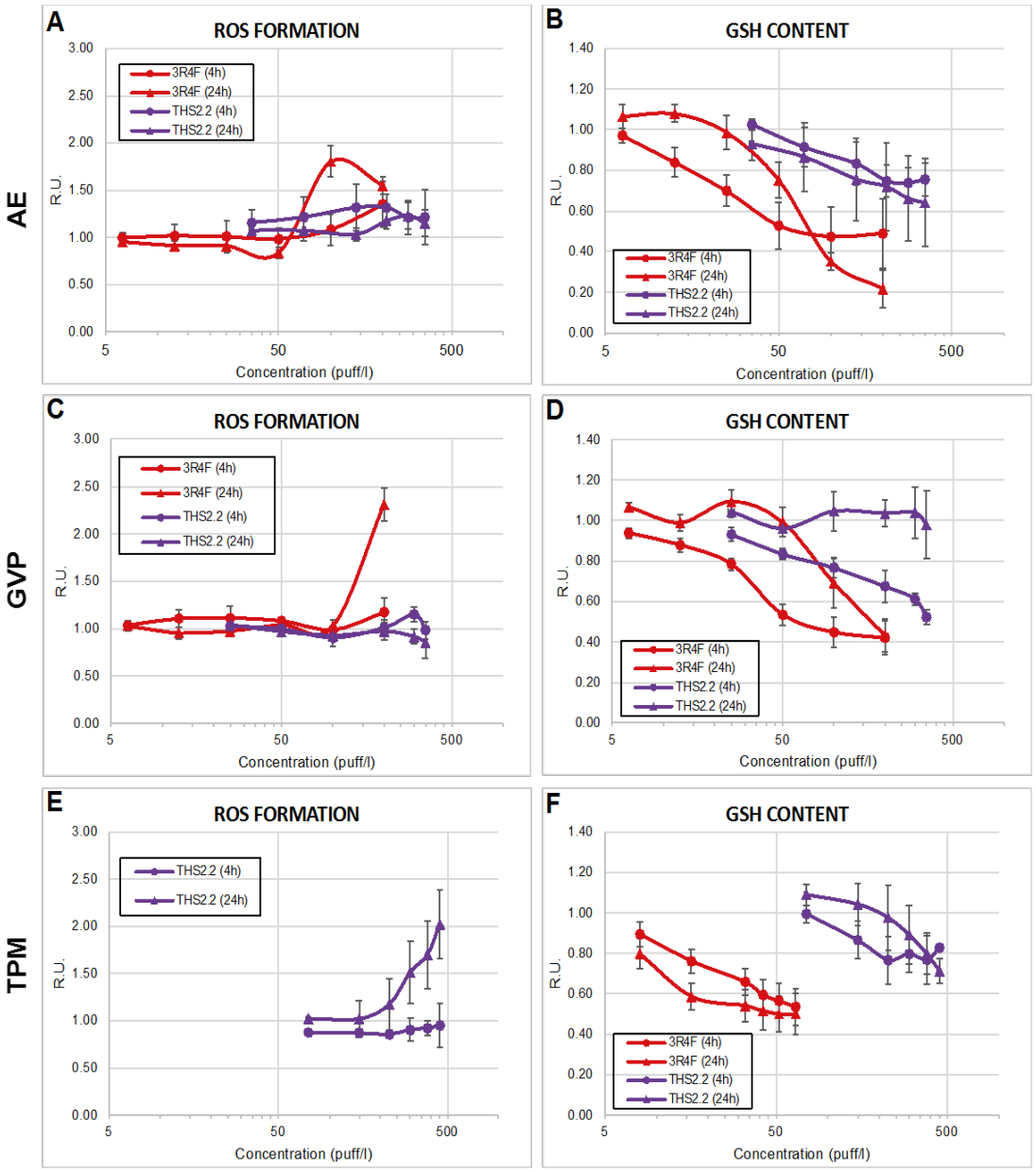


Figure 5. Oxidative stress in normal human bronchial epithelial cells exposed to 3R4F cigarette smoke or THS2.2 aerosol fractions.

Oxidative stress was assessed by measurements of ROS formation and GSH content in normal human bronchial epithelial cells exposed to (A, B) aqueous extracts (AE), (C, D) gas-vapor phase (GVP), or (E, F) total particulate matter (TPM) from 3R4F cigarette smoke (red) or THS2.2 aerosol (purple) for 4 or 24 hours. Values are normalized to the vehicle control and are means ± SEM from three independent experiments.

The genotoxic potential of the THS2.2 aerosol relative to that of 3R4F CS was evaluated by immunostaining cells for γH2AX, an indicator of DSBs. Exposure of NHBECs to 3R4F extract at the two highest doses increased γH2AX staining at 4 hours, a result that was comparable to that at the highest doses of 3R4F GVP (Figure 6A, B). Treatment with TPM from reference cigarettes for 4 hours increased DSBs in a dose-dependent manner

and a similar dose-dependent effect was observed with all 3R4F smoke fractions at the 24-hour time point (Figure 6). However, after longer treatments, there was a dramatic reduction in cell viability, indicating cytotoxicity-induced genotoxicity. With THS TPM exposures, only doses far exceeding those of the comparable 3R4F fraction caused dose-dependent DNA damage at both 4 and 24 hours. Neither THS GVP nor aerosol increased the number of γH2AX-positive cells (Figure 6).

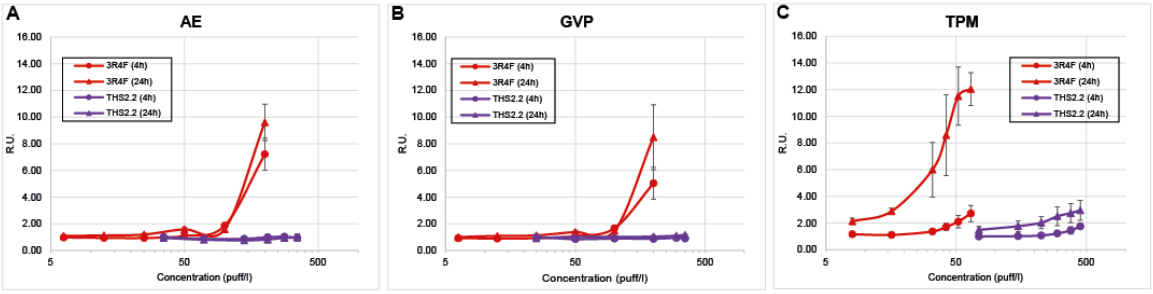


Figure 6. Genotoxic stress in normal human bronchial epithelial cells exposed to 3R4F cigarette smoke or THS2.2 aerosol fractions.

Genotoxic stress was estimated based on formation of γH2AX, a marker for DNA double-strand breaks, in normal human bronchial epithelial cells exposed to (A) aqueous extracts (AE), (B) gas-vapor phase (GVP), or (C) total particulate matter (TPM) from 3R4F cigarette smoke (red) or THS2.2 aerosol (purple) for 4 or 24 hours. Values are normalized to the vehicle control and are means ± SEM from three independent experiments.

The various fractions were then further evaluated with respect to their impacts on the NHBEC transcriptome. Exposure of NHBECs to 3R4F CSE for 4 hours gradually increased the number of DEGs in a dose-dependent manner. In contrast, a 4-hour exposure to THS2.2 AE, at comparable doses, did not result in significant changes in gene expression. Only 28 DEGs could be identified in NHBECs treated with THS2.2 AE at a concentration 3.5-fold higher than the highest 3R4F dose tested. Prolonged exposure to 3R4F AE for 24 hours did not yield any significantly altered genes, nor did treatment with THS2.2 AE at comparable doses. Only at the highest THS2.2 extract concentration were a small number of DEGs identified. In addition, SRPs indicated a large number of DEGs in cells treated with the low and high concentrations of 3R4F GVP, while 4-hour treatment with the medium concentration elicited only a small effect, possibly caused by highly variable gene expression changes among the replicate samples. In contrast, exposure to THS2.2 GVP at the lowest concentration for 4 hours led to few significant gene expression changes and no differentially expressed genes met the significance cutoff in cells treated for 4 hours with THS2.2 GVP at medium or high doses. There were, however, a small number of DEGs when NHBECs were exposed to THS2.2 GVP at a concentration that was 3.5 times higher than that of the highest 3R4F GVP concentration. After a 24-hour exposure to GVP, no significant changes in gene expression were detected in the 3R4F GVP-treated cells (excluding the highest concentration that caused high cytotoxicity) or the THS2.2 GVP-treated cells, with the exception of the lowest concentration which exhibited an SRP similar to that seen after the 4-hour treatment (data not shown). Furthermore, SRPs from NHBECs treated with TPM from both reference

and test items indicated a dose-dependent increase in significantly altered genes following 3R4F treatment for 4 hours. Prolonged 3R4F exposure increased the number of DEGs even more. In comparison, treating NHBECs with the selected THS2.2 TPM concentrations for 4 hours resulted in only 2 significantly altered genes, while no DEGs were identified in THS2.2 TPM-treated cells at the 24-hour time point.

Interrogating these data further with the mechanistic network approach highlighted the strongest biological impact for the 4-hour treatment with the highest concentration of 3R4F TPM (RBIF = 100%, REF; Figure 7). At comparable doses, treatment with 3R4F CSE for 4 hours elicited a stronger impact than with THS2.2 AE, causing perturbations in the CPR, CST, and Senescence networks. Such perturbations were also noted with the lower 3R4F CSE concentrations, albeit with an much lower impact. At 24 hours, RBIF values for both reference and test items were lower than at the 4-hour time point. Nevertheless, the biological impact of exposure to THS2.2 extract was also lower than that of exposure to 3R4F CSE at this time point (Figure 7).

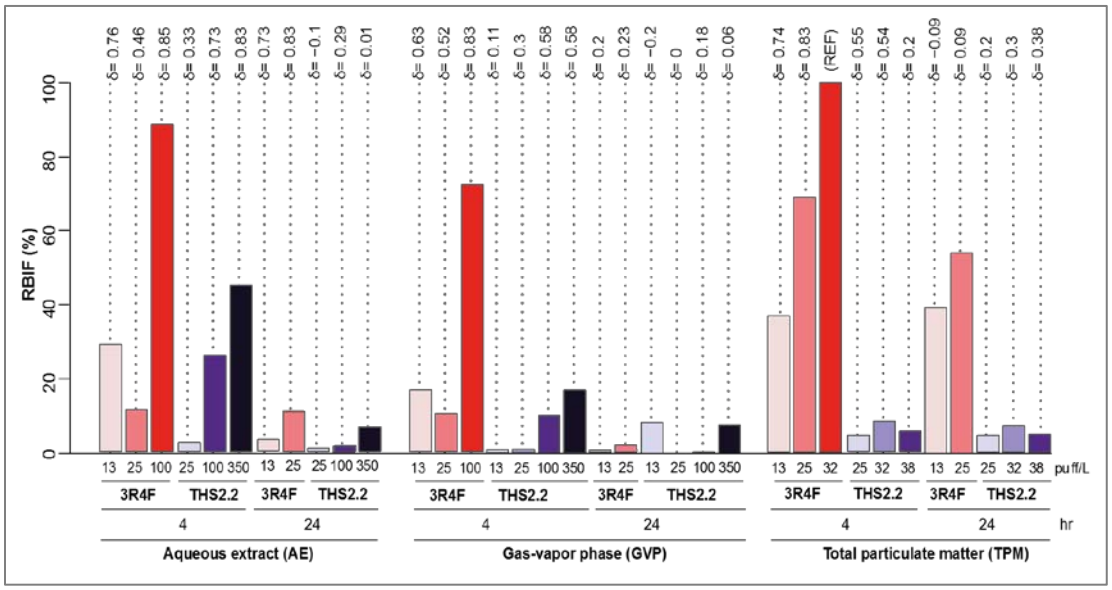


Figure 7. Network model-based analysis of the biological impact factor (BIF) in normal human bronchial epithelial cells exposed to 3R4F cigarette smoke or THS2.2 aerosol fractions.

The bar plot depicts BIF values relative to the maximum response (REF, RBIF = 100%). The δ values (−1 to 1) indicate how similar the underlying network perturbations are with respect to the REF. Scores were computed using transcriptomics profiling data from NHBE cells exposed to vehicle, aqueous extracts (AE), gas-vapor phase (GVP) or total particulate matter (TPM) from 3R4F cigarette smoke (red bars) or THS2.2 aerosol (purple bars) for 4 or 24 hours.

All CST subnetworks, with the exception of Hypoxic Stress and Endoplasmic Reticulum Stress, were affected by exposure of NHBECs to 3R4F CSE for 4 hours, while the impact of the 24-hour treatment shifted almost exclusively to the Xenobiotic Metabolism Response subnetwork, leaving other stress responses unaffected. In contrast, short-term treatment with THS2.2 AE primarily affected processes related to oxidative stress and

xenobiotic metabolism, with additional impacts on hypoxic and osmotic stress responses becoming noticeable after prolonged exposure with this aerosol fraction (Figure 8). While there was little difference in the nature of the mechanistic drivers between the reference and test items, the extent of network perturbations following treatment with extract derived from THS2.2 was considerably less than that seen with 3R4F CSE.

Network perturbations that contributed most to the observed impact of 3R4F GVP at 4 hours predominantly occurred in networks describing cell stress, proliferation and senescence biology. In cells treated for 24 hours with this fraction, CST and CPR networks continued to be most perturbed, albeit to a lesser extent. In comparison, the impact of THS2.2 GVP on NHBECs was considerably lower than that of 3R4F GVP at comparable concentrations, independent of treatment time. Similar, but far more moderate, perturbations were noted in THS2.2 GVP-treated NHBECs (Figure 8). Perturbations in the Oxidative Stress and NFE2L2 Signaling subnetworks contributed most to the CST network perturbations following exposure of NHBECs to GVP from both reference and test items, and the underlying biology was very similar between effects of 3R4F and THS2.2 GVP.

After 4 hours of exposure to 3R4F TPM at the lower dose, all networks except the Necroptosis network exhibited significant perturbations, with those in the CPR, IPN and CST networks contributing the most to the RBIF. At 24 hours, the character of network perturbations caused by exposure to 3R4F TPM was similar to that seen at the earlier time point, although the extent of perturbation was noticeably less. Mechanisms captured by the CPR, CST and IPN networks continued to be significant and predominant contributors to the observed perturbations. With THS2.2 TPM, and independent of treatment duration, cell stress processes were the most perturbed, albeit to a lesser extent than the 3R4F TPM-induced perturbations (Figure 8). Among the perturbed CST subnetworks, Xenobiotic Metabolism Response, Oxidative Stress and NFE2L2 Signaling were most affected by exposure of NHBECs to TPM from 3R4F cigarettes. Similar mechanisms were identified as possible causes for the network perturbations following 3R4F and THS2.2 TPM exposures. However, the extent of these perturbations was considerably less than those seen with 3R4F TPM.

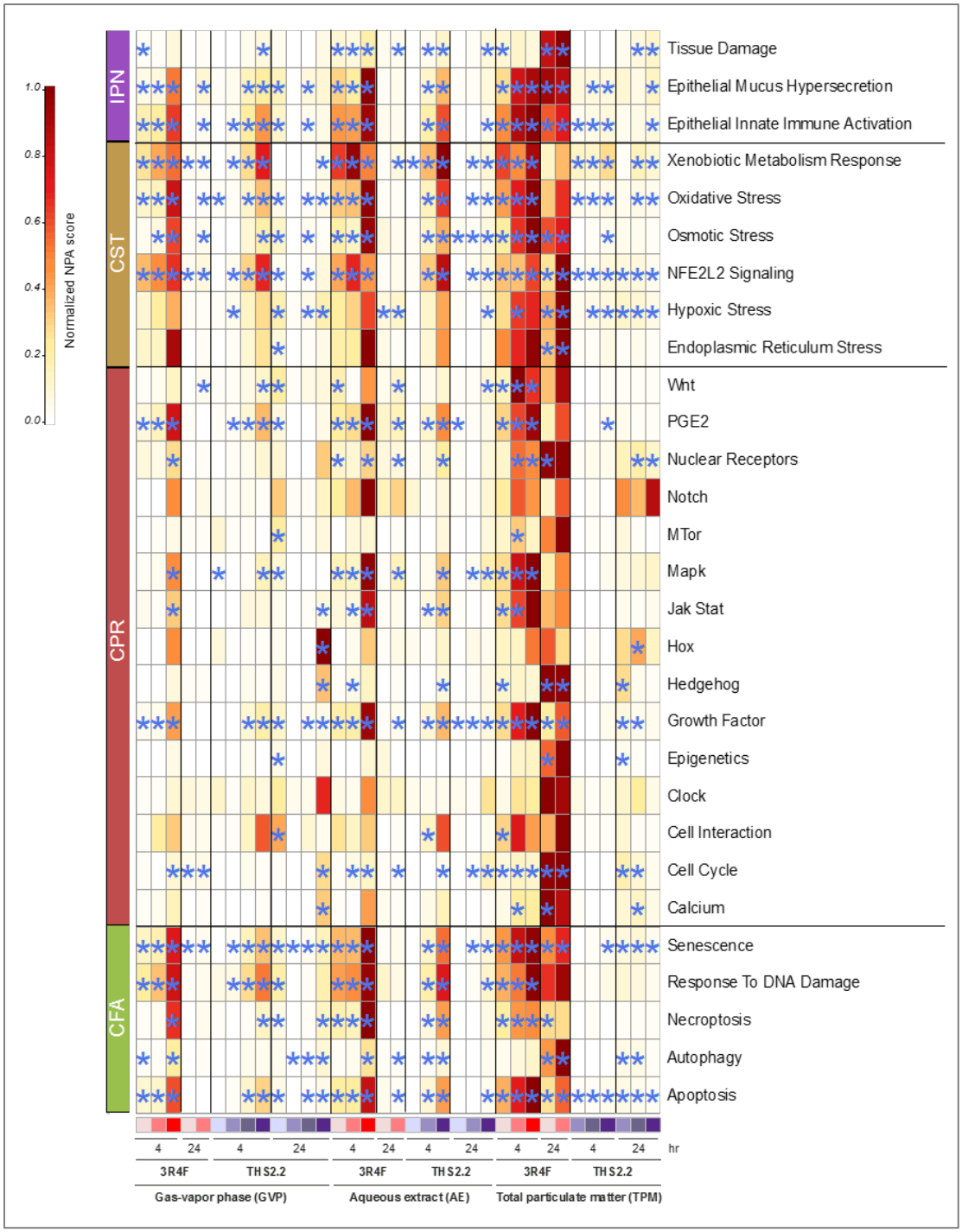


Figure 8. Network perturbations in normal human bronchial epithelial cells exposed to 3R4F cigarette smoke or THS 2.2 aerosol fractions.

Heatmap of Network Perturbation Amplitude scores summarizing subnetworks which were significantly perturbed with at least one treatment. A network is considered as perturbed if, in addition to the significance of the NPA score with respect to the experimental variation, the two companion statistics (O and K), derived to inform on the specificity of the NPA score with respect to the biology described in the network, are significant. Significantly perturbed networks are indicated by * (*i.e.*, O and K statistics *p*-values <0.05 and significant with respect to the experimental variation). CFA: Cell Fate; CPR: Cell Proliferation; CST: Cell Stress; IPN: Inflammatory Process Network.

Taken together, these results showed that fractions of 3R4F CS had a much higher potential to induce cytotoxicity, as well as oxidative and genotoxic stresses, in NHBECs compared with fractions derived from THS2.2 aerosol. 3R4F CS-derived TPM exerted the highest biological impact on primary human airway epithelial cells, while 3R4F GVP and CSE had lower biological impacts. While this tendency was also observed with the different THS2.2 aerosol-derived fractions, the overall impacts these fractions elicited on NHBECs were markedly lower than those caused by the 3R4F fractions (Gonzalez-Suarez et al, 2016).

LINK: 1673_Fraction Screening_SR

4.2.1.3 Oral Organotypic Study

To understand and compare the biological impacts of THS aerosol and 3R4F CS exposures in physiologically relevant systems representative of the human upper airway, human organotypic EpiOral™ tissue cultures (MatTek Corp., Ashland, MA, USA) were exposed for 28 minutes to air; to 15% or 24% (v/v in air) 3R4F mainstream smoke, equivalent to a target concentration of 0.32 or 0.54 μg/L nicotine, respectively; or to 25%, 34% or 69% (v/v in air) aerosol from THS, corresponding to target nicotine concentrations of 0.31, 0.46 or 1.09 μg/L, respectively. Cytotoxicity and SRPs were assessed at 4, 24, 48 and 72 hours following exposure. Several inflammatory mediators released into the culture supernatants were quantified at 24, 48 and 72 hours and tissue integrity evaluated at 48 and 72 hours post-exposure.

Exposure of EpiOral™ cultures to 3R4F CS resulted in tissue structural injury, as evidenced by keratinization and desquamation, and this was most prominent at the higher concentration and later time point. In contrast, the response in THS2.2 aerosol-exposed cultures was strongly attenuated. The cytotoxicity assay gave comparable results. Moreover, cultures exposed to 3R4F CS secreted higher levels of inflammatory mediators than did those exposed to air. Far fewer and less pronounced changes in levels of these mediators were observed in oral tissues exposed to THS2.2 aerosol at comparable or even higher nicotine levels.

At the 72-hour post-exposure time point, 3R4F CS exposure at the lowest dose had the highest impact on the cultures (RBIF = 100%; REF). Shorter post-exposure times also elicited a high biological impact, which initially declined during the post-exposure period, but rose again at 72 hours post-exposure. Overall, lower BIF values were observed for all THS2.2 concentrations at the different post-exposure time points, compared with the corresponding 3R4F exposure groups (Figure 9).

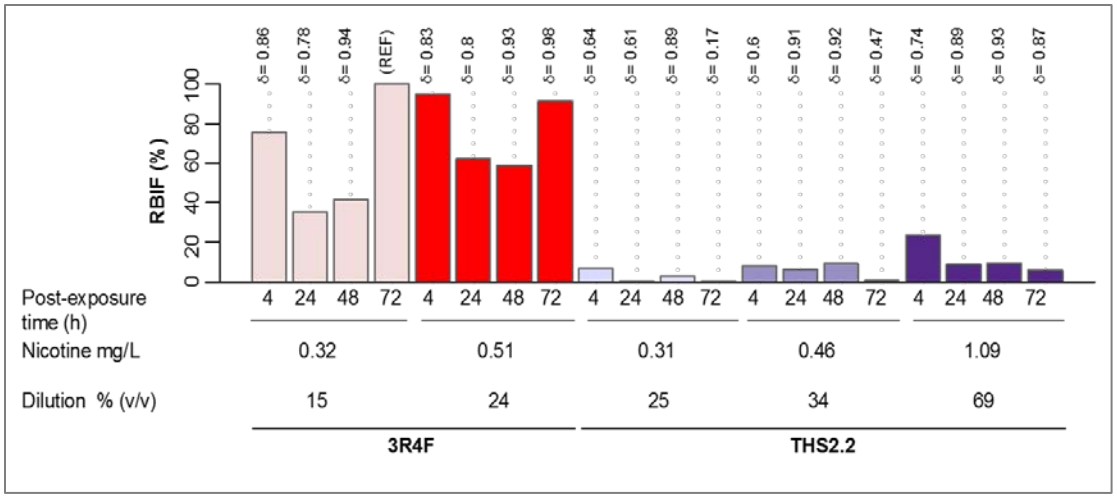


Figure 9. Network model-based analysis of the biological impact factor (BIF) in EpiOral™ cultures exposed to 3R4F cigarette smoke or THS2.2 aerosol, compared with air controls.

The bar plot depicts BIF values relative to the maximum response (REF, RBIF = 100%). The δ values (−1 to 1) indicate how similar the underlying network perturbations are with respect to the REF. Scores were computed using transcriptomics profiling data from EpiOral™ cultures that were exposed to air, 3R4F cigarette smoke (red bars) or THS2.2 aerosol (purple bars) for 28 minutes and collected for analysis at 4, 24, 48 or 72 hours post-exposure.

Examining the affected networks contributing to the observed biological impact of exposure to 3R4F CS indicated that the majority of networks were perturbed. Following the trend of the BIF pattern, the impact of 3R4F CS exposure, independent of concentration, decreased at 24 and 48 hours post-exposure and increased again at the 72-hour time point. Exposure of EpiOral™ tissues to 3R4F CS affected all CFA subnetworks describing the biology of senescence, necroptosis and apoptosis, but also affected some of the IPN subnetworks. The CPR network family was less affected, with fewer significantly altered sub-networks. Of note, with the exception of the Endoplasmic Reticulum Stress subnetwork, CS exposure also affected all CST subnetworks including Oxidative Stress and NFE2L2 Signaling (Figure 10). In contrast, THS2.2 aerosol exposure at comparable nicotine concentrations did not result in substantial perturbations of the same networks. In general, the observed perturbations following exposure to THS2.2 aerosol were of a markedly lower amplitude (NPA score) and EpiOral™ cultures exhibited broad network perturbations only at the highest nicotine concentration at all post-exposure time points. Nevertheless, the extent of those perturbations was lower compared with the impact of the highest concentration of 3R4F CS at corresponding post-exposure time points (Figure 10).

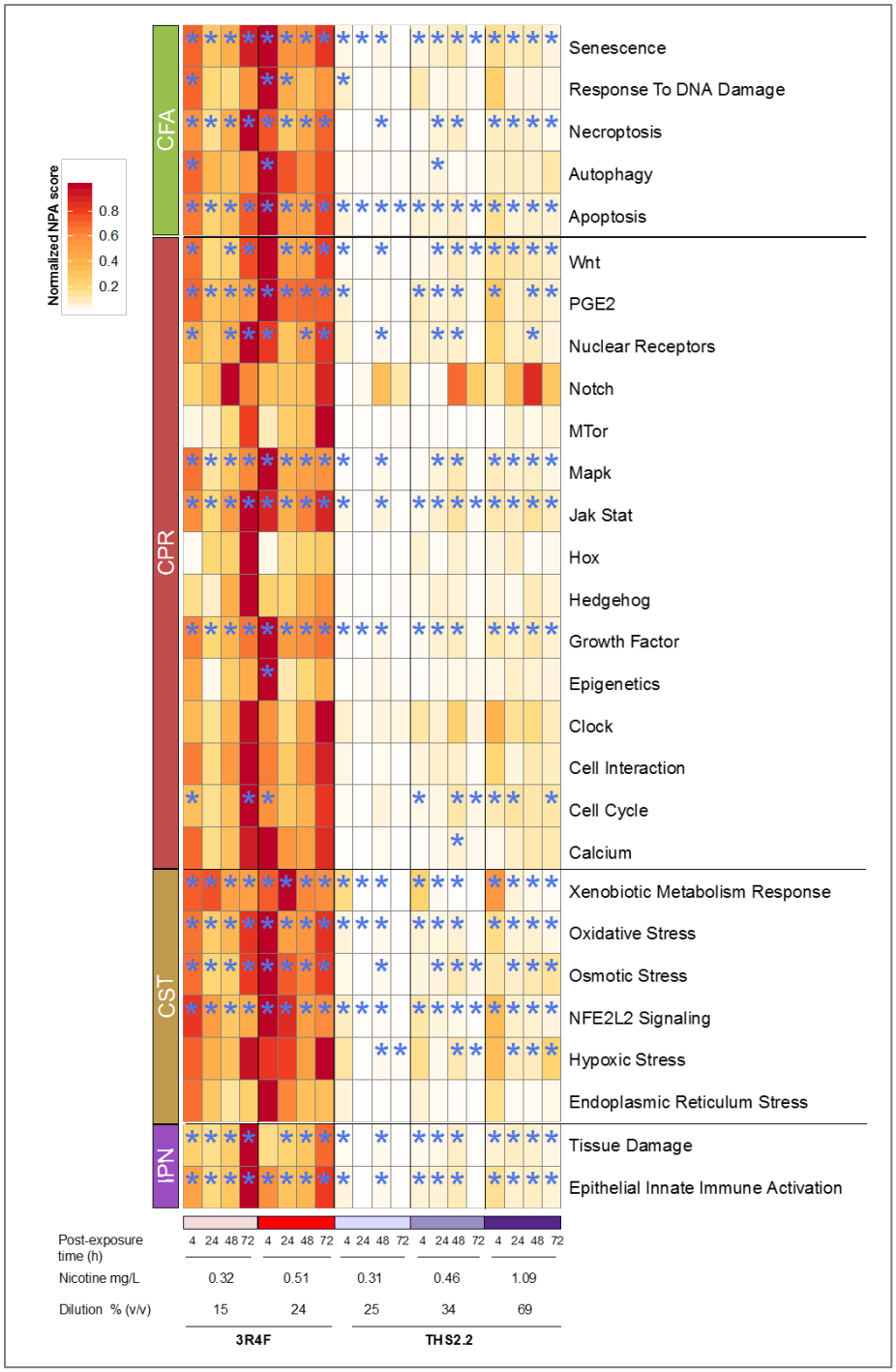


Figure 10. Network perturbations in EpiOral™ cultures exposed to 3R4F cigarette smoke or THS2.2 aerosol, compared with air controls.

Heatmap of Network Perturbation Amplitude scores summarizing subnetworks which were significantly perturbed with at least one treatment. A network is considered as perturbed if, in addition to the significance of the NPA score with respect to the experimental variation, the two companion statistics (O and K), derived to inform on the specificity of the NPA score with respect to the biology described in the network, are significant. Significantly perturbed networks are indicated by * (*i.e.*, O and K statistics *p*-values <0.05 and significant with respect to the experimental variation). CFA: Cell Fate; CPR: Cell Proliferation; CST: Cell Stress; IPN: Inflammatory Process Network.

Oxidative Stress and NFE2L2 Signaling NPA scores for EpiOral™ tissues exposed to 3R4F CS matched the RBIF values, with strong perturbations noted at 4 hours post-exposure which subsequently declined before increasing again at 72 hours post-exposure. In contrast, THS2.2 aerosol exposure elicited a markedly lower impact on these subnetworks, with NPA scores never reaching those obtained after 3R4F CS exposure (Figure 11). The predicted mechanisms underlying the network perturbations elicited by 3R4F exposure were the same as those predicted for THS2.2 aerosol exposure. However, their contributions to the NPA score were significantly greater. Similarly, mechanisms predicted to drive perturbations of the NFE2L2 Signaling subnetwork were not different with 3R4F CS and THS2.2 aerosol exposures. However, perturbation amplitudes were much lower in EpiOral™ cultures exposed to THS2.2 aerosol than in those exposed to 3R4F CS.

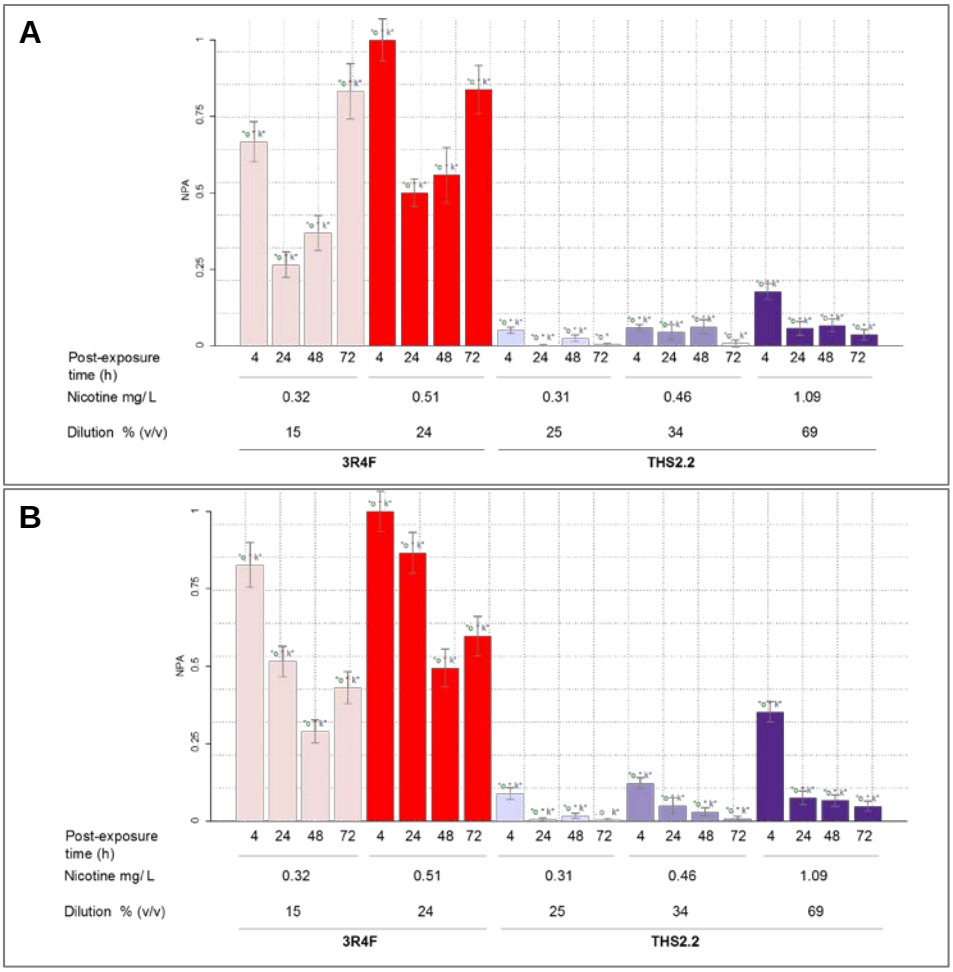


Figure 11. Relative Network Perturbation Amplitude (NPA) scores of specific CST subnetworks in EpiOral™ cultures exposed to 3R4F cigarette smoke or THS2.2 aerosol, compared with air controls.

The relative NPA scores for the Oxidative Stress (A) and NFE2L2 Signaling (B) subnetwork models are shown with confidence intervals accounting for experimental variation. The percentages indicate the relative NPA scores for the subnetworks compared with the reference (treatment comparison showing the highest perturbation). In addition, companion statistics derived to inform on the specificity of the NPA score, with respect to the biology described in the respective subnetwork models, are shown as *O and K*, respectively, if their *p*-values were below the significance level. Symbol legend:*, O and K statistic *p*-values <0.05; .O and K, *p*-values between 0.05 and 0.1.

There were a number of significant alterations in the expression of genes associated with oxidative stress responses. In 3R4F CS-exposed EpiOral™ cultures, expression levels of heme oxygenase 1 (*HMOX1*), glutamate-cysteine ligase regulatory subunit (*GCLM*), glutamate-cysteine ligase catalytic subunit (*GCLC*), thioredoxin reductase 1 (*TXNRD1*), NAD(P)H quinone dehydrogenase 1 (*NQO1*) and glutathione peroxidase 2 (*GPX2*), among others, were substantially increased, while the expression of genes encoding antioxidant enzymes such as catalase (*CAT*), superoxide dismutase 1 (*SOD1*) and xanthine dehydrogenase (*XDH*) was downregulated. For the majority of these upregulated genes, similar responses were seen only in EpiOral™ tissues exposed to THS2.2 aerosol at the highest nicotine concentration. Lower doses of THS2.2 aerosol did

not cause extensive changes in the expression of genes linked to oxidative stress responses in this 3D organotypic model of the oral mucosa (Figure 12).

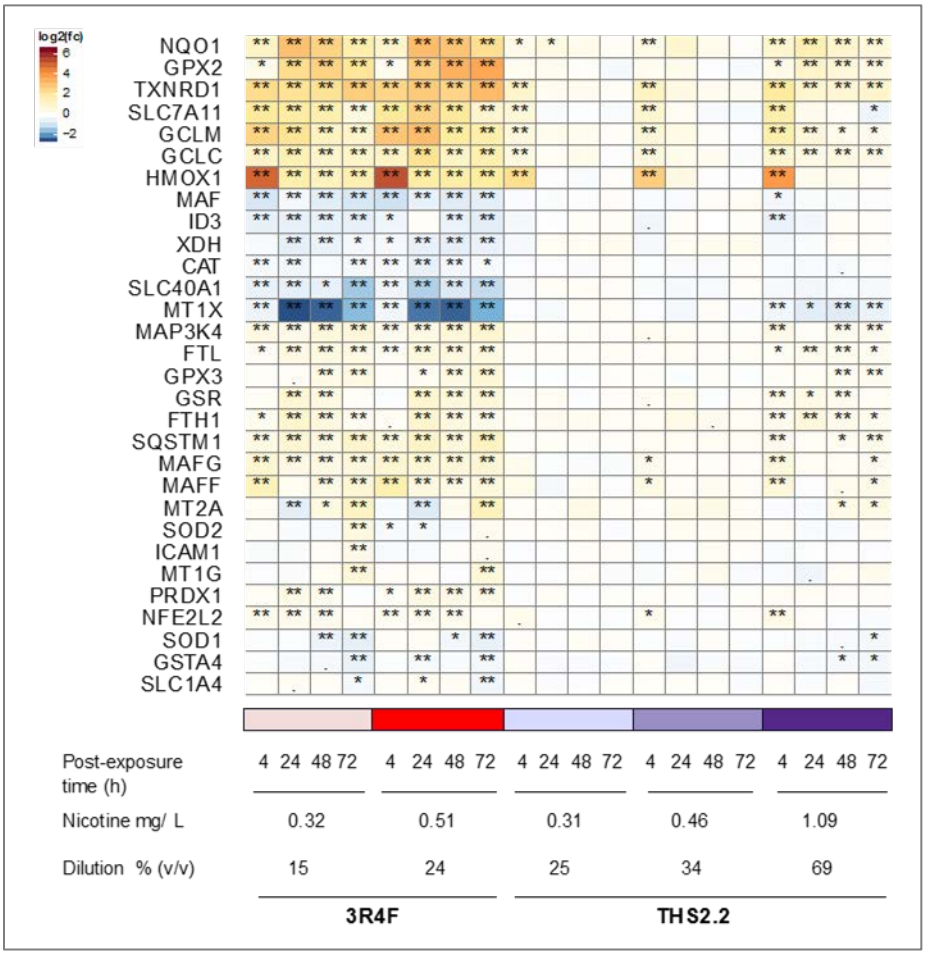


Figure 12. Altered expression levels of genes linked to the oxidative stress response in EpiOral™ cultures exposed to 3R4F cigarette smoke or THS2.2 aerosol, compared with air controls.

The heatmap depicts changes in gene expression for oxidative stress-related genes (gene symbols listed on the left), relative to expression in corresponding air-exposed controls. These changes are expressed as $\log_2$(fold change (fc)). Up- and downregulation of gene expression are represented by orange and blue shades, respectively, with darker colors indicating greater absolute fold changes. Statistically significant fold changes are highlighted by ** (adjusted $p < 0.05$) and * (adjusted $p < 0.1$).

In summary, these results showed that exposure of human oral epithelial organotypic tissues to 3R4F CS led to time- and dose-dependent cytotoxicity, tissue damage and oxidative stress. In contrast, effects of exposure to matching concentrations of THS2.2 aerosol were only transient, eliciting far less extensive stress responses that rapidly subsided (Zanetti et al, 2016).

LINK: 1743_Organotypic_Buccal_SR

4.2.1.4 Nasal Organotypic Study

In addition to studies in oral organotypic cultures, the impacts of exposure to 3R4F CS or THS2.2 aerosol were further studied in 3D organotypic nasal models. Human nasal MucilAir™ organotypic tissue cultures (Epithelix Sarl, Geneva, Switzerland) were exposed for 28 minutes to air; to 8% or 15% (v/v in air) 3R4F mainstream smoke, equivalent to target concentrations of 0.15 or 0.25 µg/L nicotine, respectively; or to 15%, 24% or 31% (v/v in air) aerosol from THS2.2, corresponding to target nicotine concentrations of 0.15, 0.27 or 0.44 µg/L, respectively. Cytotoxicity and tissue integrity, as well as SRPs, were assessed at 4, 24, 48 and 72 hours following exposure. Inflammatory mediators released into the culture supernatants were measured at 24, 48 and 72 hours post-exposure.

While exposure to 8% 3R4F CS induced little to no cytotoxicity at any time point, exposure to 15% 3R4F CS elicited substantial cytotoxicity and tissue damage at 24, 48 and 72 hours post-exposure. However, exposure to various concentrations of THS2.2 aerosol did not cause any cytotoxicity. Histological examination confirmed that exposure to 3R4F CS resulted in more tissue damage than did exposure to THS2.2 aerosol, with cultures exhibiting less damage at 48 hours than at 72 hours post-exposure. Since exposure to the high concentration of 3R4F CS was detrimental to the nasal organotypic cultures and led to tissue loss, detachment from the membrane and development of regions of a squamous phenotype at 48 and 72 hours post-exposure, these tissues were excluded from further systems biology analysis.

Using a threshold-free computational network approach, the strongest biological impact was detected 4 hours post-exposure in nasal MucilAir™ cultures exposed to 8% 3R4F CS (RBIF = 100%; REF) and this impact decreased over the 72-hour post-exposure period. In contrast, the impact on the nasal cultures after 4 hours exposure to THS2.2 aerosol at matched nicotine concentrations was only a fraction of that seen following exposure to 3R4F CS and the effects diminished rapidly with further post-exposure. When nasal tissues were exposed to higher concentrations of THS2.2 aerosol, the biological impact observed at 4 hours post-exposure was somewhat more extensive than at the lower dose, reaching RBIF values of 28% and 41% at THS2.2 aerosol dilutions of 24% and 31%, respectively. Again, the RBIF values decreased rapidly and markedly at prolonged post-exposure periods (Figure 13).

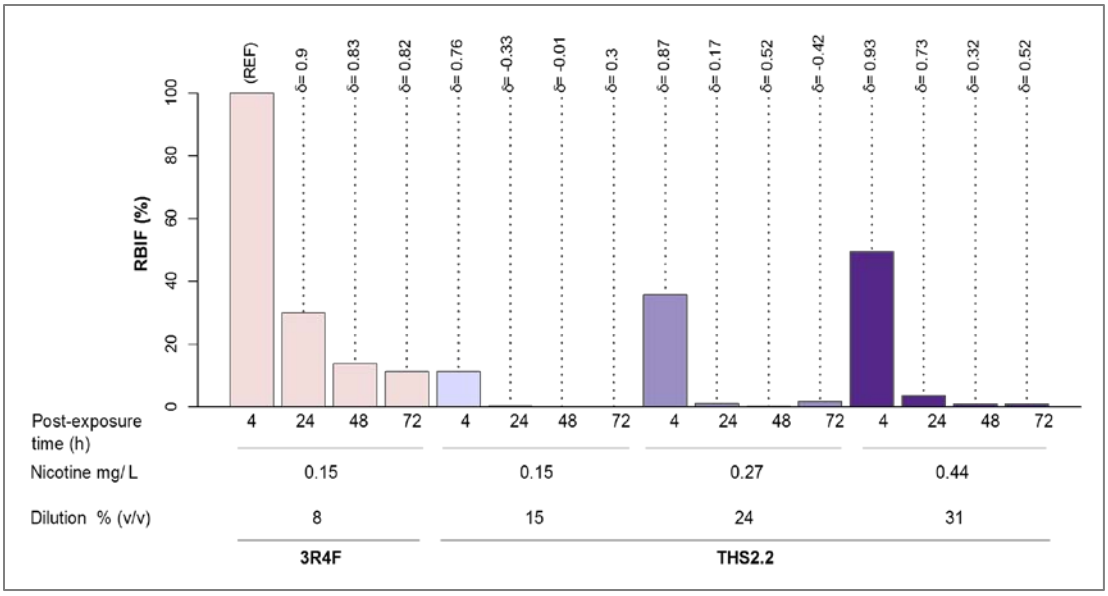


Figure 13. Network model-based analysis of the biological impact factor (BIF) in nasal MucilAir™ cultures exposed to 3R4F cigarette smoke or THS2.2 aerosol, compared with air controls.

The bar plot depicts BIF values relative to the maximum response (REF, RBIF = 100%). The δ values (−1 to 1) indicate how similar the underlying network perturbations are with respect to the REF. Scores were computed using transcriptomics profiling data from nasal MucilAir™ cultures that were exposed to air, 3R4F cigarette smoke (red bars) or THS2.2 aerosol (purple bars) for 28 minutes and collected for analysis at 4, 24, 48 or 72 hours post-exposure.

Exposure to 3R4F CS caused significant perturbations predominantly in networks capturing the biology of senescence, apoptosis, DNA damage, MAPK and Jak/Stat-mediated cell proliferation, inflammatory processes and those reflecting cell stress responses. Among the latter, the Xenobiotic Metabolism Response, Oxidative Stress and NFE2L2 Signaling subnetworks were affected at all post-exposure time points, exhibiting the highest NPA scores at 4 hours post-exposure and decreasing as the post-exposure time increased. There was also an early significant osmotic stress response, while the Hypoxic Stress subnetwork was significantly perturbed only at 72 hours post-exposure (Figure 14). Of note, at matching nicotine concentrations, exposure of nasal MucilAir™ tissues to THS2.2 aerosol affected far fewer networks and significant perturbations in the IPN and the CFA network were restricted to the early post-exposure time point. This was different than for the CST network; low doses of THS2.2 aerosol impacted CST network processes related to xenobiotic metabolism, osmotic and and oxidative stress at 4 and 24 hours post-exposure, while hypoxic stress was affected later. At the highest THS2.2 aerosol concentrations, network perturbations similar to those caused by exposure to 3R4F CS were observed and these persisted throughout the post-exposure period. However, with very few exceptions, the extent of these pertubations was noticeably less than that of the network perturbations caused by 3RF CS exposure (Figure 14).

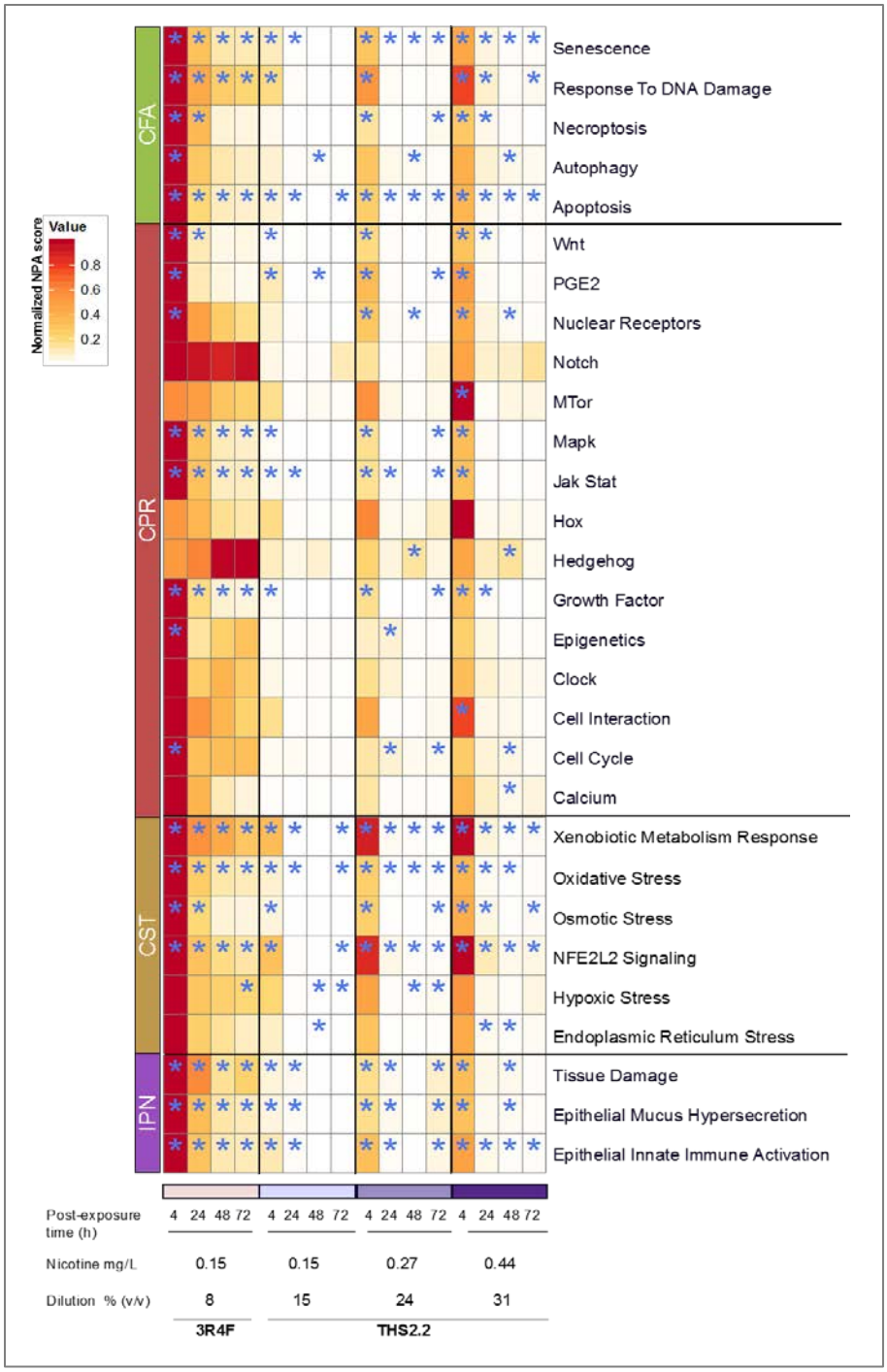


Figure 14. Network perturbations in nasal MucilAir™ cultures exposed to 3R4F cigarette smoke or THS2.2 aerosol, compared with air controls.

Heatmap of Network Perturbation Amplitude scores summarizing subnetworks which were significantly perturbed by at least one treatment. A network is considered as perturbed if, in addition to the significance of the NPA score with respect to the experimental variation, the two companion statistics (O and K), derived to inform on the specificity of the NPA score with respect to the biology described in the network, are significant. Significantly perturbed networks are indicated by * (*i.e.*, O and K statistics *p*-values <0.05 and significant with respect to the experimental variation). CFA: Cell Fate; CPR: Cell Proliferation; CST: Cell Stress; IPN: Inflammatory Process Network.

There were no major differences between 3R4F CS and THS2.2 aerosol exposures in the underlying mechanisms predicted to be the drivers of the observed stress responses. Closer examination of changes in expression of genes linked to oxidative stress was consistent with this finding. Exposure to THS2.2 aerosol affected expression of the same oxidative stress genes as did exposure to 3R4F CSE. Similar to changes previously noted in exposed 3D oral organotypic cultures, expression of the antioxidant enzyme-encoding genes *HMOX1*, *GCLC*, *GCLM*, *NQO1*, *GPX2* and *TXNRD1* was also significantly increased in this study. However, the majority of gene expression changes in THS2.2 aerosol-exposed nasal MucilAir™ tissues did not persist over the post-exposure period, while transcriptional levels affected by 3R4F CS exposure were persistently altered (Figure 15).

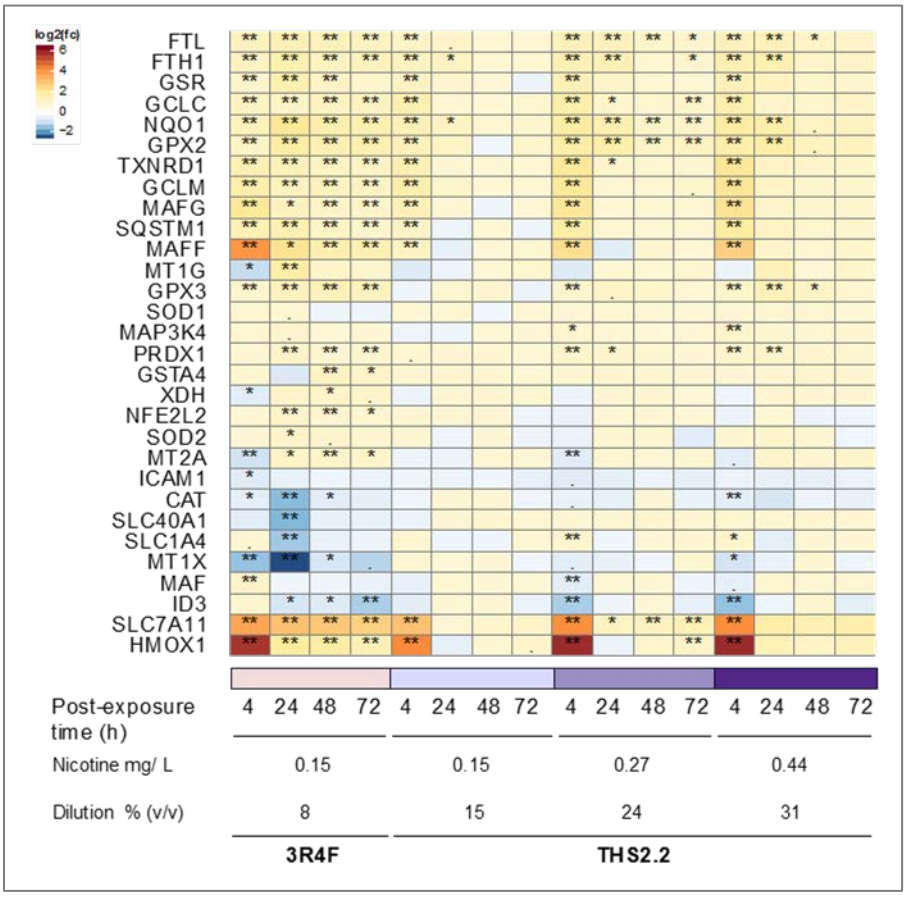


Figure 15. Altered expression levels of genes linked to the oxidative stress response in nasal MucilAir™ cultures following exposure to 3R4F cigarette smoke or THS2.2 aerosol, compared with air controls.

The heatmap depicts changes in gene expression for oxidative stress-related genes (gene symbols listed on the left) relative to those in corresponding air-exposed controls expressed as $\log_2$(fold change (fc)). Up- and downregulation of gene expression levels are represented by orange and blue shades, respectively, with darker colors indicating greater absolute fold changes. Statistically significant fold changes are highlighted by ** (adjusted $p < 0.05$) and * (adjusted $p < 0.1$).

In conclusion, these data demonstrated that exposure of human organotypic nasal epithelial tissues to whole smoke generated from 3R4F reference cigarettes resulted in time- and dose-dependent cytotoxicity, tissue damage and increased secretion of inflammatory mediators. In contrast, exposure of the cultures to the corresponding concentrations of THS2.2 aerosol (matched by nicotine levels) had effects more comparable to those of fresh air exposures, with negligible cytotoxicity or tissue damage and markedly reduced oxidative stress responses (Iskandar et al, 2016).

LINK: 1722_Organotypic_Nasal_SR

4.2.1.5 Bronchial Organotypic Study

Similar to studies in 3D organotypic oral and nasal tissues, 3D organotypic bronchial tissues (bronchial MucilAir™ (Epithelix Sarl) or bronchial EpiAirway™ (MatTek Corporation) were exposed to air; to 8% or 15% (v/v in air) 3R4F CS; or to 15%, 24% or 31% (v/v in air) THS2.2 aerosol. These cultures were then examined for exposure-related effects at 4, 24, 48 and 72 hours post-exposure.

At the earliest time point following exposure, no cytotoxicity was noted, independent of the type of exposure. However, cultures exposed to 3R4F CS showed more cytotoxicity from 24 hours post-exposure onwards, with significant damage elicited by the higher CS dose. However, THS2.2 aerosol exposure did not cause cytotoxicity in bronchial MucilAir™ tissues, independent of dose and post-exposure time point. These results were confirmed by histological evaluation, highlighting that the morphology of THS2.2 aerosol-exposed cultures resembled that of those exposed to only air. Since exposure to the high 3R4F CS concentration severely damaged the bronchial organotypic cultures, these samples were excluded from further systems biology analysis.

Network model-based analysis showed that 3R4F CS exposure had the strongest impact on bronchial MucilAir™ cultures at 4 hours post-exposure (RBIF = 100%) and this impact declined over the post-exposure period. At comparable nicotine concentrations, the impact of THS2.2 aerosol exposure on the tissues was always lower than that of 3R4F CS exposure, independent of the post-exposure time point. The impact of THS2.2 aerosol exposure decreased sharply with increasing post-exposure duration. In addition, there was a dose-dependent effect of THS2.2 aerosol exposure on the RBIF at 4 hours post-exposure (Figure 16).

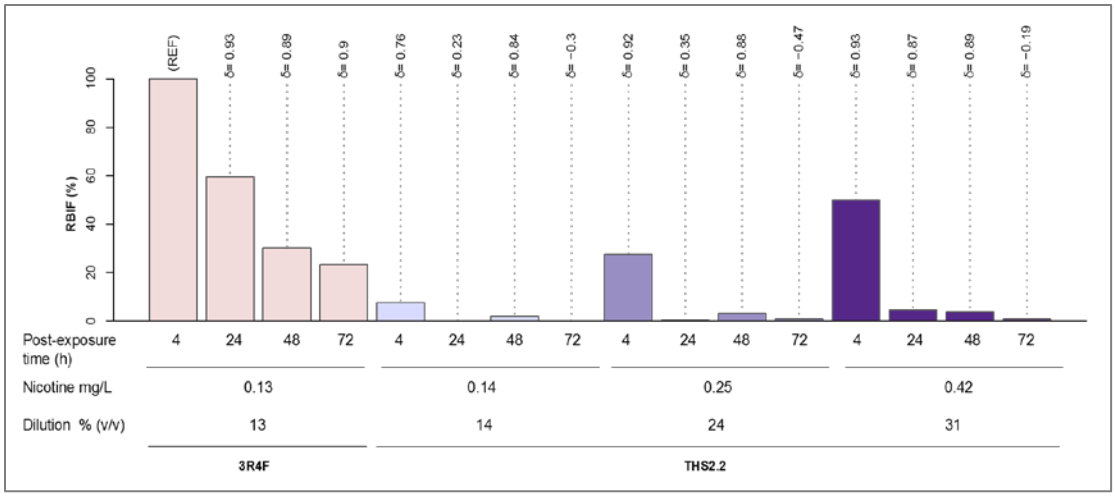


Figure 16. Network model-based analysis of the biological impact factor (BIF) in bronchial MucilAir™ cultures exposed to 3R4F cigarette smoke or THS2.2 aerosol, compared with air controls.

The bar plot depicts BIF values relative to the maximum response (REF, RBIF = 100%). The δ values (−1 to 1) indicate how similar the underlying network perturbations are with respect to the REF. Scores were computed using transcriptomics profiling data from bronchial MucilAir™ cultures that were exposed to air, 3R4F cigarette smoke (red bars) or THS2.2 aerosol (purple bars) for 28 minutes and collected for analysis at 4, 24, 48 or 72 hours post-exposure.

Network analysis of the transcriptomic changes induced by exposure to 3R4F CS indicated that significant perturbations occurred at all post-exposure time points in networks incorporating senescence, necroptosis and apoptosis biology, mechanisms of cell proliferation associated with growth factor, Wnt, nuclear receptor, MAPK and Jak-Stat signaling, inflammatory and other cellular stress responses. With very few exceptions, THS2.2 aerosol exposure affected the same networks, but perturbations were typically of lower amplitude and often not sustained over the entire post-exposure period. For both, 3R4F CS and THS2.2 aerosol exposures, network pertubations initially peaked at 4 hours post-exposure, gradually decreasing until the 72-hour time point (Figure 17).

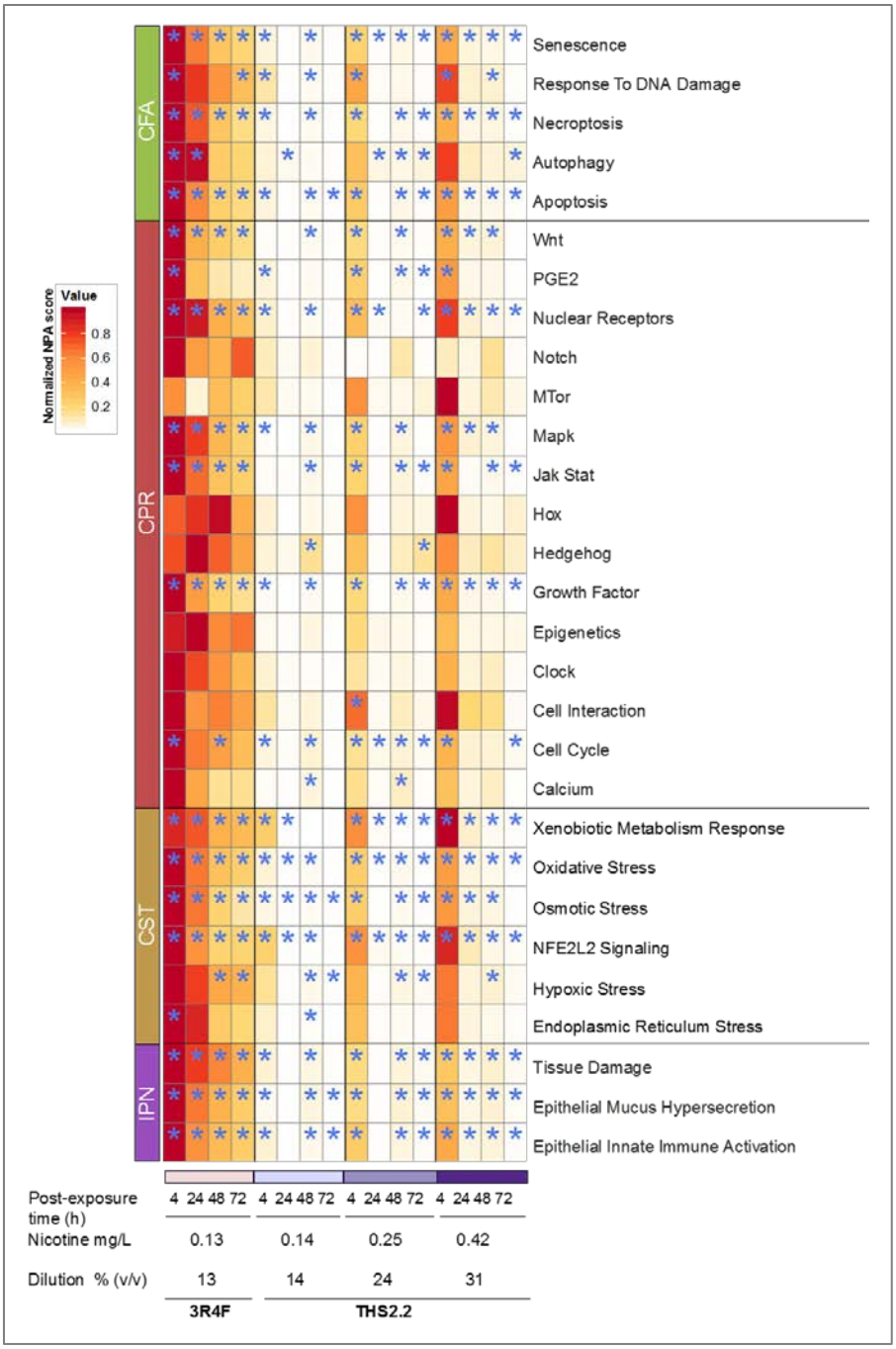


Figure 17. Network perturbations in bronchial MucilAir™ cultures exposed to 3R4F cigarette smoke or THS2.2 aerosol, compared with air controls.

Heatmap of Network Perturbation Amplitude scores summarizing subnetworks which were significantly perturbed by at least one treatment. A network is considered as perturbed if, in addition to the significance of the NPA score with respect to the experimental variation, the two companion statistics (O and K), derived to inform on the specificity of the NPA score with respect to the biology described in the network, are significant. Significantly perturbed networks are indicated by * (*i.e.*, O and K statistics *p*-values <0.05 and significant with respect to the experimental variation). CFA: Cell Fate; CPR: Cell Proliferation; CST: Cell Stress; IPN: Inflammatory Process Network.

Among the CST networks, the Oxidative Stress and NFE2L2 Signaling subnetworks were strongly affected by the exposures and throughout the post-exposure period, with no apparent differences in the underlying biology between effects of 3R4F CS and THS2.2 aerosol exposures. In concordance with previous observations in the oral and nasal 3D culture systems, the majority of perturbations caused by THS2.2 aerosol exposure were of smaller amplitude.

Increased expression of many genes linked to oxidative stress responses (*SLC7A11*, *MAFF*, *HMOX1*, *NQO1*, *GSR*, *FTH1*, *GCLC*, *GPX2*, *TXNRD1*, *GCLM*, *MAFG*, *SQSTM1*, *SOD2* and *FTL*) was seen in bronchial MucilAir™ cultures exposed to 3R4F CS at all post-exposure time points. The expression of the majority of these genes was also increased in THS2.2 aerosol-exposed tissues. However, THS2.2 aerosol exposure only transiently affected the levels of these genes, in most cases not leading to sustained deregulation after 4 hours post-exposure (Figure 18).

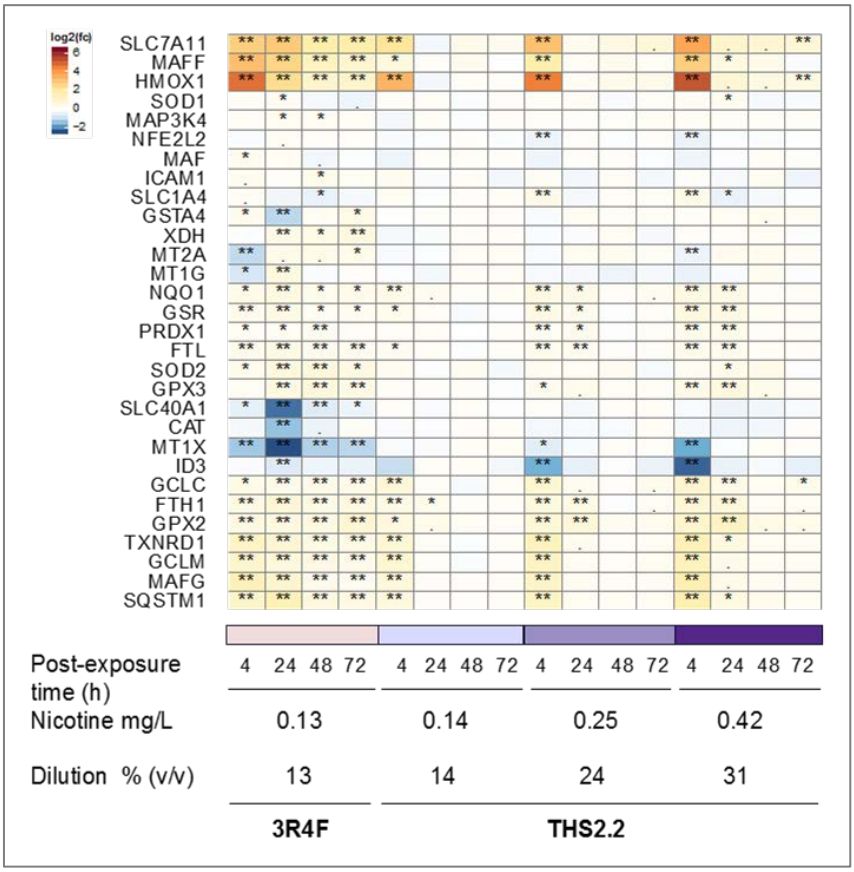


Figure 18. Altered expression levels of genes linked to the oxidative stress response in bronchial organotypic cultures exposed to 3R4F cigarette smoke or THS2.2 aerosol, compared with air controls.

The heatmap depicts changes in gene expression for oxidative stress-related genes (gene symbols listed on the left) relative to those in corresponding air exposed controls, expressed as log2(fold change (fc)). Up- and downregulation of gene expression levels are represented by orange and blue shades, respectively, with darker colors indicating greater absolute fold changes. Statistically significant fold changes are highlighted by ** (adjusted $p < 0.05$) and * (adjusted $p < 0.1$).

Taken together, these results demonstrated that exposure to THS2.2 aerosol, in contrast to 3R4F CS exposure, caused little to no cytotoxicity, tissue damage and oxidative stress in 3D bronchial organotypic tissues *in vitro.*

LINK: 1709_Organotypic_Bronch_SR; 1709_Organotypic_Bronch_Pub

4.2.2 Results from *In Vivo* Studies

4.2.2.1 Rat OECD Studies

Two independent 90-day inhalation studies were conducted with THS2.2 (Rat-THS-TG413) and THS2.2 Menthol (Rat-THSM-TG413) according to OECD guideline TG413, comparing toxicity of CS from 3R4F to that of aerosols from THS and its mentholated version. For this purpose, male and female Sprague-Dawley rats were nose-only exposed to filtered fresh air (sham), 3 target nicotine concentrations of 3R4F CS (8, 15 or 23 µg/L) or aerosol from THS/THS menthol (15, 23 or 50 µg/L) for 6 h/day, 5 days/week for 13 weeks. Additional groups of animals were included for exposure to THS aerosol at the highest nicotine concentration for 13 weeks, followed by a 42-day recovery period, to investigate the reversibility or persistence of test substance-related effects. In addition to the OECD endpoints, pulmonary inflammation was assessed by BALF cell counts and quantification of BALF inflammatory mediators at the end of exposure (90 days) and following the post-exposure period (90+42 days). Furthermore, potential molecular changes as a consequence of exposure were evaluated by employing transcriptomics, proteomics and lipidomics analyses.

The results of the OECD TG413 toxicological assessments in rats have been described in another section of this dossier (link to 6.1.2 Preclinical Safety). This part of the document will focus on the results of the oxidative stress-related endpoints that were obtained from the additional integrative systems toxicological evaluation of samples from the OECD inhalation studies (the “OECD Plus” part).

4.2.2.1.1 Rat OECD THS2.2 Study

Evidence for stress-related changes in the airway epithelium were noted upon histological evaluation of the respiratory tract organs—nose, larynx, trachea and lungs—of the exposed rats. For example, exposure to 3R4F CS over a 90-day period resulted in the development of moderate to marked reserve cell hyperplasia, marked squamous metaplasia with and without cornification, particularly in animals exposed to higher concentrations, and loss of goblet cells in the rat respiratory nasal epithelium. In addition, slight infiltration by neutrophilic granulocytes was observed. Similarly, reserve cell hyperplasia and squamous metaplasia were also observed in rats exposed to THS2.2 aerosols. However, lesions in these animals showed remarkably less cornification and loss of goblet cells than those seen in the 3R4F groups. There were no differences in incidence and severity of these nasal lesions between the two genders, independent of exposure. Moreover, with the exception of squamous metaplasia, severity of lesions decreased following a 42-day post-exposure period, suggesting that the observed changes represented a local adaptation to irritant inhalation.

Histopathological evaluation at nose level 2 also identified reserve cell hyperplasia and squamous metaplasia in the nasal respiratory and olfactory epithelium of animals exposed to medium and high doses of 3R4F CS which were, at least in part, fully reversible following post-exposure. In contrast, exposure to THS2.2 aerosol led to limited reserve cell hyperplasia in some, but not all, animals and did not result in the development of squamous metaplasia in either the respiratory or olfactory epithelium of the exposed rats.

Examination of the laryngeal tissues showed marked squamous metaplasia with extensive cornification in male and female rats exposed to 3R4F CS and less severe metaplastic lesions that were not cornified following a 42-day post-exposure period in animals from the 3R4F high-dose group. Squamous metaplasia was also seen at the base of the epiglottis and floor of the larynx in rats of both genders exposed to THS2.2 aerosol. In contrast to findings in 3R4F CS-exposed rats, these lesions were less severe and exhibited a lower extent of cornification. In addition, 42 days after the last exposure those lesions had noticeably regressed.

There were no marked increases in goblet cells or squamous transdifferentiation at the tracheal bifurcation of rats exposed to either 3R4F CS or THS2.2 aerosol. However, exposure to 3R4F CS resulted in the development of goblet cell hyperplasia in bronchial epithelium, with a dose-dependent increase in severity of the lesion that was more pronounced in male than in female rats. In contrast, the bronchial epithelium of rats exposed to THS2.2 aerosol did not present with extensive goblet cell hyperplasia in either male or female rats. Of note, these lesions appeared to regress noticeably in animals that were permitted a post-exposure recovery.

Gene expression profiles of respiratory nasal epithelia from exposed rats of both genders were analyzed and demonstrated a clear concentration-dependent response with respect to the number of significant DEGs in 3R4F CS-exposed and, to a lesser extent, in THS2.2 aerosol-exposed animals. There was a clear difference in the magnitude of the changes in respiratory nasal epithelial samples between matching nicotine concentrations of 3R4F CS and THS2.2 aerosol exposures. After the 42-day recovery period, gene expression changes were much reduced in all groups, except in nasal epithelia from rats exposed to the medium and high 3R4F CS concentrations. Systems toxicological evaluation of the nasal epithelial transcriptome from 3R4F CS-exposed rats further highlighted extensive perturbations in nearly all networks, with significant perturbations becoming apparent at a dose equivalent to 15 μg/L nicotine. In contrast, not even the highest THS2.2 aerosol dose elicited as strong an impact on the networks of interest (Figure 19).

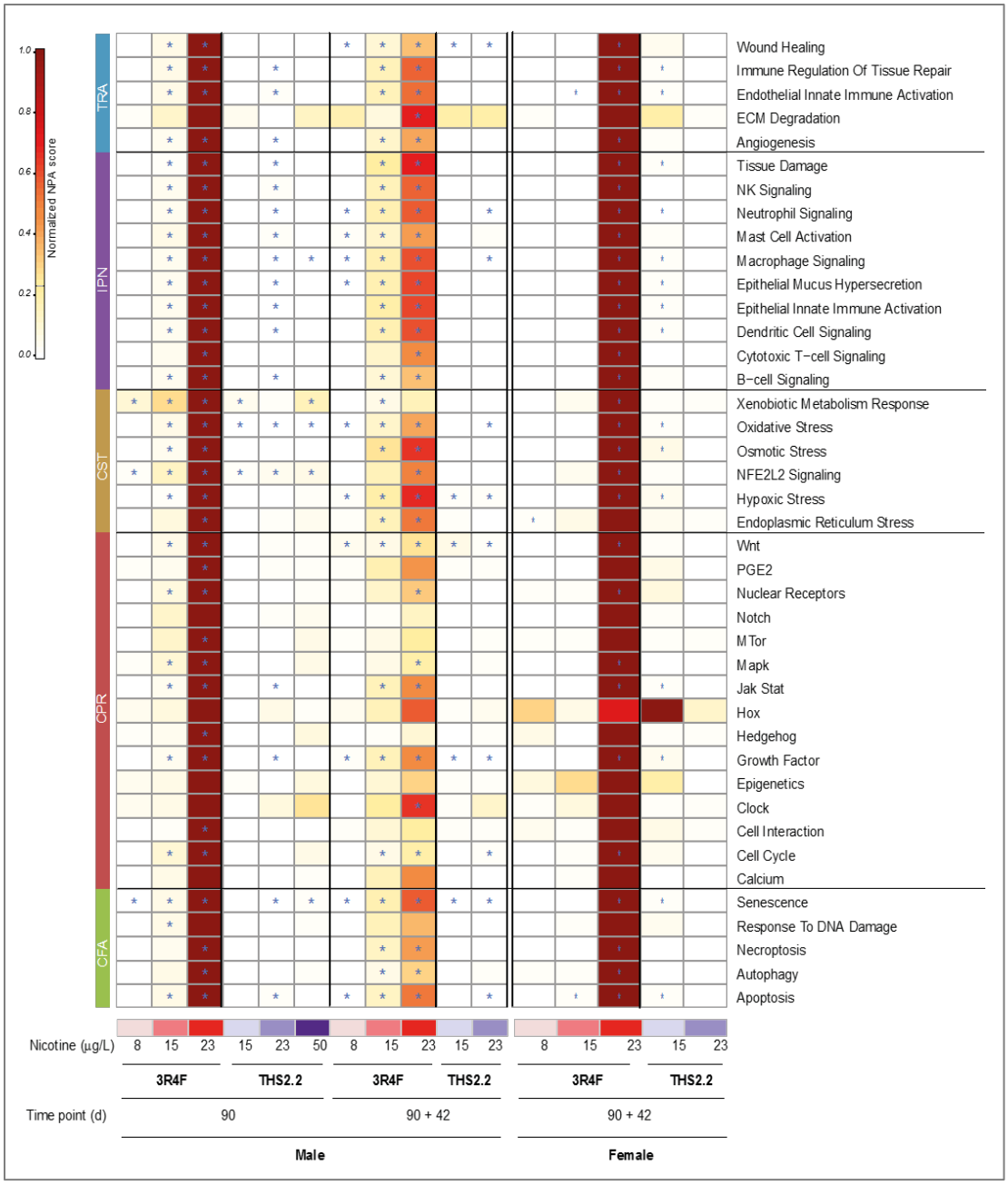


Figure 19. Network perturbations in rat nasal epithelial tissues following exposure to 3R4F cigarette smoke or THS2.2 aerosol, compared with air-exposed controls.

Heatmap of Network Perturbation Amplitude scores summarizing subnetworks which were significantly perturbed with at least one treatment. A network is considered as perturbed if, in addition to the significance of the NPA score with respect to the experimental variation, the two companion statistics (O and K), derived to inform on the specificity of the NPA score with respect to the biology described in the network, are significant. Significantly perturbed networks are indicated by * (i.e., O and K statistics *p*-values <0.05 and significant with respect to the experimental variation). CFA: Cell Fate; CPR: Cell Proliferation; CST: Cell Stress; IPN: Inflammatory Process Network; TRA: Tissue Repair and Angiogenesis.

Note: RNA extracted from nasal epithelia of only the female rats at 90+42 days passed quality check criteria for subsequent gene expression and network analyses.

The Xenobiotic Metabolism Response and NFE2L2 Signaling subnetworks were among the few significantly perturbed by exposure of male rats to 3R4F CS at the low nicotine concentration. Perturbations were noted in all CST subnetworks except for the Endoplasmic Reticulum Stress subnetwork on exposure to 3R4F CS corresponding to 15 μg/L nicotine. At the highest 3R4F CS dose, all stress-related networks were impacted and this appeared to be irreversible because most of these perturbations were still detectable after the post-exposure recovery period. This was in contrast to results obtained in nasal epithelia from male rats exposed to THS2.2 aerosol. In these animals, only the Xenobiotic Metabolism Response, Oxidative Stress and NFE2L2 Signaling subnetworks were affected and to a lesser extent than with 3R4F CS exposures. At the end of the post-exposure period, only the Oxidative Stress subnetwork remained significantly perturbed, and additional pertubations were noted in the Hypoxic Stress subnetwork (Figure 19).

Moreover, mechanistic analysis of transcriptomics data from nasal respiratory epithelia of exposed male rats indicated dose-dependent effects of both 3R4F CS and THS2.2 aerosol exposures on the Oxidative Stress and NFE2L2 Signaling subnetworks. The impact on the Oxidative Stress subnetwork was only partially reversible in 3R4F CS-exposed samples, even at the low dose, whereas the impact on the NFE2L2 Signaling subnetwork was significant only for the high 3R4F concentration. Similarly, minor perturbations in the Oxidative Stress subnetwork persisted in the nasal epithelium of animals exposed to THS2.2 aerosol corresponding to 23 μg/L nicotine. However, no continued perturbation was observed in nasal samples from THS2.2 aerosol-exposed animals at day 42 post-exposure (Figure 20).

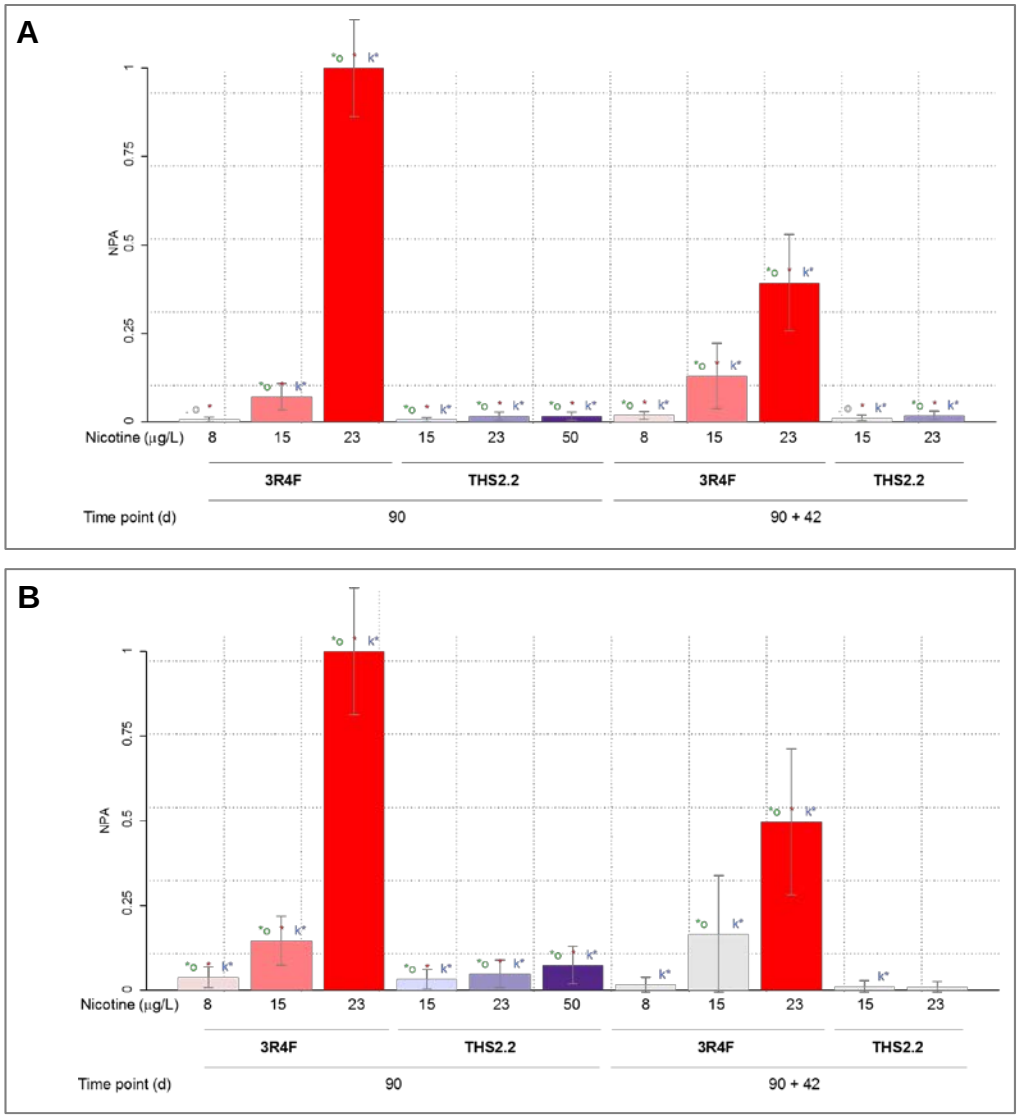


Figure 20. Relative network perturbation amplitude (NPA) of specific cell stress subnetworks in nasal epithelial tissues following exposure of male rats to 3R4F cigarette smoke or THS2.2 aerosol, compared with air-exposed controls.

The relative NPA scores for the Oxidative Stress (A) and NFE2L2 Signaling (B) subnetwork models are shown with their confidence intervals accounting for experimental variation. The percentages give the relative NPA scores for the subnetworks compared with the reference (treatment comparison showing the highest perturbation). In addition, companion statistics, derived to inform on the specificity of the NPA score with respect to the biology described in the respective subnetwork models, are shown as *O and K*, respectively, if their *p*-values were below the significance level. Symbol legend:*, O and K statistic *p*-values <0.05; O and K, *p*-values between 0.05 and 0.1.

Many oxidative stress response genes did not exhibit significantly altered expression levels in response to exposure to 3R4F CS at low and medium nicotine concentrations. However, at the highest dose, significant gene expression changes were detected for *GSR*, *CAT*, *TXNRD1*, *SOD2*, *GCLM*, *GCLC*, *HMOX1*, *XDH*, *ICAM1*, *SLC7A11*, *MAF* and

GPX2 in the nasal epithelium of male animals. These changes did not persist once exposure had ceased (Figure 21).

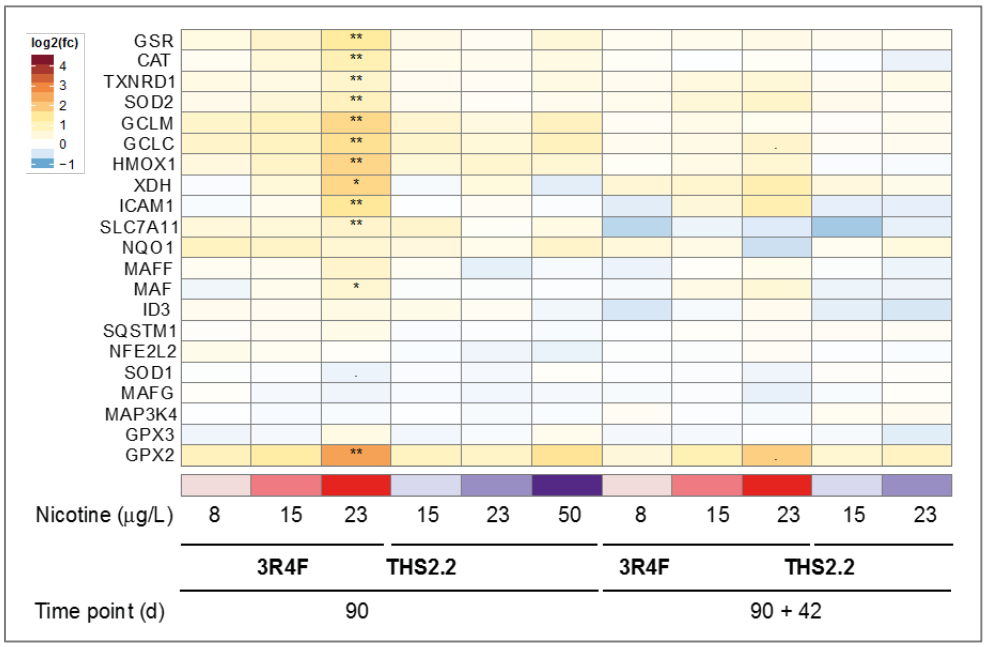


Figure 21. Altered expression levels of genes linked to the oxidative stress response in nasal epithelial tissues of male rats following exposure to 3R4F cigarette smoke or THS2.2 aerosol, compared with air-exposed controls.

The heatmap depicts changes in gene expression for oxidative stress-related genes (gene symbols listed on the left) relative to those in corresponding air-exposed controls in nasal epithelia of (A) male and (B) female rats expressed as $\log_2$(fold change (fc)). Up- and downregulation of gene expression levels are represented by orange and blue shades, respectively, with darker colors indicating greater absolute fold changes. Statistically significant fold changes are highlighted by ** (adjusted $p < 0.05$) and * (adjusted $p < 0.1$).

Evaluation of lung SRPs from exposed male and female rats indicated that only a few genes showed significant deregulation following exposure to 3R4F CS. This response was dose-dependent and, at least in part, reversible in animals that were allowed a 42-day post-exposure recovery. There were no obvious differences in SRPs in male and female rats. In comparison, exposure to THS2.2 aerosol induced a markedly less pronounced systems response, even at the highest concentration. In addition, gene expression changes following THS2.2 aerosol exposure fully reverted during the post-exposure period. Systems toxicological analysis of the transcriptomics data revealed significant perturbations in all network families in the lungs of 3R4F CS-exposed rats. In particular, the majority of subnetworks belonging to the IPN and Tissue Repair and Angiogenesis (TRA) network were affected by the exposure and this impact was sustained throughout the recovery period. The IPN also exhibited significant perturbations following THS2.2 aerosol exposure. However, these perturbations were generally of smaller amplitude and the exposure effects did not persist (Figure 22).

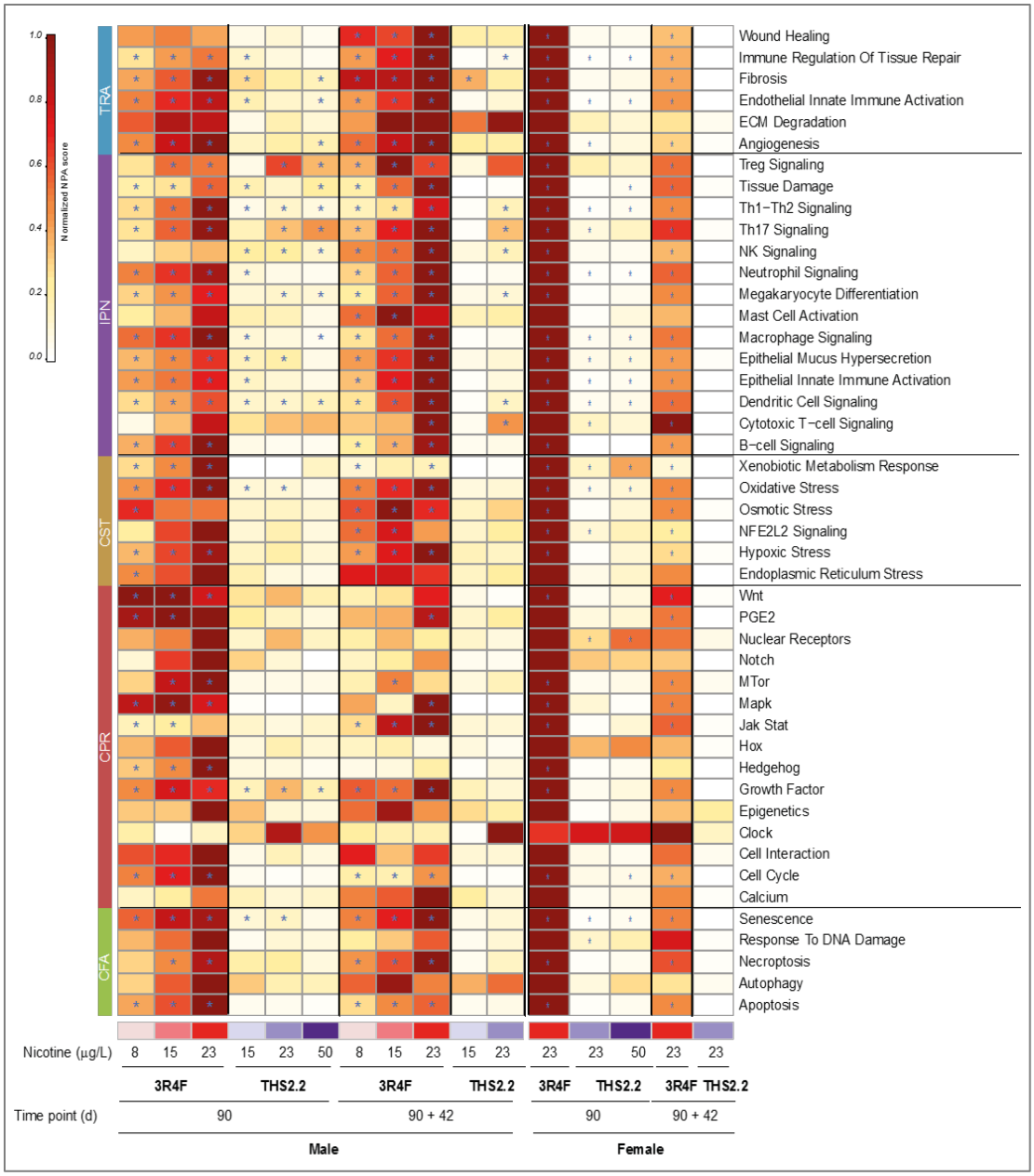


Figure 22. Network perturbations in rat lung tissues following exposure to 3R4F cigarette smoke or THS2.2 aerosol, compared with air-exposed controls.

Heatmap of Network Perturbation Amplitude scores summarizing subnetworks which were significantly perturbed with at least one treatment. A network is considered as perturbed if, in addition to the significance of the NPA score with respect to the experimental variation, the two companion statistics (O and K), derived to inform on the specificity of the NPA score with respect to the biology described in the network, are significant. Significantly perturbed networks are indicated by * (*i.e.*, O and K statistics *p*-values <0.05 and significant with respect to the experimental variation). CFA: Cell Fate; CPR: Cell Proliferation; CST: Cell Stress; IPN: Inflammatory Process Network; TRA: Tissue Repair and Angiogenesis.

Similar to the observations in the nose, transcriptomics data further indicated involvement of several types of cellular stress responses in the lungs of exposed animals. There was pronounced activation of the xenobiotic, hypoxic, osmotic and oxidative stress responses in the lungs of 3R4F CS-exposed male rats, effects not observed in animals exposed to the THS2.2 aerosol. Notably, the impact on the Oxidative Stress subnetwork was dose-dependent in male animals exposed to 3R4F CS and the extent of network perturbations was not markedly diminished following the 42-day post-exposure period. In contrast, the impact on the Oxidative Stress subnetwork elicited by THS2.2 aerosol exposure was no longer significant at the end of the recovery phase (Figure 23). In the lungs of female rats exposed to 3R4F CS, the same CST subnetworks were significantly perturbed. In contrast, THS2.2 aerosol-exposed female animals showed perturbations of predominantly the Xenobiotic Metabolism Response and Oxidative Stress subnetworks and these effects were less pronounced and were reversible upon cessation of exposure.

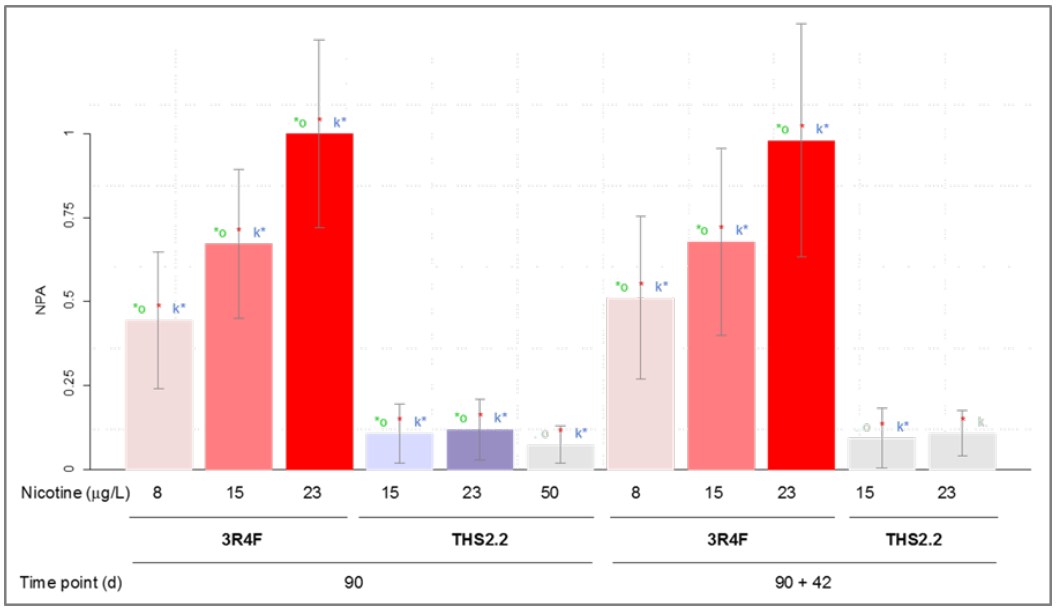


Figure 23. Relative network perturbation amplitude (NPA) of the oxidative stress subnetwork in lung tissues of male rats following exposure to 3R4F cigarette smoke or THS2.2 aerosol, compared with air-exposed controls.

The relative NPA scores for the oxidative stress subnetwork model are shown with their confidence intervals accounting for experimental variation. The percentages give the relative NPA score for the subnetworks compared with the reference (treatment comparison showing the highest perturbation). In addition, companion statistics derived to inform on the specificity of the NPA score, with respect to the biology described in the respective subnetwork models, are shown as *O and K*, respectively, if their *p*-values were below the significance level. Symbol legend:*, O and K statistic *p*-values <0.05; O and K, *p*-values between 0.05 and 0.1.

Close examination of a set of genes known to be involved in mediating oxidative stress responses showed only a few significant alterations in their transcriptional levels. For example, *SOD2* and *SLC7A11* gene expression was increased in lungs of male rats following exposure to 3R4F CS at the medium and high concentrations. The *NQO1*

expression level was also elevated, but only when animals were exposed to 3R4F CS corresponding to the highest nicotine concentration. None of these changes were still present after 42 days post-exposure recovery. Furthermore, at matching nicotine or even higher concentrations none of the selected oxidative stress genes displayed any significant changes in their expression levels in the lungs of male rats exposed to THS2.2 aerosol (Figure 24A).

Compared with in males, slightly more genes were affected by 3R4F CS exposure in the lungs of female animals. These included *TXRND1*, *NQO1, SOD2*, *HMOX1*, *SQSTM1* and *SLC7A11*, all upregulated, and *MAFF* which was downregulated. With the exception of *SOD2* expression levels, most of these changes were less pronounced at 90+42 days. Similar to the observations in male animals, no significant changes in expression of oxidative stress genes were identified in the lungs of female rats exposed to THS2.2 aerosol (Figure 24B).

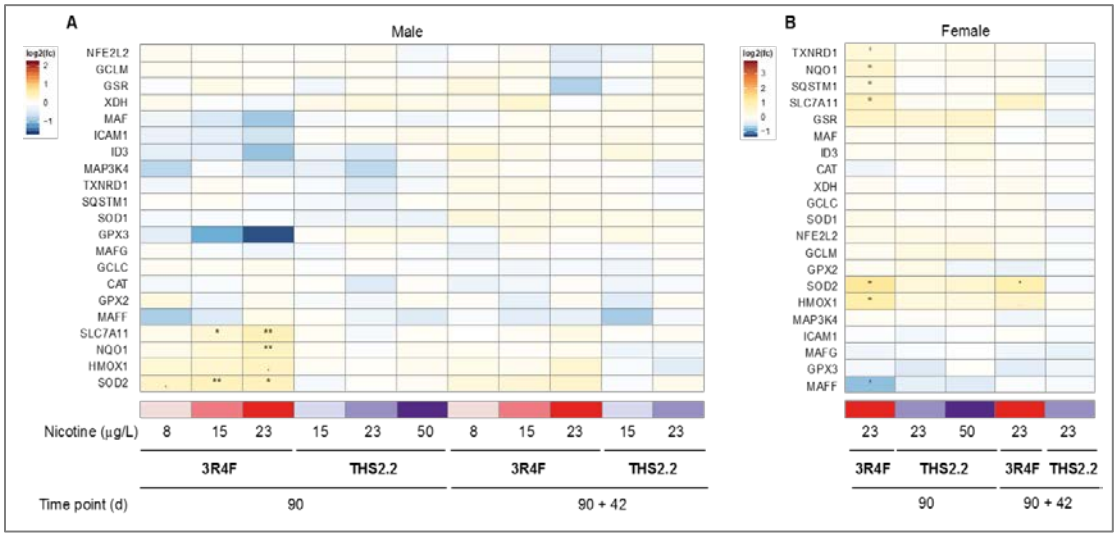


Figure 24. Altered expression levels of genes linked to the oxidative stress response in rat lung tissues following exposure to 3R4F cigarette smoke or THS2.2 aerosol, compared with air-exposed controls.

The heatmap depicts changes in gene expression for oxidative stress-related genes (gene symbols listed on the left) relative to those in corresponding air-exposed controls in the lungs of (A) male and (B) female rats expressed as $\log_2$(fold change (fc)). Up- and downregulation of gene expression levels are represented by orange and blue shades, respectively, with darker colors indicating greater absolute fold changes. Statistically significant fold changes are highlighted by ** (adjusted $p < 0.05$) and * (adjusted $p < 0.1$).

LINK: 15006_150082_150083 THS SR; 15006_150082_150083 THS PUB

4.2.2.1.2 Rat OECD THS2.2 Menthol Study

The second 90-day inhalation study was conducted with a mentholated version of the THS2.2 MRTP prototype (THSM), comparing toxicity of CS from 3R4F to that of aerosol from THS2.2 Menthol. In this study, rats were exposed to filtered fresh air (sham); to CS from 3R4F or two mentholated reference cigarettes (MRCs), all corresponding to 23 μg/L nicotine; or to low, medium or high concentrations of the aerosol from THS 2.2 Menthol, corresponding to 15, 23 and 50 μg/L nicotine, respectively. MRC Low Menthol (LM) and MRC High Menthol (HM) were designed to meet the tar, nicotine, CO and cigarette diameter specifications of 3R4F reference cigarettes and to produce approximately 1.2 and 2.4 mg menthol in smoke, respectively, when smoked according to ISO standard 3308. As in the previous OECD study, respiratory tract organs from animals of all exposure groups were subjected to histopathological evaluation following the 90-day inhalation, and pulmonary inflammation was assessed at the end of exposure (90 days) and following the 42-day post-exposure period (90+42 days). Furthermore, potential molecular changes as a consequence of exposure were evaluated by employing transcriptomics, proteomics and lipidomics analyses.

Changes in the nasal respiratory epithelium were observed in rats following exposure to CS and THS2.2M aerosol over a 90-day period and consisted of squamous cell metaplasia, goblet cell hyperplasia with and without loss of goblet cells, and reserve cell hyperplasia. Squamous metaplasia was predominantly seen in animals exposed to smoke from reference cigarettes without marked differences in lesion severity among the three items. Squamous metaplasia was also incidentally found in animals exposed to a high concentration of THS2.2M aerosol. However, squamous metaplastic changes in nasal respiratory epithelia of the High THS2.2M group animals were less severe than in animals in the 3R4F and MRC HM groups. Reserve cell hyperplasia was also less severe in animals from the THS2.2M groups than in rats exposed to smoke from the reference cigarettes, independent of the presence or concentration of menthol in smoke. Importantly, there was nearly complete regression of these adaptive epithelial changes following a recovery period of 42 days, independent of the exposure, suggesting that they represented local adaptive changes to irritant inhalation. In contrast, goblet cell hyperplasia was observed in all exposed female animals, compared with in sham-exposed controls. Although the changes were not severe or extensive, they persisted throughout the post-exposure period and even worsened in severity. However, goblet cell hyperplasia was still less severe in THS2.2M-exposed rats compared with those exposed to any of the reference cigarettes.

Similar exposure-related alterations, in particular squamous metaplasia and reserve cell hyperplasia, were also noted in the nasal olfactory epithelium in animals exposed to smoke from any of the reference cigarettes. The severity of these adaptive lesions decreased in female rats during the recovery period. In contrast, THS2.2M-exposed animals exhibited squamous metaplasia and reserve cell hyperplasia at this location only incidentally and also did not display any major abnormalities in distal nasal epithelium.

Squamous metaplasia was also a morphological feature observed in laryngeal epithelium, at the base of the epiglottis and arytenoid projections, in all exposed animals. Generally, lesions were more severe in rats exposed to smoke from the reference cigarettes than in those exposed to THS2.2M aerosol and grading was similar in male and female rats.

Moreover, lesions regressed in animals allowed a recovery period, suggesting that these were predominantly adaptive and reversible epithelial changes.

The bronchial epithelium of rats exposed to THS2.2M aerosol did not exhibit any marked increase in goblet cells or squamous metaplastic lesions. However, exposure to reference CS, with or without menthol, resulted in the development of goblet cell hyperplasia in bronchial epithelium that was more advanced than that observed in THS2.2M aerosol-exposed animals. Notably, goblet cell hyperplasia in the bronchial epithelium regressed noticeably in female animals permitted a post-exposure recovery.

Examining the biological impact of exposures on the nasal epithelium using a mechanistic network approach identified exposure to MRC LM as having the greatest biological impact in both male and female rats (RBIF = 100%, REF). Of note, this was nearly identical to the biological impact of exposure to MRC HM in female rats, and was close to the impact elicited by 3R4F CS exposure. In the nose of male rats exposed to MRC HM, the impact was approximately half that of MRC LM exposure. The 3R4F CS exposure had a biological impact falling between the effects of exposures to the two mentholated reference cigarettes. A marked effect of THS2.2M aerosol exposure on the biological networks occurred only at the highest concentration. In addition, while the impact caused by THS2.2M aerosol exposure almost entirely abated following post-exposure recovery, the effects of 3R4F CS and MRC HM CS exposure were only diminished, suggesting that they were only partially irreversible.

Interrogating the affected network families further, a broad range of biological processes and mechanisms in the nose were affected by exposure to reference CS. These included those related to cell proliferation, stress responses, programmed cell death and senescence, tissue repair and angiogenesis and innate and adaptive immune responses. There were no gender-associated differences in these patterns of network perturbations. Furthermore, in female rats exposed to smoke from any of the reference cigarettes, all perturbations were sustained, albeit with a smaller amplitude. In comparison, exposure to aerosol from THS2.2M led to few perturbations, most of which reflected cellular stress responses and, at medium and high concentrations, cell death mechanisms, tissue repair and epithelial immune responses. However, perturbations caused by THS2.2M exposure, independent of dose, did not reach the same amplitude achieved with exposure to any of the reference products and were mostly diminished during the 42-day post-exposure period (Figure 25).

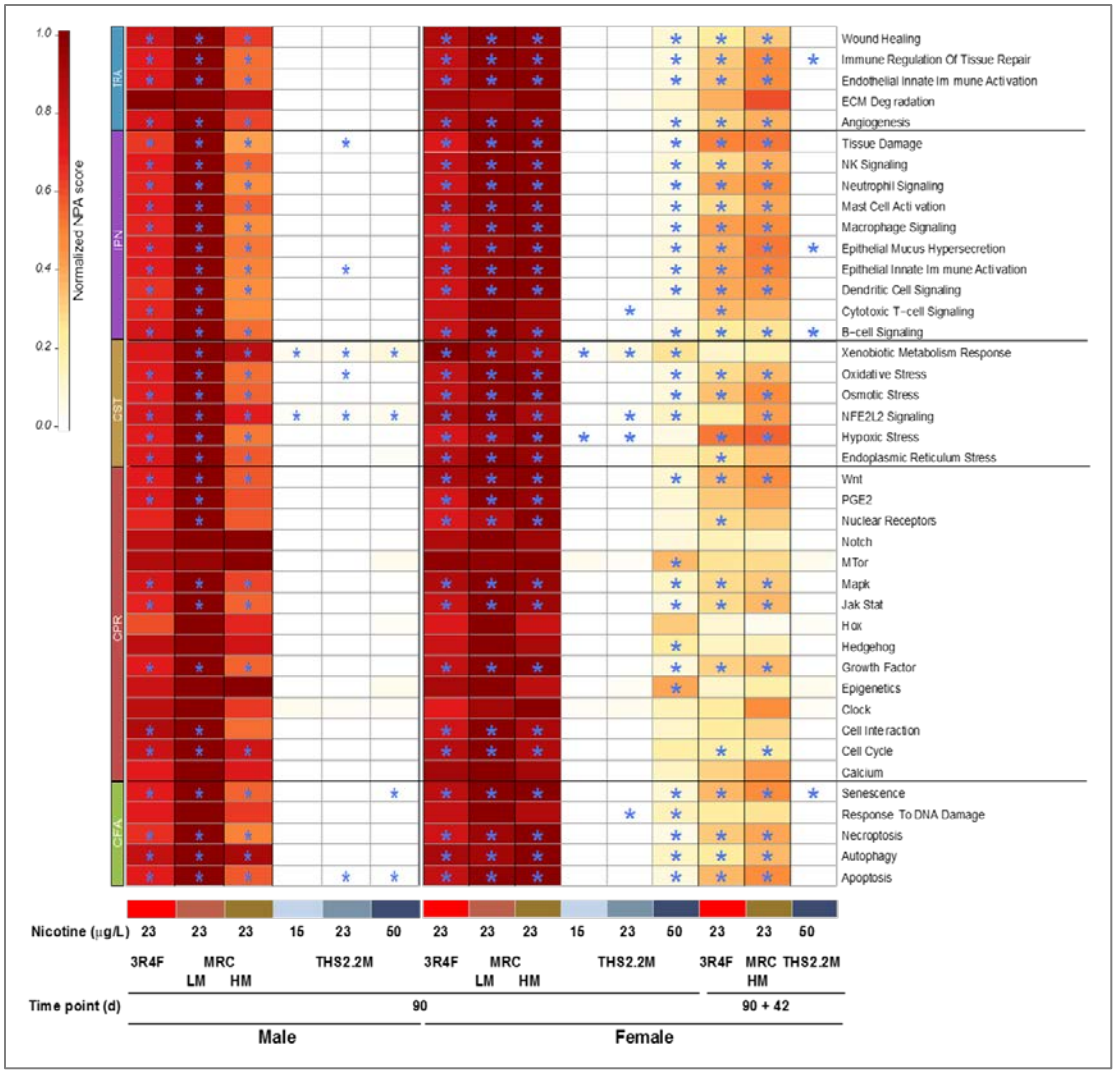


Figure 25. Network perturbations in rat nasal epithelial tissues following exposure to 3R4F cigarette smoke or THS2.2M aerosol, compared with air-exposed controls.

Heatmap of Network Perturbation Amplitude scores summarizing subnetworks which were significantly perturbed with at least one treatment. A network is considered as perturbed if, in addition to the significance of the NPA score with respect to the experimental variation, the two companion statistics (O and K) derived to inform on the specificity of the NPA score with respect to the biology described in the network, are significant. Significantly perturbed networks are indicated by * (*i.e.*, O and K statistics *p*-values <0.05 and significant with respect to the experimental variation). CFA: Cell Fate; CPR: Cell Proliferation; CST: Cell Stress; IPN: Inflammatory Process Network; TRA: Tissue Repair and Angiogenesis.

While all CST subnetworks were significantly impacted by exposure to CS from any of the reference cigarettes, only two of the cell stress responses appeared to play a major role in adaptive repair processes in the nose of THS2.2M aerosol-exposed rats. Besides a significant xenobiotic stress response for all exposure arms, there was also a marked Nrf2-mediated oxidative stress response. In addition, a pronounced hypoxic stress response was noticeable in female rats exposed to low and medium concentrations of

THS2.2M aerosol, whereas high concentrations also caused pertubations in the Osmotic Stress subnetwork. In contrast to observations in the nose of animals exposed to CS from the reference cigarettes, perturbations in the Endoplasmic Reticulum Stress subnetwork did not occur in the nasal epithelium of THS2.2M aerosol-exposed rats (Figure 26).

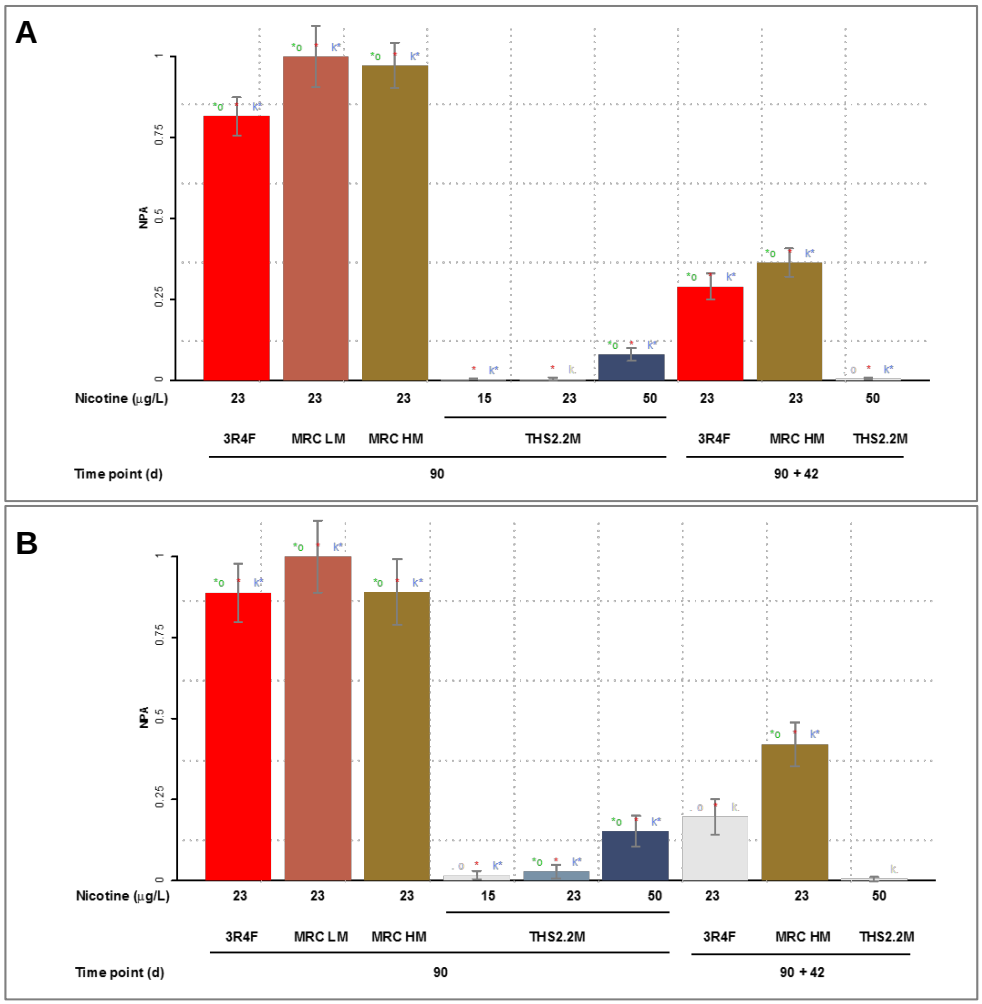


Figure 26. Relative network perturbation amplitude (NPA) of the oxidative stress subnetworks in nasal epithelial tissues of female rats following exposure to 3R4F cigarette smoke or THS2.2 aerosol, compared with air-exposed controls.

The relative NPA scores for the (A) Oxidative Stress and (B) NFE2L2 Signaling subnetwork models are shown with their confidence intervals accounting for experimental variation. The percentages give the relative NPA scores for the subnetworks compared with the reference (treatment comparison showing the highest perturbation). In addition, companion statistics, derived to inform on the specificity of the NPA score with respect to the biology described in the respective subnetwork models, are shown as *O and K*, respectively, if their *p*-values were below the significance level. Symbol legend:*, O and K statistic *p*-values <0.05; O and K, p-values between 0.05 and 0.1.

A number of oxidative stress-related genes were significantly upregulated in nasal epithelia of rats exposed to smoke from reference cigarettes. *ICAM1*, *HMOX1*, *SOD2*, *TXRND1*, *GPX2*, *GPX3*, *MAF*, *GSR*, *GCLC*, *GCLM*, *XDH* and *SQSMT1* gene expression levels were elevated in both male and female animals, with similar fold changes across the three conditions and with no obvious effects of menthol. Similarly, expression levels of *SOD1* and *MAFG* decreased in the nose of CS-exposed rats. This was in contrast to observations in THS2.2M aerosol-exposed animals. In those, exposure at the highest nicotine concentration caused only a slight elevation of *HMOX1* expression levels in males, whereas *HMOX1* and other genes encoding antioxidant enzymes including, *XDH*, *CAT* and *TXRND1*, were upregulated in the nasal epithelia of female animals. As noted with the network perturbations, the majority of gene expression changes induced by CS exposure were still detectable after the 42-day recovery period. Upon recovery following THS2.2M aerosol exposure, however, no significantly altered genes could be detected, indicating that gene expression changes were transient, reflecting a rapid oxidative stress response that was not sustained once exposure ceased (Figure 27).

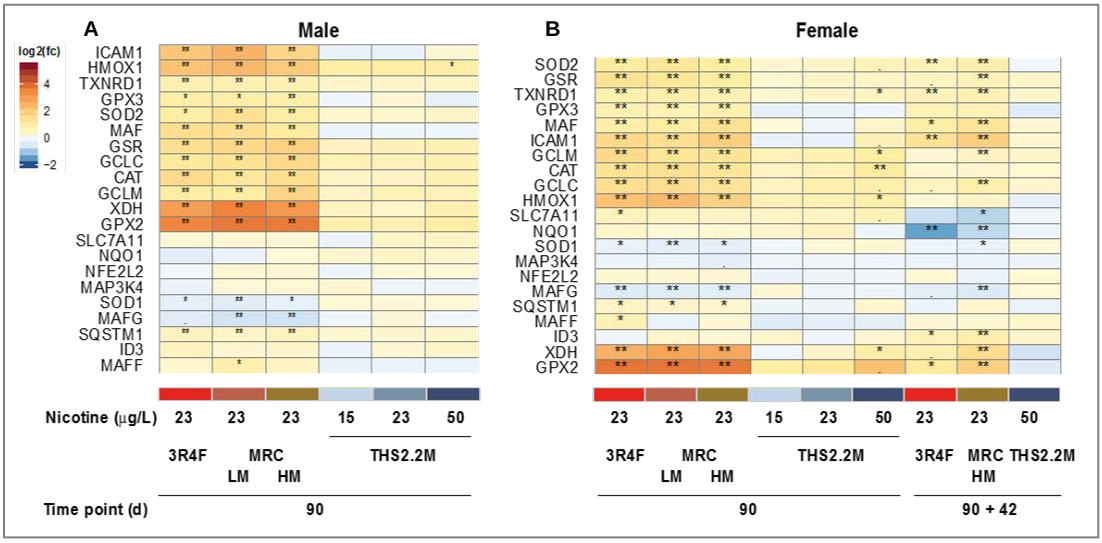


Figure 27. Altered expression levels of genes linked to the oxidative stress response in rat nasal epithelial tissues following exposure to 3R4F cigarette smoke or THS2.2 aerosol, compared with air-exposed controls.

The heatmap depicts changes in gene expression for oxidative stress-related genes (gene symbols listed on the left) relative to those in corresponding air-exposed controls in the lungs of (A) male and (B) female rats expressed as $\log_2$(fold change (fc)). Up- and downregulation of gene expression levels are represented by orange and blue shades, respectively, with darker colors indicating greater absolute fold changes. Statistically significant fold changes are highlighted by ** (adjusted $p < 0.05$) and * (adjusted $p < 0.1$).

Evaluation of the lung SRPs from exposed male and female rats indicated that only a few genes were significantly deregulated following exposure to 3R4F CS. This response was dose-dependent, and, at least in part, reversible in animals that were allowed a 42-day post-exposure recovery. There was no obvious difference between male and female rats' SRPs. In comparison, exposure to THS2.2 aerosol induced a markedly less pronounced

systems response, even at the highest concentration. In addition, gene expression changes following THS2.2 aerosol exposure fully reverted during the post-exposure period. Systems toxicological analysis of the transcriptomics data revealed significant perturbations in all network families in the lungs of 3R4F CS-exposed rats. In particular, the majority of subnetworks belonging to the IPN and TRA networks were affected by the exposure, and this impact was sustained throughout the recovery period. The CST network also exhibited significant perturbations following THS2.2 aerosol exposure. However, these perturbations were generally of markedly smaller amplitude and the exposure effects did not persist (Figure 28).

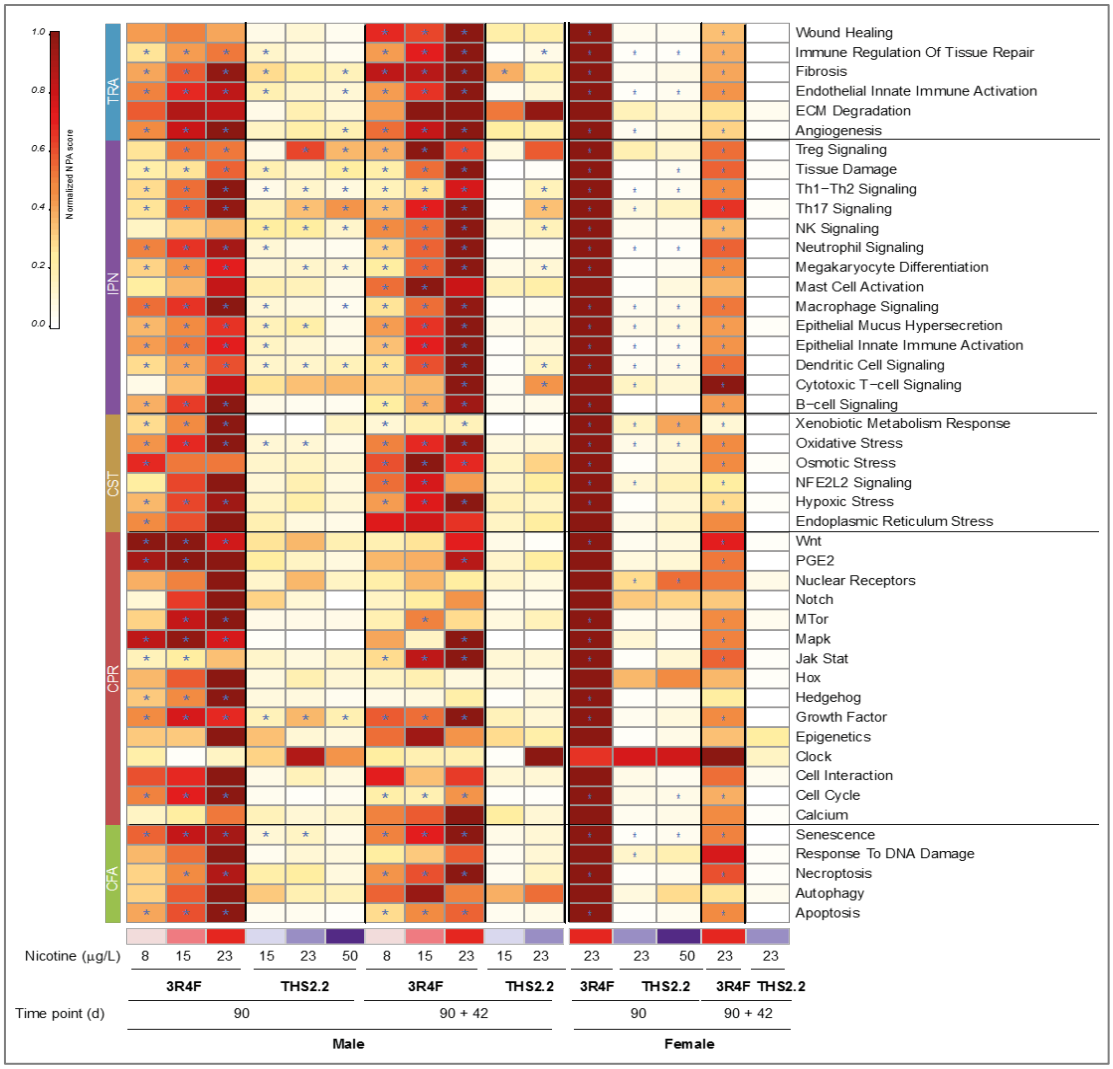


Figure 28. Network perturbations in rat lung tissues following exposure to 3R4F cigarette smoke or THS2.2 aerosol, compared with air-exposed controls.

Heatmap of Network Perturbation Amplitude Scores summarizing subnetworks which are significantly perturbed in at least one treatment. A network is considered as perturbed if, in addition to the significance of the NPA score with respect to the experimental variation, the two companion statistics (O and K) derived to inform on the specificity of the NPA score with respect to the biology described in the network, are significant. Significantly perturbed networks are indicated by * (i.e., O and K statistics *p*-values <0.05 and significant with respect to the experimental variation). CFA: Cell Fate; CPR: Cell Proliferation; CST: Cell Stress; IPN: Inflammatory Process Network; TRA: Tissue Repair and Angiogenesis.

Moreover, 3R4F CS exposure resulted in altered expression of oxidative stress genes, regardless of the reference product or gender. This effect was mostly irreversible in female rats, while gene expression reverted in males. However, gene expression changes were not observed in the lungs of THS2.2M aerosol-exposed animals (Figure 29).

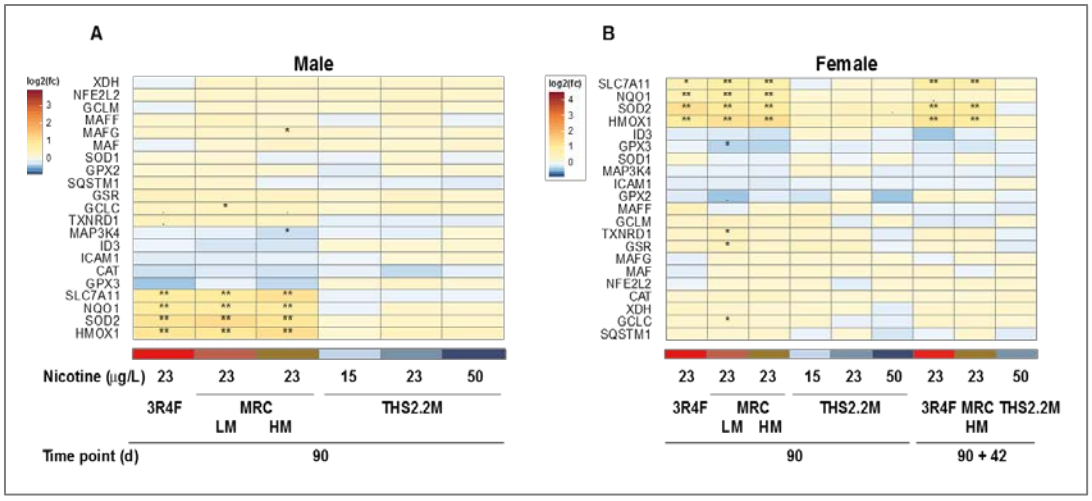


Figure 29. Altered expression levels of genes linked to the oxidative stress response in rat lung tissues following exposure to 3R4F cigarette smoke or THS2.2 aerosol, compared with air-exposed controls.

The heatmap depicts changes in gene expression for oxidative stress-related genes (gene symbols listed on the left) relative to those in corresponding air-exposed controls in the lungs of (A) male and (B) female rats expressed as $\log_2$(fold change (fc)). Up- and downregulation of gene expression levels are represented by orange and blue shades, respectively, with darker colors indicating greater absolute fold changes. Statistically significant fold changes are highlighted by ** (adjusted $p < 0.05$) and * (adjusted $p < 0.1$).

In summary, adaptive epithelial changes were noted in the upper respiratory tract in rats exposed to 3R4F, MRC LM and MRC HM CS. These changes were comparable in incidence and severity in male and female animals exposed to any of the reference products. In contrast, there were only incidental exposure-related findings in the respiratory tracts of animals from the Low and Medium THS2.2M groups. While exposure to THS2.2M aerosol at high concentrations did produce epithelial alterations, these changes were typically mild in severity or rare compared with effects of the reference items, even though the aerosol nicotine concentration was more than twice as high as that of the reference cigarettes. Moreover, a broad range of stress responses, some not reversible, were mounted in the upper respiratory tracts of rats exposed to CS. In contrast, exposure to THS2.2M aerosol induced fewer and less extensive stress responses, all of which subsided during post-exposure recovery.

LINK: 15025_176500 THS SR; 15025_176500 THS PUB

4.2.2.2 *Apoe*$^{-/-}$ THS Switching Study

Development and progression of COPD and CVD were evaluated in apolipoprotein E-deficient (*Apoe*$^{-/-}$) mice chronically exposed to 3R4F mainstream CS at a target nicotine concentration of 29.9 µg/L, to an aerosol from THS2.2 at a matched nicotine concentration, or to filtered fresh air. All exposures were given for 3 hours per day, 5 days per week for up to 8 months. After 2 months exposure to 3R4F CS, designated groups of animals were switched to THS2.2 aerosol exposure (switching group) or

exposed to filtered air (cessation group) for up to 6 months, following the same daily exposure regimen. At designated time points (months 1, 2, 3, 6 or 8 after commencing exposure), the animals were examined for multiple parameters to comprehensively assess development and progression of COPD or CVD indicators. These included hematology and clinical chemistry, pulmonary inflammation measurements, assessment of pulmonary function, lung histopathology and morphometry, evaluation of atherosclerotic plaque formation in the aortic arch and descending aorta and the examination of molecular changes in various tissues throughout the exposure period by transcriptomics, proteomics and lipidomics.

The size of atherosclerotic plaques increased following 3R4F CS exposure over time. Although animals in the THS2.2 group were exposed to matched aerosol nicotine levels, their plaque sizes were only minimally different from those in sham animals. Moreover, cessation and switching appeared to halt plaque growth and did not further aggravate CS exposure-related effects.

Typical CS exposure-related effects, including reserve cell hyperplasia and squamous metaplasia, were noted in the nasal respiratory epithelium. The incidence and severity of these lesions diminished towards the more distal regions of the nose. Such marked effects were not seen in the THS2.2 aerosol-exposed mice, although mild reserve cell hyperplasia was noted in the nasal respiratory epithelium at month 6 and month 8. This did not worsen until the completion of exposure. Within one and three months, both cessation and switching resulted in a rapid repair of CS-related metaplastic and hyperplastic lesions, respectively, in the nasal epithelium, indicating the transient nature of these pathological changes.

The bronchial epithelium displayed mild to moderate reserve cell hyperplasia in 3R4F CS-exposed animals and this diminished in severity upon cessation and switching. In contrast, continuous exposure to THS2.2 aerosol caused reserve cell hyperplasia in some, but not all, animals with minimal alterations to the bronchial epithelium. Similarly, the lungs of THS2.2 aerosol-exposed mice also lacked the inflammatory cell infiltrates in the alveolar lumen and interstititum and pigmented and unpigmented macrophages accumulating over time; these effects, in contrast, were the most pronounced histopathological findings in the lungs of *Apoe*$^{-/-}$ mice exposed to 3R4F CS but decreased in incidence and severity when animals were switched to fresh air or THS2.2 aerosol. Histopathological and morphometric assessment of the lungs also confirmed the presence of emphysematous lesions in animals exposed to 3R4F CS, but not in those exposed to THS2.2 aerosol. Although very mild age-dependent emphysematous lesions were noted in all animals, both cessation and switching led to notable lung tissue regeneration and repair.

For the analysis of biomarkers of exposure and oxidative stress, urine was collected from selected *Apoe*$^{-/-}$ mice from each study arm. CS exposure resulted in elevated 8-OHdG levels, compared with in sham animals, though this increase was not significant. There were no changes in urinary 8-OHdG levels following continuous THS exposure or with switching or cessation. Both MDA and 4-HNE, markers of lipid peroxidation, were detected at significantly higher levels in mice exposed to 3R4F CS than in sham animals at months 6 and 8. Again, no differences were noted in levels of these markers in urine from THS aerosol-exposed mice and mice subjected to cessation or switching protocols, suggesting an overall lower oxidative burden.

Analysis of the transcriptomics data using a systems toxicology approach showed the highest biological impact with 8-month 3R4F CS exposure (RBIF = 100%; REF). The impacts were much lower at the earlier time points or with continued THS2.2 aerosol exposure. Importantly, switching to fresh air or THS2.2 aerosol greatly reduced the biological impacts of 3R4F CS exposure over time (Figure 30).

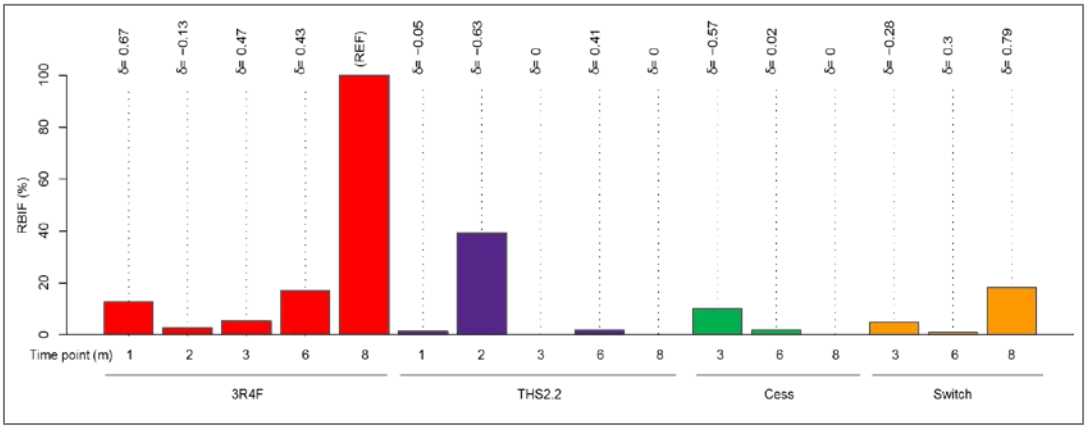


Figure 30. Network model-based analysis of the biological impact factor (BIF) in nasal epithelia from *Apoe*$^{-/-}$ mice exposed to 3R4F cigarette smoke or THS2.2 aerosol, compared with air-exposed controls.

The bar plot depicts BIF values relative to the maximum response (REF, RBIF = 100%). The δ values (−1 to 1) indicate how similar the underlying network perturbations are with respect to the REF. Scores were computed using transcriptomics profiling data from nasal tissues following continuous, 8-month exposure of *Apoe*$^{-/-}$ mice to air, 3R4F cigarette smoke (red bars) or THS2.2 aerosol (purple bars), or from animals that were switched from a 2-month 3R4F cigarette smoke exposure to air (cessation; Cess; green bars) or THS2.2 aerosol (switch; yellow bars).

Further examination of the mechanisms contributing to the observed biological impacts on the nose of 3R4F CS-exposed *Apoe*$^{-/-}$ mice revealed significant perturbations of the Cell Cycle and Senescence subnetworks in addition to a sustained xenobiotic metabolism response. These perturbations increased in amplitude over time and at 8 months a number of additional networks in all network families were also significantly impacted. In contrast, exposure to THS2.2 aerosol for 2 months had the strongest biological impact on predominantly the CST network and IPN and, to a lesser degree, subnetworks capturing apoptosis, sensecence, and cell proliferation biology. Notably, with the exception of perturbations in the Cell Cycle, Senescence and Xenobiotic Metabolism Response subnetworks, THS2.2 aerosol exposure did not cause a significant impact after the 2-month time point. Moreover, upon cessation, the majority of network perturbations were abated within a short time. While this was also true with switching, some cell stress and inflammatory responses remained active in the nasal epithelium of the *Apoe*$^{-/-}$ mice that were switched to THS2.2 aerosol (Figure 31).

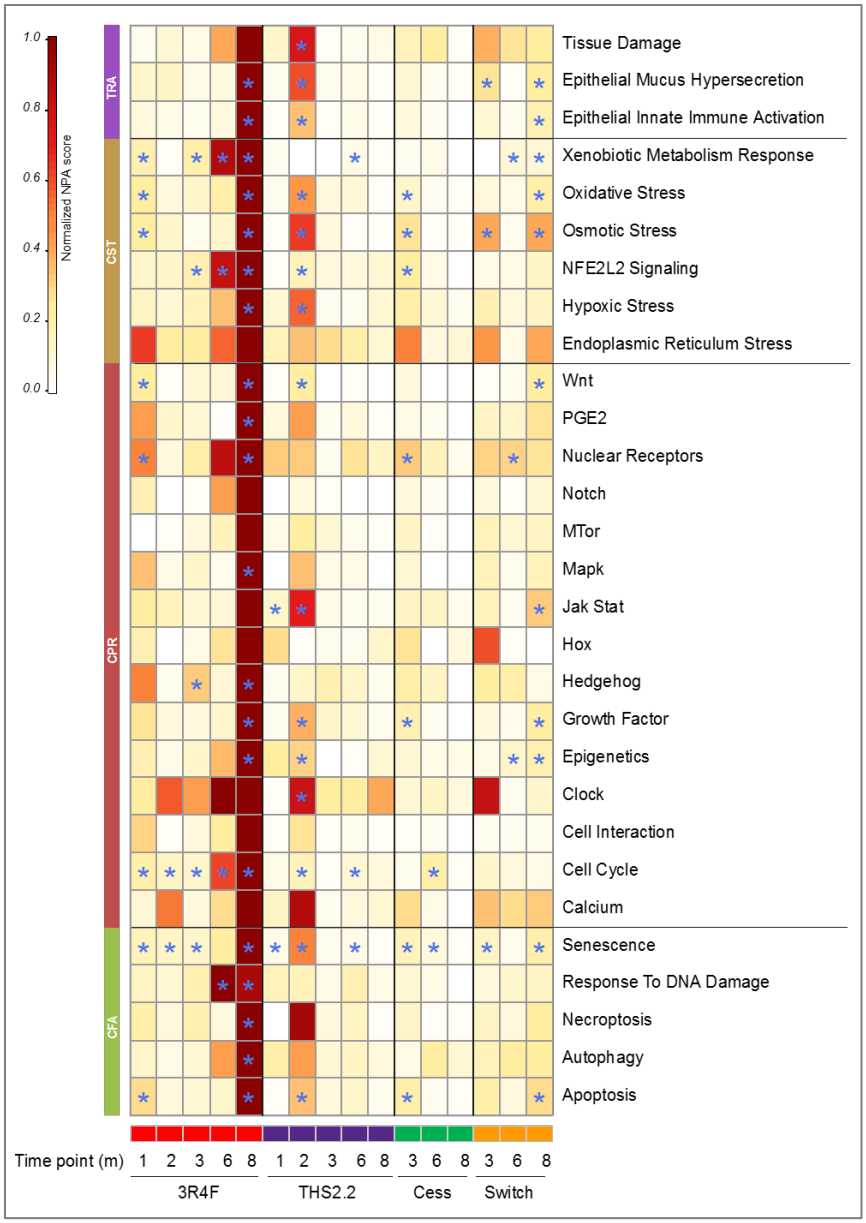


Figure 31. Network perturbations in *Apoe*$^{-/-}$ mouse nasal tissues following exposure to 3R4F cigarette smoke or THS2.2M aerosol, compared with air-exposed controls.

Heatmap of Network Perturbation Amplitude scores summarizing subnetworks which were significantly perturbed with at least one treatment. A network is considered as perturbed if, in addition to the significance of the NPA score with respect to the experimental variation, the two companion statistics (O and K), derived to inform on the specificity of the NPA score with respect to the biology described in the network, are significant. Significantly perturbed networks are indicated by * (*i.e.*, O and K statistics p-values <0.05 and significant with respect to the experimental variation). Cess: Cessation; Switch: switching. CFA: Cell Fate; CPR: Cell Proliferation; CST: Cell Stress; IPN: Inflammatory Process Network; TRA: Tissue Repair and Angiogenesis.

Closer inspection of the Oxidative Stress subnetwork also showed that exposure of *Apoe*$^{-/-}$ mice to 3R4F CS for 8 months exerted the greatest perturbation on this mechanism in nasal epithelia and that THS2.2 aerosol exposure had a significant impact on the oxidative stress response at month 2. In addition, perturbations were markedly reduced within 1 month of cessation to eventually become insignificant. While a reduction in the amplitude of the Oxidative Stress subnetwork perturbation was also noted when animals were switched to THS2.2 aerosol exposure, some residual activity of this mechanism was still present after switching (Figure 32).

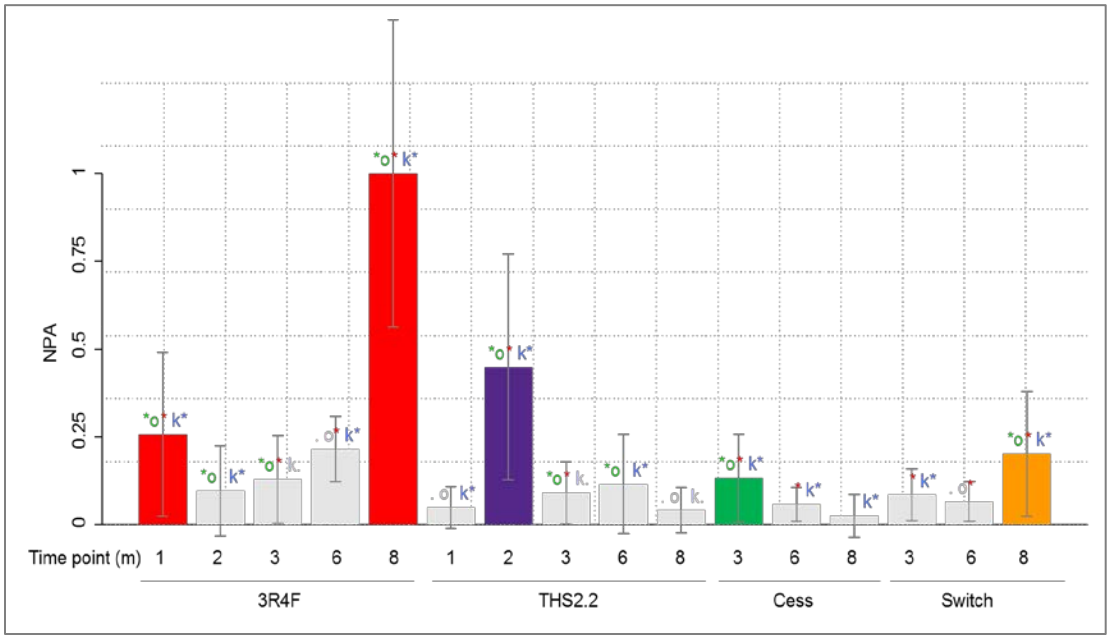


Figure 32. Relative network perturbation amplitude (NPA) of the Oxidative Stress subnetwork in *Apoe*$^{-/-}$ mouse nasal tissues following exposure to 3R4F cigarette smoke or THS2.2 aerosol, compared with air-exposed controls.

The relative NPA scores for the oxidative stress subnetwork model are shown with their confidence intervals accounting for experimental variation. The percentages give the relative NPA scores for the subnetworks compared with the reference (treatment comparison showing the highest perturbation). In addition, companion statistics derived to inform on the specificity of the NPA score, with respect to the biology described in the respective subnetwork models, are shown as *O and K*, respectively, if their *p*-values were below the significance level. Symbol legend:*, O and K statistic *p*-values <0.05; O and K, *p*-values between 0.05 and 0.1.

Similar to observations in nasal samples, lung SRPs revealed an increasing number of DEGs in 3R4F CS-exposed compared with sham-exposed mice over time, while no DEGs were identified in lung tissues from THS2.2 aerosol-exposed mice or in those from the cessation and switching groups. Biological impact analysis indicated a major impact of 3R4F CS at the first three time points, peaking at 6 months of exposure (RBIF = 100%; REF) before declining slightly. In comparison, continued THS2.2 aerosol exposure had a considerably lower impact on the lungs of *Apoe*$^{-/-}$ mice. Moreover, both

cessation and switching resulted in marked reductions of the 3R4F CS exposure effects, suggesting that they were, at least in part, reversible (Figure 33).

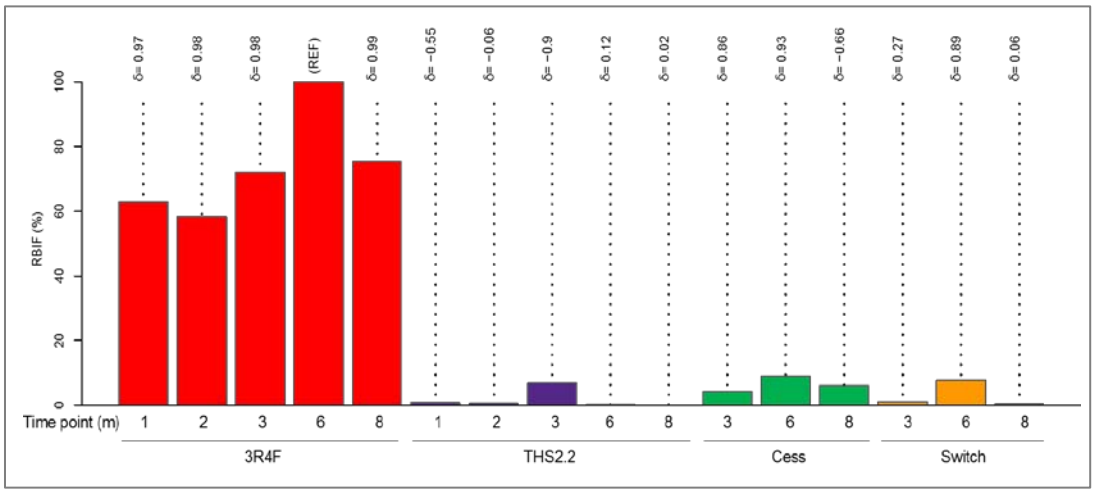


Figure 33. Network model-based analysis of the biological impact factor (BIF) in lungs from *Apoe*$^{-/-}$ mice exposed to 3R4F cigarette smoke or THS2.2 aerosol, compared with air-exposed controls.

The bar plot depicts BIF values relative to the maximum response (REF, RBIF=100%). The δ values (−1 to 1) indicate how similar the underlying network perturbations are with respect to the REF. Scores were computed using transcriptomics profiling data from lung tissues following continuous 8-month exposure of *Apoe*$^{-/-}$ mice to air, 3R4F cigarette smoke (red bars) or THS2.2 aerosol (purple bars), or from animals that were switched from a 2-month 3R4F cigarette smoke exposure to air (cessation; Cess; green bars) or THS2.2 aerosol (switch; yellow bars).

Early drivers of THS2.2 aerosol exposure effects were restricted to the networks describing tissue repair and oxidative stress-related processes. More extensive involvement of other cell stress as well as innate and adaptive immune reponses was not apparent until month 3. After this time point, however, very few networks remained significantly perturbed. In contrast, the mechanisms underlying the observed biological impact of 3R4F CS exposure encompassed all network models, with a predominant involvement of the TRA network and IPN families, followed by the CST, CPR and CFA networks. Most of the affected networks remained significantly perturbed throughout the cessation period, although the extent of perturbations was markedly lower. This was different from findings in the lungs of animals from the switching group. In those mice, most of the network perturbations declined until they were no longer significant, suggesting that switching to THS2.2 aerosol exposure for this period of time did not worsen the effects of prior 3R4F CS exposure and also did not cause any additional effects on the lungs (Figure 34).

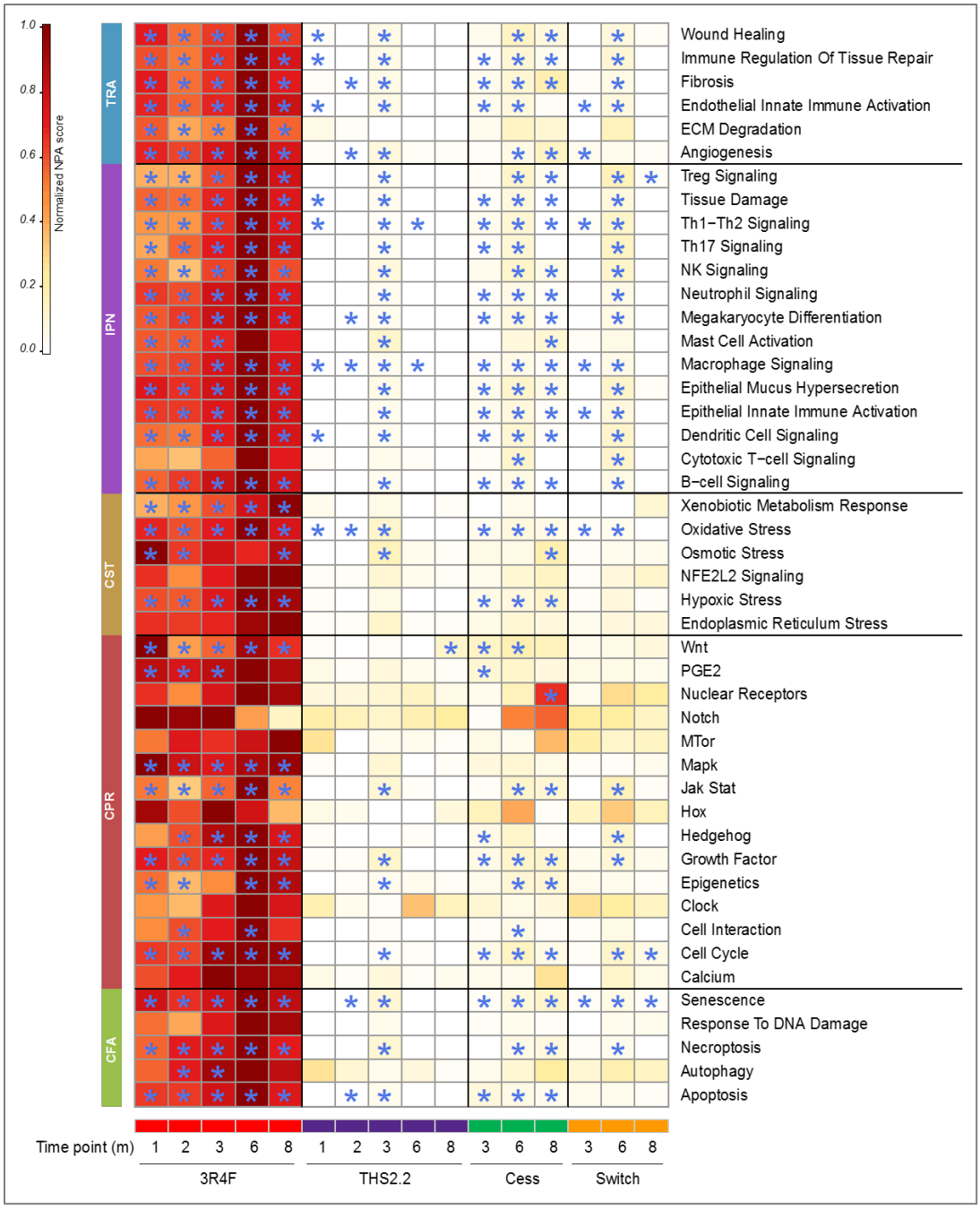


Figure 34. Network perturbations in *Apoe*$^{-/-}$ mouse lung tissues following exposure to 3R4F cigarette smoke or THS2.2M aerosol, compared with air-exposed controls.

Heatmap of Network Perturbation Amplitude scores summarizing subnetworks which were significantly perturbed with at least one treatment. A network is considered as perturbed if, in addition to the significance of the NPA score with respect to the experimental variation, the two companion statistics (O and K), derived to inform on the specificity of the NPA score with respect to the biology described in the network, are significant. Significantly perturbed networks are indicated by * (*i.e.*, O and K statistics *p*-values <0.05 and significant with respect to the experimental variation). CFA: Cell Fate; CPR: Cell Proliferation; CST: Cell Stress; IPN: Inflammatory Process Network; TRA: Tissue Repair and Angiogenesis.

An overview of the Oxidative Stress network perturbation amplitudes illustrates these observations further. While 3R4F CS exposure exerted a prominent effect on this CST subnetwork, its impact was markedly reduced upon cessation and switching. However, prolonged exposure to THS2.2 aerosol had only transient effects on oxidative stress mechanisms (Figure 35).

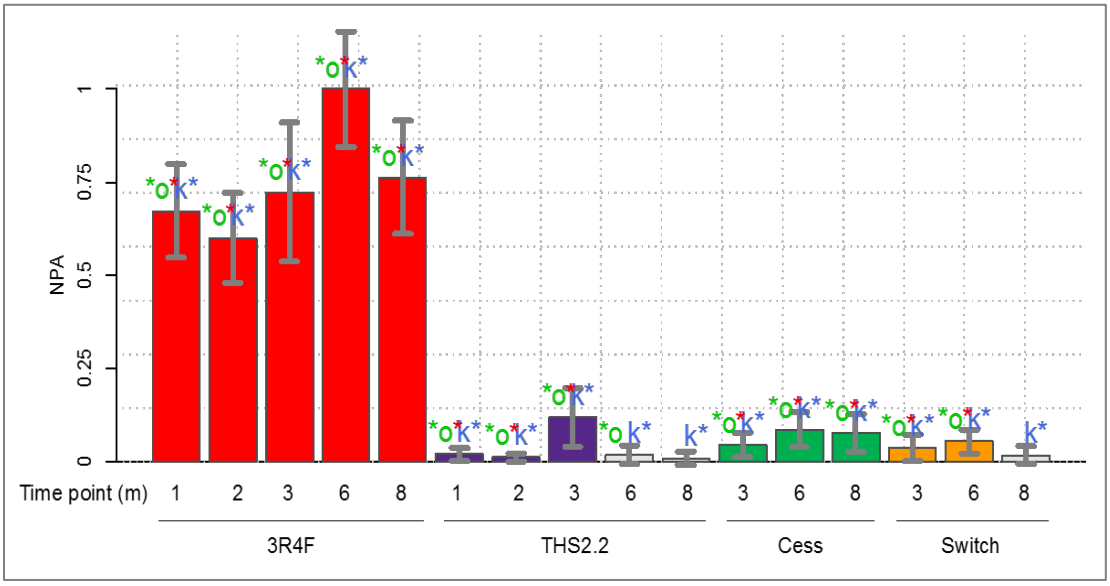


Figure 35. Relative network perturbation amplitude (NPA) of the Oxidative Stress subnetwork in *Apoe*$^{-/-}$ mouse lung tissues following exposure to 3R4F cigarette smoke or THS2.2 aerosol, compared with air-exposed controls.

The relative NPA scores for the oxidative stress subnetwork model are shown with their confidence intervals accounting for experimental variation. The percentages give the relative NPA scores for the subnetworks compared with the reference (treatment comparison showing the highest perturbation). In addition, companion statistics derived to inform on the specificity of the NPA score, with respect to the biology described in the respective subnetwork models, are shown as *O and K*, respectively, if their *p*-values were below the significance level. Symbol legend:*, O and K statistic *p*-values <0.05; O and K, *p*-values between 0.05 and 0.1.

Together, these results demonstrated that exposure of *Apoe*$^{-/-}$ mice to THS2.2 aerosol for up to 8 months resulted in changes at the anatomical, physiological, and molecular levels that were largely indistinguishable from those seen in animals exposed to fresh air. Furthermore, following exposure to CS for 2 months, both cessation and switching to THS2.2 aerosol exposure did not further aggravate CS exposure-induced alterations in lung function or the extent of atherosclerotic plaques and resulted in the regression of inflammatory changes and reduction of molecular responses across a broad range of biological processes and mechanisms (Lo Sasso et al, 2016a; Lo Sasso et al, 2016b; Phillips et al, 2016).

LINK: 15015_CVD_Resp_ApoE_SW_SR_Part 1

4.2.2.3 A/J Lung Cancer Study

To assess the impact of lifetime exposure to THS2.2 aerosol, compared with 3R4F CS, on development of emphysema and on lung tumor incidence and multiplicity, female A/J mice were exposed to fresh air (sham), 3R4F mainstream CS corresponding to 13.4 µg nicotine/L, or aerosol from THS2.2 aerosol equivalent to nicotine concentrations of 6.7 (Low), 13.4 (Medium) or 26.8 µg/L (High). Mice were exposed for 6 hours per day, 5 days per week, for up to 18 months following OECD Test Guideline 453 (OECD 2009b). In addition, two groups of male A/J mice were also exposed to fresh air (sham) and THS aerosol at 26 µg nicotine/L. Histopathological evaluation of respiratory tract organs and muscle tissues were performed at interim dissections of female mice, following 1, 5 and 10 months of exposure. The mice were also assessed at these time points for hematological and clinical chemistry parameters, lung function and pulmonary inflammation (the latter at months 1 and 5 only). Samples of nasal epithelium and lungs were collected from exposed female animals for transcriptomics and proteomics analyses.

Since this study is currently ongoing, this part of the dossier describes only the available histopathological findings and the transcriptomics data from nasal respiratory epithelial and trachea samples collected during the interim dissections at months 1, 5 and 10. Whether lifetime exposure to THS2.2 aerosol affects lung tumor incidences and multiplicities or causes pathologies in other than the respiratory organs will require analysis of samples obtained at terminal dissection.

Nasal respiratory and olfactory epithelium displayed morphological changes, identified as reserve cell and goblet cell hyperplasia and squamous metaplasia, following exposure to 3R4F CS and THS2.2 aerosol. However, the incidence and severity of these adapative lesions were generally lower in the THS2.2 aerosol-exposed mice. Similarly, reserve cell hyperplasia and squamous metaplasia in anterior and posterior laryngeal tissues were prominent histopathological findings in 3R4F CS-exposed animals and occurred less frequently and were less extensive in those exposed to THS2.2 aerosol, independent of concentration. In addition, typical CS exposure-related epithelial changes, including epithelial hyperplasia and squamous metaplasia, were found at the carina of bifurcation at months 5 and 10, while tracheas from A/J mice exposed to THS2.2 aerosol did not exhibit any remarkable exposure-related effects.

The lungs of 3R4F CS-exposed animals exhibited inflammatory cell infiltrates from month 1 onward and these were absent in the animals from the THS2.2 and sham study groups. Pigmented and unpigmented macrophages were more frequent in A/J mice exposed to 3R4F CS from month 5, while this effect was not found in those exposed to THS2.2 aerosol. Furthermore, histopathological evaluation confirmed the presence of mild to moderate emphysematous lesions in mice exposed to 3R4F CS for 5 and 10 months. In contrast, lungs of THS2.2 aerosol-exposed mice showed no signs of the alveolar destruction typical of emphysema. Neoplastic lung lesions, including nodular hyperplasia of the alveolar epithelium and bronchiolo-alveolar adenoma, were also detected from month 5 onward. Since incidence of these lesions was low at both time points, the sample number was small ($n \leq 10$) and the lesions were found across all study groups, it would be premature to draw conclusions concerning the effects of THS2.2 aerosol exposure on lung tumor incidence and/or multiplicity.

To date, transcriptomics analysis of nasal respiratory and tracheal epithelia from female animals was performed to gain insights into the potential mechanisms involved in mediating exposure effects in this mouse strain. Nasal SRPs indicated an increase in the number of DEGs, with time, when A/J mice were exposed to 3R4F CS, relative to air-exposed animals. In comparison, THS2.2 aerosol exposure caused upregulation of only one gene, *HMOX1*, in the nasal epithelium at month 10, independent of dose. Evaluating the data with the more sensitive systems toxicology approach approach indicated that the highest biological impact occurred with exposure to 3R4F CS for 10 months (RBIF = 100%; REF), whereas the impact of THS2.2 aerosol exposure on the nose was much lower and appeared to subside with time (Figure 36).

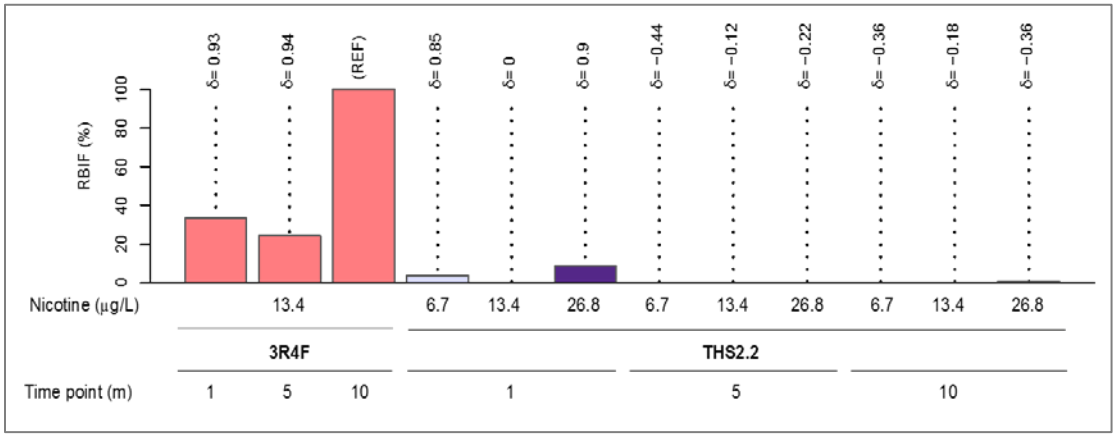


Figure 36. Network model-based analysis of the biological impact factor (BIF) in nasal tissues from A/J mice exposed to 3R4F cigarette smoke or THS2.2 aerosol, compared with air-exposed controls.

The bar plot depicts BIF values relative to the maximum response (REF, RBIF = 100%). The δ values (−1 to 1) indicate how similar the underlying network perturbations are with respect to the REF. Scores were computed using transcriptomics profiling data from lung tissues following continuous 8-month exposure of A/J mice to air, 3R4F cigarette smoke (red bars) or THS2.2 aerosol (purple bars).

Nearly all networks were already affected by month 1 with exposure to 3R4F CS and these perturbations, with very few exceptions, persisted over time. Notably, exposure to a matching (by nicotine) concentration of THS2.2 aerosol did not cause comparable network perturbations. THS2.2 aerosol at the highest concentration had a more widespread impact, albeit of smaller amplitude than did exposure to 3R4F CS. In contrast, 1-month exposure to a low dose of THS2.2 aerosol predominantly impacted networks incorporating the biology of inflammation and tissue repair, while effects on other networks were restricted to specific processes including senescence, apoptosis and oxidative stress. Prolonged exposure to THS2.2 aerosol, independent of concentration, resulted in far fewer and less extensive network perturbations than were initially seen at the earlier time point. While most networks affected by THS2.2 aerosol exposure for 5 months indicated an involvement of inflammatory processes, others, namely tissue repair and cell stress responses, appeared to be more significantly affected at month 10 (Figure 37).

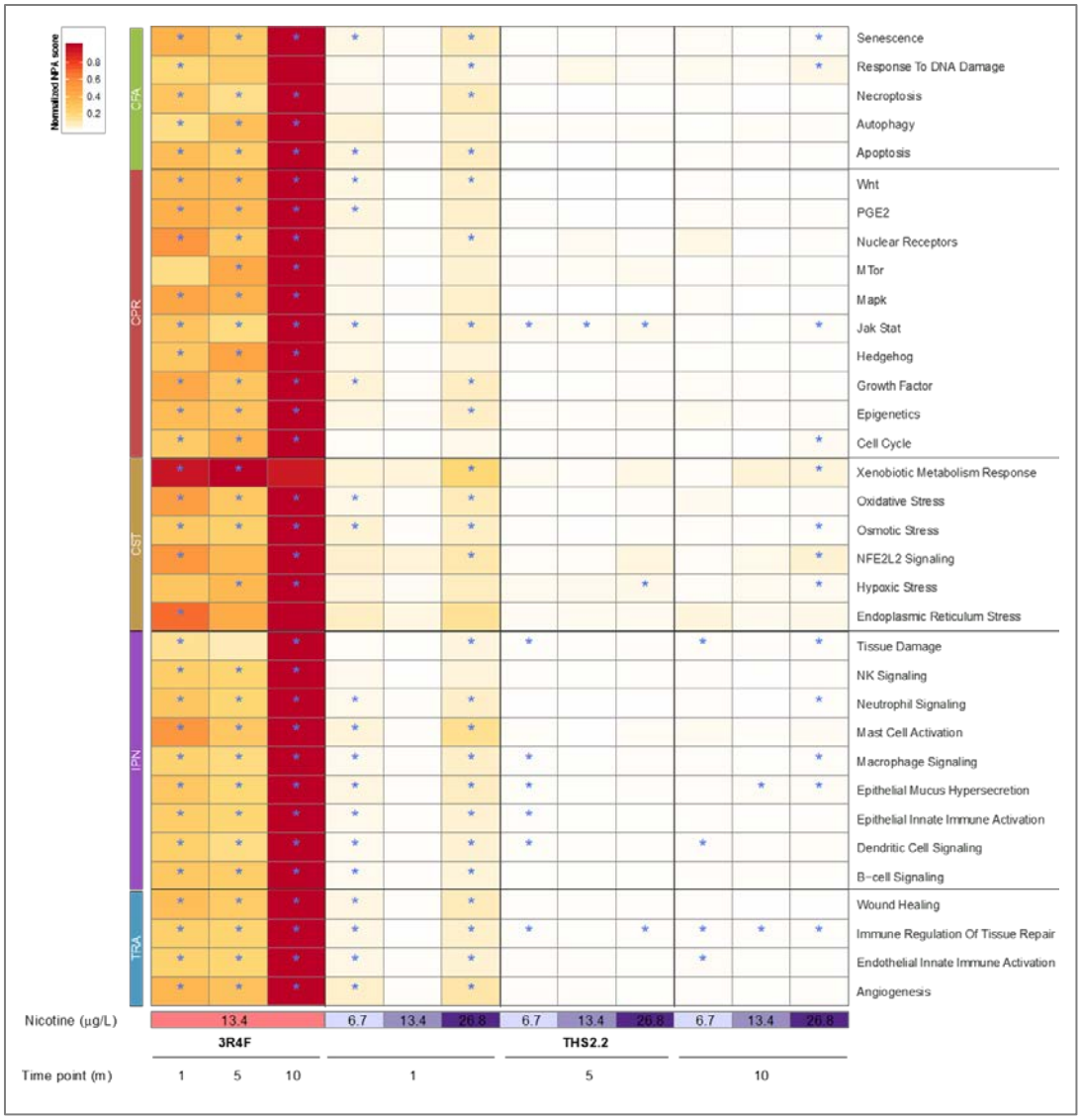


Figure 37. Network perturbations in A/J mouse nasal tissues following exposure to 3R4F cigarette smoke or THS2.2M aerosol, compared with air-exposed controls.

Heatmap of Network Perturbation Amplitude scores summarizing subnetworks which were significantly perturbed by at least one treatment. A network is considered as perturbed if, in addition to the significance of the NPA score with respect to the experimental variation, the two companion statistics (O and K), derived to inform on the specificity of the NPA score with respect to the biology described in the network, are significant. Significantly perturbed networks are indicated by * (*i.e.*, O and K statistics *p*-values <0.05 and significant with respect to the experimental variation). CFA: Cell Fate; CPR: Cell Proliferation; CST: Cell Stress; IPN: Inflammatory Process Network; TRA: Tissue Repair and Angiogenesis.

Among the cell stress responses, those related to xenobiotic metabolism, osmotic and oxidative stress were most affected by exposure to THS2.2 at the highest concentration for 1 or 10 months. However, the amplitudes of these perturbations never reached those observed in the nasal epithelium of 3R4F CS-exposed A/J mice (Figure 38).

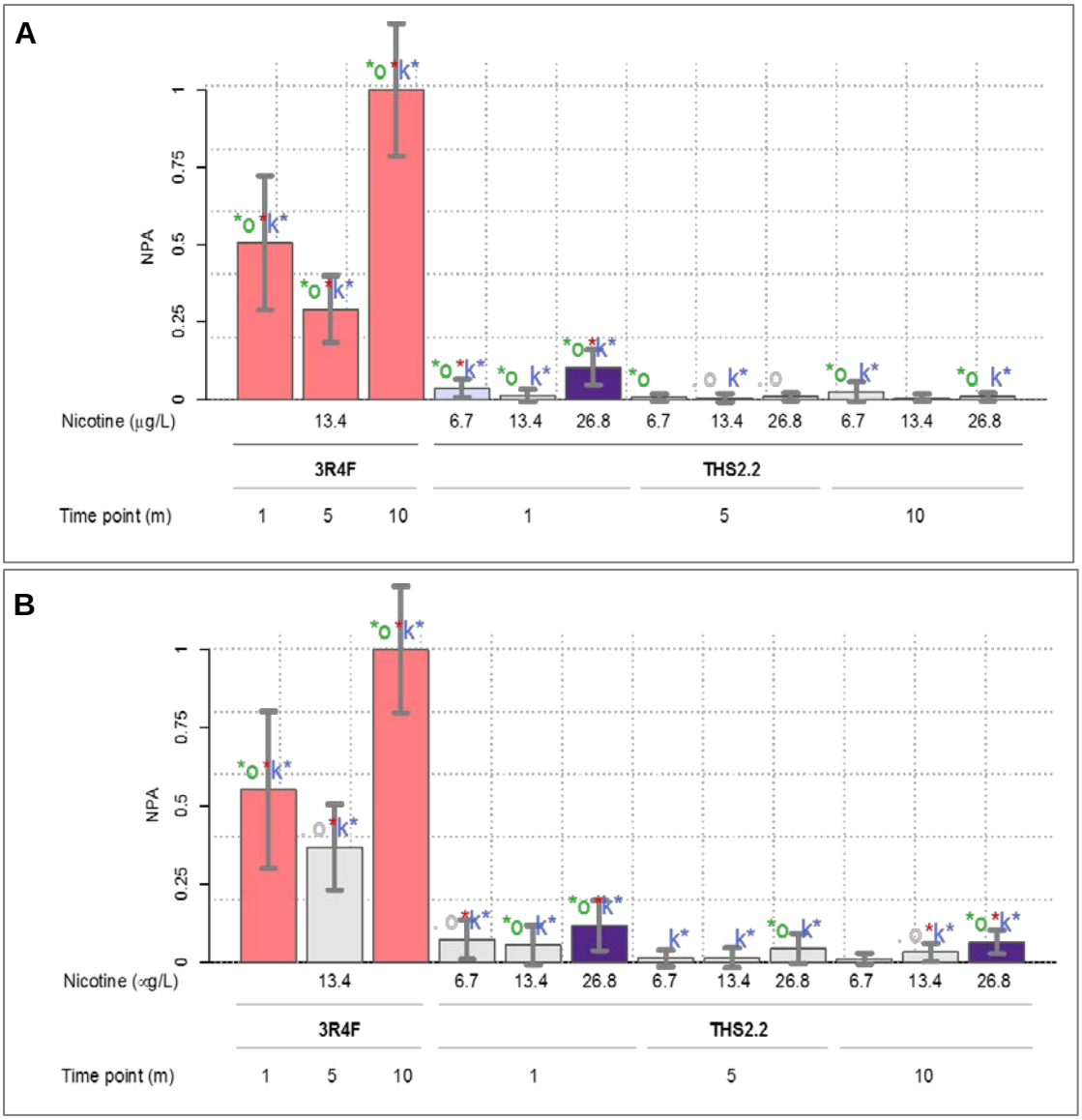


Figure 38. Relative network perturbation amplitude (NPA) of the Oxidative Stress subnetwork in A/J mouse nasal tissues exposed to 3R4F cigarette smoke or THS2.2 aerosol.

The relative NPA scores for the Oxidative Stress subnetwork model are shown with their confidence intervals accounting for experimental variation. The percentages give the relative NPA score for the subnetworks compared with the reference (treatment comparison showing the highest perturbation). In addition, companion statistics, derived to inform on the specificity of the NPA score with respect to the biology described in the respective subnetwork models, are shown as *O and K*, respectively, if their *p*-values are below the significance level. Symbol legend:*, O and K statistic *p*-values <0.05; O and K, *p*-values between 0.05 and 0.1.

Similar to the observations in nasal epithelial samples, SRPs of the trachea exhibited an increasing number of DEGs, over time, with 3R4F CS exposure. In contrast, exposure to low and medium concentrations of THS2.2 aerosol did not cause a deregulation of gene expression in this tissue. However, in animals exposed to THS2.2 aerosol at the highest

nicotine concentration for 10 months, tracheal SRPs showed significant transcriptional changes. Systems toxicology analysis of the transcriptomics data found the highest impact in tracheal samples from animals exposed to 3R4F CS (RBIF = 100%; REF), only slightly greater than that seen at month 5. THS2.2 aerosol exposure exerted a dose-dependent effect, with small differences in amplitude at various time points and, overall, smaller amplitudes than those associated with 3R4F CS exposures (Figure 39).

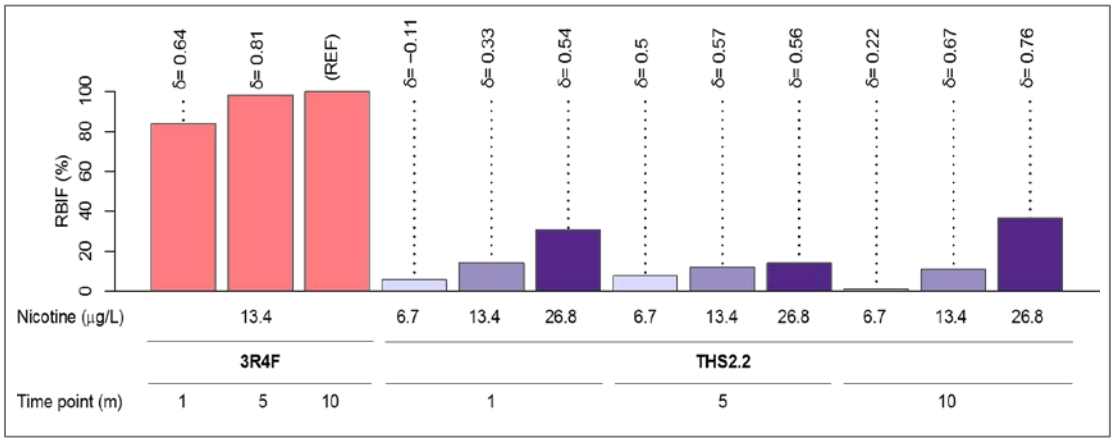


Figure 39. Network model-based analysis of the biological impact factor (BIF) in tracheal tissues from A/J mice exposed to 3R4F cigarette smoke or THS2.2 aerosol, compared with air-exposed controls.

The bar plot depicts BIF values relative to the maximum response (REF, RBIF = 100%). The δ values (−1 to 1) indicate how similar the underlying network perturbations are with respect to the REF. Scores were computed using transcriptomics profiling data from lung tissues following continuous 8-month exposure of A/J mice to air, 3R4F cigarette smoke (red bars) or THS2.2 aerosol (purple bars).

Examining the underlying biology of the 3R4F CS exposure effects identified network perturbations implicating a broad range of mechanisms. While most processes captured in the CFA network were increasingly affected by CS over time, those reflecting various mechanisms governing cell proliferation appeared to be less significantly perturbed as exposure duration increased. At matching nicotine concentrations, exposure to THS2.2 aerosol caused perturbations in many of the same networks that were also affected by 3R4F CS exposure, but these perturbations were of smaller amplitudes, with the exception of cell proliferation involving calcium signaling at month 1. Over time, perturbations in the Senescence, PGE2, Nuclear Receptor and Calcium subnetworks diminished and no longer contributed significantly to the overall impact of THS2.2 aerosol exposure. In contrast, networks encompassing mechanisms of tissue repair and innate and adaptive immune responses remained significantly impacted. Higher nicotine concentrations in THS2.2 aerosol amplified some, but not all of these responses, an effect most pronounced after 5 months of exposure (Figure 40).

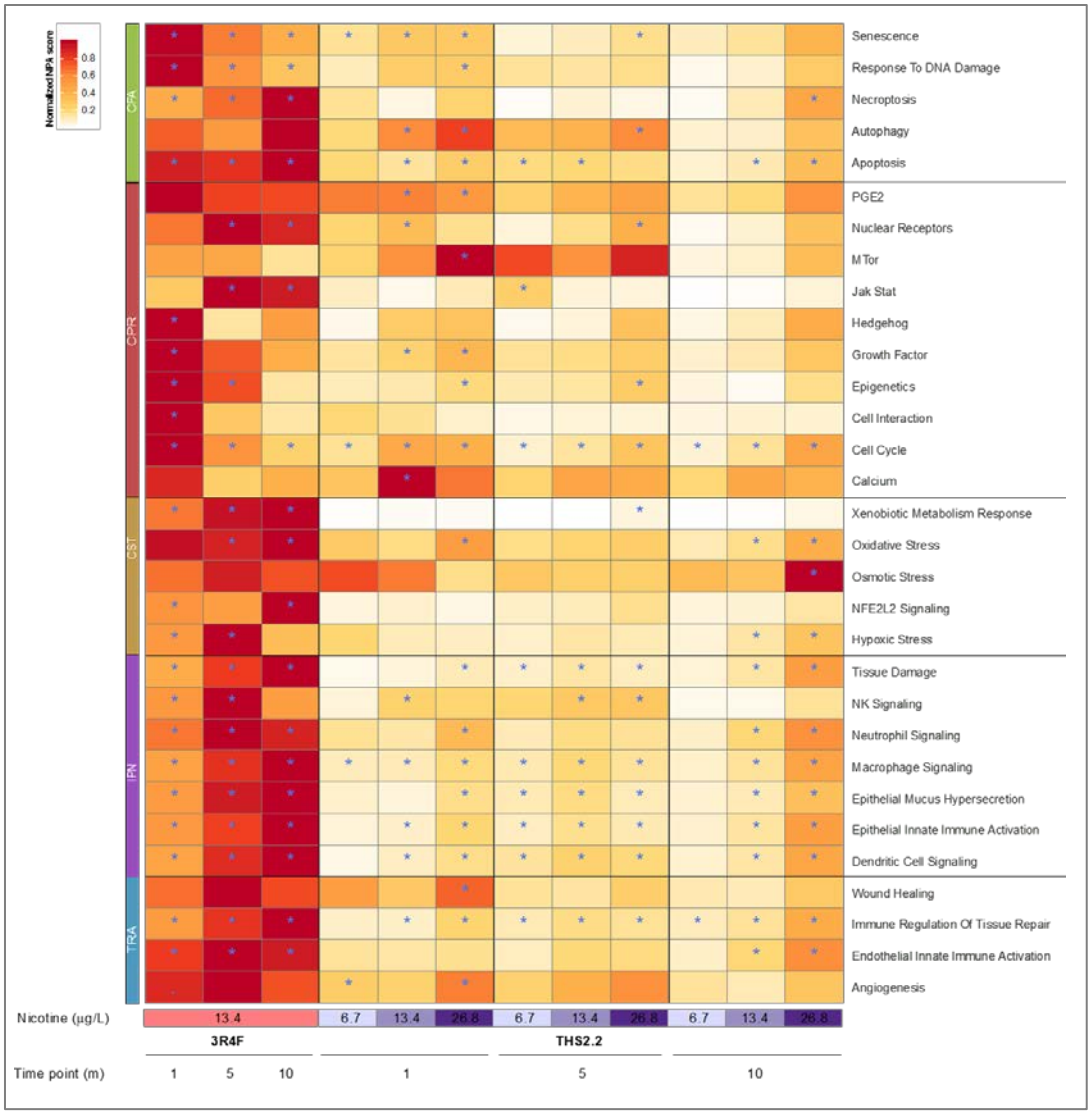


Figure 40. Network perturbations in A/J mouse tracheal tissues following exposure to 3R4F cigarette smoke or THS2.2M aerosol, compared with air-exposed controls.

The relative NPA scores for the oxidative stress subnetwork model are shown with their confidence intervals accounting for experimental variation. The percentages give the relative NPA scores for the subnetworks compared with the reference (treatment comparison showing the highest perturbation). In addition, companion statistics derived to inform on the specificity of the NPA score, with respect to the biology described in the respective subnetwork models, are shown as *O and K*, respectively, if their *p*-values are below the significance level. Symbol legend:*, O and K statistic *p*-values <0.05; O and K, *p*-values between 0.05 and 0.1. Cess: Cessation; Switch: switching. CFA: Cell Fate; CPR: Cell Proliferation; CST: Cell Stress; IPN: Inflammatory Process Network; TRA: Tissue Repair and Angiogenesis.

Rapid cell stress responses were mounted to 3R4F CS exposure, with significant contributions by xenobiotic, hypoxic and oxidative stress, but this was not seen in tracheal tissues from A/J mice exposed to THS2.2 aerosol. In these mice, significant perturbation of the Oxidative Stress subnetwork was noted only for exposures at the

matched nicotine concentration at month 10 and at the highest concentration at months 1 and 10 (Figure 41).

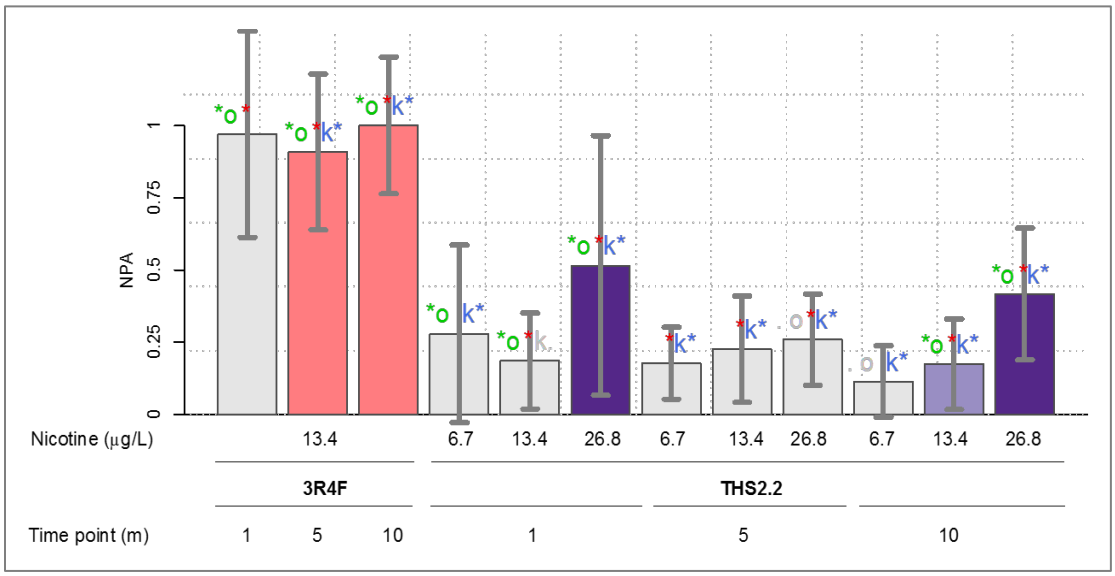


Figure 41. Relative network perturbation amplitude (NPA) of the Oxidative Stress subnetwork in A/J mouse tracheal tissues following exposure to 3R4F cigarette smoke or THS2.2 aerosol.

The relative NPA scores for the oxidative stress subnetwork model are shown with their confidence intervals accounting for experimental variation. The percentages give the relative NPA scores for the subnetworks compared with the reference (treatment comparison showing the highest perturbation). In addition, companion statistics, derived to inform on the specificity of the NPA score with respect to the biology described in the respective subnetwork models, are shown as *O and K*, respectively, if their *p*-values are below the significance level. Symbol legend:*, O and K statistic *p*-values <0.05; O and K, *p*-values between 0.05 and 0.1.

Together these preliminary data showed moderate to severe adaptive and degenerative changes in the upper respiratory tract organs of 3R4F CS-exposed A/J mice, while such adaptative changes were far less frequent and severe in the THS2.2 aerosol-exposed animals. In addition, molecular changes observed in the nasal respiratory and tracheal epithelium following 3R4F CS exposure were extensive, affecting a broad range of mechanisms. In comparison, the biological impact of THS2.2 aerosol exposure was much less pronounced and sustained.

LINK: 15020_AJ LC_QA-checked Interim Report

5. CONCLUSIONS

Any change in the cellular environment can induce stress to a cell and is generally counteracted by the initiation of an intricate, tightly regulated cellular stress response aimed at either amelioration of or adaptation to the stress (Milisav, 2011b). Stress response profiles or stress pathway activation patterns are thought to provide useful insights into the specific stress signatures that are linked to cell fate and the mechanisms of action of suspected toxicants. Thus, "stress signatures" could be employed to assess toxicity of chemical compounds or compound mixtures in *in vitro* and *in vivo* biological systems (Demirovic & Rattan, 2013; Simmons et al, 2009). Utilizing 'omics technologies to elucidate mechanisms governing stress reponses as previously proposed (Bross et al, 2010), together with a number of novel computational tools, has enabled complex analysis of the impact a compound exerts on any biological system.

In vitro studies in endothelial and monocytic cells demonstrated that exposure to THS2.2 aerosol had little effect on monocyte adhesion and caused only transient cellular stress responses. Similarly, studies in NHBECs confirmed that THS2.2 aerosol fractions had little or no cytotoxic and genotoxic potential, eliciting predominantly physiological stress responses. Results from organotypic studies, using a variety of reconstructed human epithelia that closely mimic the upper aerodigestive tract, corroborated findings of low biological impact with THS2.2 aerosol exposures. These experiments showed that exposure to 3R4F CS resulted in time- and dose-dependent cytotoxicity, tissue damage and oxidative stress, while exposure effects following THS2.2 aerosol exposure were far less extensive and limited in duration. Furthermore, the results of *in vivo* inhalation studies demonstrated that exposure to THS2.2 aerosol, at matching or even higher nicotine concentrations, elicited epithelial morphological changes in the respiratory organs of rats and mice that were generally less frequent and less severe than with exposure to CS from 3R4F. Mechanistic analyses in nasal respiratory epithelial, bronchial epithelial and lung parenchyma samples from the exposed animals identified several types of cellular stress responses to THS2.2 aerosol exposure. Of note, these stress responses were considerably weaker than those evoked by exposure to 3R4F CS, confirming an overall lower biological impact in experimental *in vivo* systems. In addition, switching to THS2.2 aerosol exposure after 2-month 3R4F CS exposure did not cause further aggravation of CS exposure-related cellular stress responses, as shown by the reduction in cellular stress subnetwork perturbations in a mouse model of CVD and emphysema. On the contrary, switching appeared to rapidly alleviate cellular stress responses, with sustained low activity over extended periods of time. These trends were also seen for the inflammatory responses investigated in the same studies (see companion document on inflammation in this dossier).

Overall, the data obtained in these nonclinical studies demonstrated that exposure to THS2.2 aerosol did not cause systemic toxicity and caused very low or no toxicity in the respiratory tracts of laboratory animals. Therefore, and in combination with the *in vitro* systems toxicology data collected, it is most likely that human adults using THS2.2 will not be exposed to additional hazards, as compared with those smoking conventional cigarettes.

6. REFERENCES

(GOLD) GIfCOLD. (2013) Global Strategy for the Diagnosis, Management and Prevention of COPD.

Adams MR, Jessup W, Celermajer DS (1997) Cigarette smoking is associated with increased human monocyte adhesion to endothelial cells: reversibility with oral L-arginine but not vitamin C. Journal of the American College of Cardiology 29: 491-497

Adamson J, Phillips G, Haswell LE, Gaça MD (2011) In Vitro Models of Chronic Obstructive Pulmonary Disease (COPD): INTECH Open Access Publisher.

Albino A, Huang X, Jorgensen E, Yang J, Gietl D, Traganos F, Darzynkiewicz Z (2004) Induction of H2AX phosphorylation in pulmonary cells by tobacco smoke: a new assay for carcinogens. Cell Cycle 3: 1060-1066

Albino AP, Huang X, Jorgensen ED, Gietl D, Traganos F, Darzynkiewicz Z (2006) Induction of DNA double-strand breaks in A549 and normal human pulmonary epithelial cells by cigarette smoke is mediated by free radicals. International Journal of Oncology 28: 1491-1505

Anguissola S, Garry D, Salvati A, O'Brien PJ, Dawson KA (2014) High content analysis provides mechanistic insights on the pathways of toxicity induced by amine-modified polystyrene nanoparticles.

Aoshiba K, Zhou F, Tsuji T, Nagai A (2012) DNA damage as a molecular link in the pathogenesis of COPD in smokers. European Respiratory Journal 39: 1368-1376

Aramburu J, Drews-Elger K, Estrada-Gelonch A, Minguillón J, Morancho B, Santiago V, López-Rodríguez C (2006) Regulation of the hypertonic stress response and other cellular functions by the Rel-like transcription factor NFAT5. Biochemical Pharmacology 72: 1597-1604

Arunachalam G, Sundar IK, Hwang J-w, Yao H, Rahman I (2010) Emphysema is associated with increased inflammation in lungs of atherosclerosis-prone mice by cigarette smoke: implications in comorbidities of COPD. Journal of Inflammation (London, England) 7: 34-34

Asmat U, Abad K, Ismail K (2015) Diabetes mellitus and oxidative stress—A concise review. Saudi Pharmaceutical Journal

Austin RC (2009) The Unfolded Protein Response in Health and Disease Antioxidants & Redox Signaling 11: 2279-2287

Barreiro E, Fermoselle C, Mateu-Jimenez M, Sánchez-Font A, Pijuan L, Gea J, Curull V (2013) Oxidative stress and inflammation in the normal airways and blood of patients with lung cancer and COPD. Free Radical Biology and Medicine 65: 859-871

Barzilai A, Yamamoto K-I (2004) DNA damage responses to oxidative stress. DNA Repair 3: 1109-1115

Basu S (2008) F2-Isoprostanes in Human Health and Diseases: From Molecular Mechanisms to Clinical Implications Antioxidants & Redox Signaling 10: 1405-1434

Benhar M, Dalyot I, Engelberg D, Levitzki A (2001) Enhanced ROS Production in Oncogenically Transformed Cells Potentiates c-Jun N-Terminal Kinase and p38 Mitogen-Activated Protein Kinase Activation and Sensitization to Genotoxic Stress. Molecular and Cellular Biology 21: 6913-6926

Benhar M, Engelberg D, Levitzki A (2002) ROS, stress-activated kinases and stress signaling in cancer. EMBO Rep 3: 420-425

Berridge MJ. (2012) Cell Stress, Inflammatory Responses and Cell Death. Cell Signalling Biology. Portland Press.

Bloomer R (2007) Decreased blood antioxidant capacity and increased lipid peroxidation in young cigarette smokers compared to nonsmokers: Impact of dietary intake. Nutrition Journal 6: 39

Boelens J, Lust S, Offner F, Bracke ME, Vanhoecke BW (2007) The Endoplasmic Reticulum: A Target for New Anticancer Drugs. In Vivo 21: 215-226

Bosio A, Knörr C, Janssen U, Gebel S, Haussmann H-J, Müller T (2002) Kinetics of gene expression profiling in Swiss 3T3 cells exposed to aqueous extracts of cigarette smoke. Carcinogenesis 23: 741-748

Boué S, De León H, Schlage WK, Peck MJ, Weiler H, Berges A, Vuillaume G, Martin F, Friedrichs B, Lebrun S (2013) Cigarette smoke induces molecular responses in respiratory tissues of ApoE−/− mice that are progressively deactivated upon cessation. Toxicology 314: 112-124

Brahimi-Horn C, Pouysségur J (2006) The role of the hypoxia-inducible factor in tumor metabolism growth and invasion. Bulletin du Cancer 93: E73-E80

Brocker C, Thompson DC, Vasiliou V (2012) The role of hyperosmotic stress in inflammation and disease. Biomol Concepts 3: 345-364

Bross P, Palmfeldt J, Hansen J, Vang S, Gregersen N (2010) Measuring consequences of protein misfolding and cellular stress using OMICS techniques. Protein Misfolding and Cellular Stress in Disease and Aging: Concepts and Protocols: 119-135

Brunet A, Sweeney LB, Sturgill JF, Chua KF, Greer PL, Lin Y, Tran H, Ross SE, Mostoslavsky R, Cohen HY, Hu LS, Cheng H-L, Jedrychowski MP, Gygi SP, Sinclair DA, Alt FW, Greenberg ME (2004) Stress-Dependent Regulation of FOXO Transcription Factors by the SIRT1 Deacetylase. Science 303: 2011-2015

Brusselle GG, Bracke KR, Maes T, D'Hulst A I, Moerloose KB, Joos GF, Pauwels RA (2006) Murine models of COPD. Pulm Pharmacol Ther 19: 155-165

Burdon RH (1995) Superoxide and hydrogen peroxide in relation to mammalian cell proliferation. Free Radical Biology and Medicine 18: 775-794

Burg MB, Ferraris JD, Dmitrieva NI (2007) Cellular Response to Hyperosmotic Stresses. Physiological Reviews 87: 1441-1474

Cabanski M, Fields B, Boue S, Boukharov N, DeLeon H, Dror N, Geertz M, Guedj E, Iskandar A, Kogel U (2015) Transcriptional profiling and targeted proteomics reveals common molecular changes associated with cigarette smoke-induced lung emphysema development in five susceptible mouse strains. Inflammation Research: 1-16

Cai H, Harrison DG (2000) Endothelial Dysfunction in Cardiovascular Diseases: The Role of Oxidant Stress. Circulation Research 87: 840-844

Caramori G, Adcock IM, Casolari P, Ito K, Jazrawi E, Tsaprouni L, Villetti G, Civelli M, Carnini C, Chung KF, Barnes PJ, Papi A (2011) Unbalanced oxidant-induced DNA damage and repair in COPD: a link towards lung cancer. Thorax 66: 521-527

Carnevali S, Petruzzelli S, Longoni B, Vanacore R, Barale R, Cipollini M, Scatena F, Paggiaro P, Celi A, Giuntini C (2003) Cigarette smoke extract induces oxidative stress and apoptosis in human lung fibroblasts. American Journal of Physiology Lung Cellular and Molecular Physiology 284: L955-L963

Catanzaro DF, Zhou Y, Chen R, Yu F, Catanzaro SE, De Lorenzo MS, Subbaramaiah K, Zhou XK, Pratico D, Dannenberg AJ (2007) Potentially reduced exposure cigarettes accelerate atherosclerosis: evidence for the role of nicotine. Cardiovascular toxicology 7: 192-201

Cavallo D, Ursini CL, Fresegna AM, Maiello R, Ciervo A, Ferrante R, Buresti G, Iavicoli S (2013) Cyto-genotoxic effects of smoke from commercial filter and non-filter cigarettes on human bronchial and pulmonary cells. Mutation Research/Genetic Toxicology and Environmental Mutagenesis 750: 1-11

Ceriello A, Motz E (2004) Is oxidative stress the pathogenic mechanism underlying insulin resistance, diabetes, and cardiovascular disease? The common soil hypothesis revisited. Arteriosclerosis, Thrombosis, and Vascular Biology 24: 816-823

Chatterjee N, Eom HJ, Choi J (2014) Effects of silver nanoparticles on oxidative DNA damage–repair as a function of p38 MAPK status: A comparative approach using human Jurkat T cells and the nematode Caenorhabditis elegans. Environmental and Molecular Mutagenesis 55: 122-133

Chehne F, Oguogho A, Lupattelli G, Budinsky AC, Palumbo B, Sinzinger H (2001) Increase of isoprostane 8-epi-PGF2 αafter restarting smoking. Prostaglandins, Leukotrienes and Essential Fatty Acids 64: 307-310

Chen H-W, Chien M-L, Chaung Y-H, Lii C-K, Wang T-S (2004) Extracts from cigarette smoke induce DNA damage and cell adhesion molecule expression through different pathways. Chemico-Biological Interactions 150: 233-241

Chen J, Higby R, Tian D, Tan D, Johnson MD, Xiao Y, Kellar KJ, Feng S, Shields PG (2008a) Toxicological Analysis of Low-Nicotine and Nicotine-Free Cigarettes. Toxicology 249: 194-203

Chen Z-H, Kim HP, Sciurba FC, Lee S-J, Feghali-Bostwick C, Stolz DB, Dhir R, Landreneau RJ, Schuchert MJ, Yousem SA, Nakahira K, Pilewski JM, Lee JS, Zhang Y, Ryter SW, Choi AMK (2008b) Egr-1 Regulates Autophagy in Cigarette Smoke-Induced Chronic Obstructive Pulmonary Disease. PLoS ONE 3: e3316

Churg A, Cosio M, Wright JL (2008) Mechanisms of cigarette smoke-induced COPD: insights from animal models. AmJ Physiol Lung Cell MolPhysiol 294: L612-L631

Churg A, Sin DD, Wright JL (2011) Everything prevents emphysema: are animal models of cigarette smoke-induced chronic obstructive pulmonary disease any use? Am J Respir Cell Mol Biol 45: 1111-1115

Churg A, Tai H, Coulthard T, Wang R, Wright JL (2006) Cigarette smoke drives small airway remodeling by induction of growth factors in the airway wall. Am J Respir Crit Care Med 174: 1327-1334

Ciccia A, Elledge SJ (2010) The DNA Damage Response: Making It Safe to Play with Knives. Molecular Cell 40: 179-204

Csordas A, Kreutmayer S, Ploner C, Braun PR, Karlas A, Backovic A, Wick G, Bernhard D (2011) Cigarette smoke extract induces prolonged endoplasmic reticulum stress and autophagic cell death in human umbilical vein endothelial cells. Cardiovascular Research 92: 141-148

Cuda G, Paternò R, Ceravolo R, Candigliota M, Perrotti N, Perticone F, Faniello MC, Schepis F, Ruocco A, Mele E, Cassano S, Bifulco M, Santillo M, Avvedimento EV (2002) Protection of Human Endothelial Cells From Oxidative Stress: Role of Ras-ERK1/2 Signaling. Circulation 105: 968-974

Daugherty A, Puré E, Delfel-Butteiger D, Chen S, Leferovich J, Roselaar SE, Rader DJ (1997) The effects of total lymphocyte deficiency on the extent of atherosclerosis in apolipoprotein E-/-mice. Journal of Clinical Investigation 100: 1575

de Nadal E, Alepuz PM, Posas F (2002) Dealing with osmostress through MAP kinase activation. EMBO Rep 3: 735-740

Deanfield JE, Halcox JP, Rabelink TJ (2007) Endothelial Function and Dysfunction: Testing and Clinical Relevance. Circulation 115: 1285-1295

DeMarini DM, Gudi R, Szkudlinska A, Rao M, Recio L, Kehl M, Kirby PE, Polzin G, Richter PA (2008) Genotoxicity of 10 cigarette smoke condensates in four test systems: Comparisons between assays and condensates. Mutation Research/Genetic Toxicology and Environmental Mutagenesis 650: 15-29

Demirovic D, Rattan SIS (2013) Establishing cellular stress response profiles as biomarkers of homeodynamics, health and hormesis. Experimental Gerontology 48: 94-98

Deng X, Luyendyk JP, Ganey PE, Roth RA (2009) Inflammatory Stress and Idiosyncratic Hepatotoxicity: Hints from Animal Models. Pharmacological Reviews 61: 262-282

Deslee G, Adair-Kirk TL, Betsuyaku T, Woods JC, Moore CH, Gierada DS, Conradi SH, Atkinson JJ, Toennies HM, Battaile JT, Kobayashi DK, Patterson GA, Holtzman MJ, Pierce RA (2010) Cigarette Smoke Induces Nucleic-Acid Oxidation in Lung Fibroblasts. American Journal of Respiratory Cell and Molecular Biology 43: 576-584

Deslee G, Woods JC, Moore C, Conradi SH, Gierada DS, Atkinson JJ, Battaile JT, Liu L, Patterson GA, Adair-Kirk TL, Holtzman MJ, Pierce RA (2009) Oxidative damage to nucleic acids in severe emphysema. CHEST Journal 135: 965-974

Dewhirst MW (2009) Relationships between cycling hypoxia, HIF-1, angiogenesis and oxidative stress. Radiation Research 172: 653-665

Di Pietro A, Visalli G, Munaò F, Baluce B, La Maestra S, Primerano P, Corigliano F, De Flora S (2009) Oxidative damage in human epithelial alveolar cells exposed in vitro to oil fly ash transition metals. International journal of hygiene and environmental health 212: 196-208

Doll R, Peto R (1981) The causes of cancer: quantitative estimates of avoidable risks of cancer in the United States today. Journal of the National Cancer Institute 66: 1191-1308

Doll R, Peto R, Boreham J, Sutherland I (2004) Mortality in relation to smoking: 50 years' observations on male British doctors. BMJ 328: 1519

Dong ZM, Brown AA, Wagner DD (2000) Prominent role of P-selectin in the development of advanced atherosclerosis in ApoE-deficient mice. Circulation 101: 2290-2295

Dovgan P, Edwards J, Zhan X, Wilde M, Agrawal D (1994) Cigarette smoking increases monocyte adherence to cultured endothelial cell monolayer. Biochemical and Biophysical Research Communications 203: 929-934

Durham AL, Adcock IM (2015) The relationship between COPD and lung cancer. Lung Cancer 90: 121-127

Dvorak A, Tilley AE, Shaykhiev R, Wang R, Crystal RG (2011) Do airway epithelium air–liquid cultures represent the in vivo airway epithelium transcriptome? American Journal of Respiratory Cell and Molecular Biology 44: 465-473

Edirisinghe I, Yang S-R, Yao H, Rajendrasozhan S, Caito S, Adenuga D, Wong C, Rahman A, Phipps RP, Jin Z-G, Rahman I (2008) VEGFR-2 inhibition augments cigarette smoke-induced oxidative stress and inflammatory responses leading to endothelial dysfunction. The FASEB Journal 22: 2297-2310

Eisner V, Criollo A, Quiroga C, Olea-Azar C, Santibañez JF, Troncoso R, Chiong M, Díaz-Araya G, Foncea R, Lavandero S (2006) Hyperosmotic stress-dependent NFκB activation is regulated by reactive oxygen species and IGF-1 in cultured cardiomyocytes. FEBS Letters 580: 4495-4500

Erler JT, Bennewith KL, Nicolau M, Dornhofer N, Kong C, Le Q-T, Chi J-TA, Jeffrey SS, Giaccia AJ (2006) Lysyl oxidase is essential for hypoxia-induced metastasis. Nature 440: 1222-1226

Facchinetti F, Amadei F, Geppetti P, Tarantini F, Di Serio C, Dragotto A, Gigli PM, Catinella S, Civelli M, Patacchini R (2007) α,β-Unsaturated Aldehydes in Cigarette Smoke Release Inflammatory Mediators from Human Macrophages. American Journal of Respiratory Cell and Molecular Biology 37: 617-623

Fahn H-J, Wang L-S, Kao S-H, Chang S-C, Huang M-H, Wei Y-H (1998) Smoking-Associated Mitochondrial DNA Mutations and Lipid Peroxidation in Human Lung Tissues. American Journal of Respiratory Cell and Molecular Biology 19: 901-909

Faux SP, Tai T, Thorne D, Xu Y, Breheny D, Gaca M (2009) The role of oxidative stress in the biological responses of lung epithelial cells to cigarette smoke. Biomarkers 14: 90-96

Fayolle C, Pourchet J, de Fromentel CC, Puisieux A, Dore J-F, Voeltzel T (2007) Gadd45a Activation Protects Melanoma Cells from Ultraviolet B-Induced Apoptosis. J Invest Dermatol 128: 196-202

Fearon IM, Faux SP (2009) Oxidative stress and cardiovascular disease: novel tools give (free) radical insight. Journal of Molecular and Cellular Cardiology 47: 372-381

Fearon IM, Gaça MD, Nordskog BK (2013) In vitro models for assessing the potential cardiovascular disease risk associated with cigarette smoking. Toxicology in Vitro 27: 513-522

Fearon IM, Phillips G, Carr T, Taylor M, Breheny D, Faux SP (2011) The Role of Oxidative Stress in Smoking-Related Diseases. Mini-Reviews in Organic Chemistry 8: 360-371

Federico A, Morgillo F, Tuccillo C, Ciardiello F, Loguercio C (2007) Chronic inflammation and oxidative stress in human carcinogenesis. International Journal of Cancer 121: 2381-2386

Finan JD, Guilak F (2010) The effects of osmotic stress on the structure and function of the cell nucleus. Journal of Cellular Biochemistry 109: 460-467

Food U, Administration D (2012) Harmful and potentially harmful constituents in tobacco products and tobacco smoke; established list. Fed Regist 77: 20034-20037

Förstermann U (2010) Nitric oxide and oxidative stress in vascular disease. Pflugers Arch - Eur J Physiol 459: 923-939

Fritsch-Decker S, Both T, Mülhopt S, Paur H-R, Weiss C, Diabaté S (2011) Regulation of the arachidonic acid mobilization in macrophages by combustion-derived particles. Particle and Fibre Toxicology 8: 23-23

Fulda S, Gorman AM, Hori O, Samali A (2010) Cellular Stress Responses: Cell Survival and Cell Death. International Journal of Cell Biology 2010

Gairola CG, Drawdy ML, Block AE, Daugherty A (2001) Sidestream cigarette smoke accelerates atherogenesis in apolipoprotein E−/− mice. Atherosclerosis 156: 49-55

Gairola CG, Howatt DA, Daugherty A (2010) Dietary coenzyme Q10 does not protect against cigarette smoke-augmented atherosclerosis in apoE-deficient mice. Free Radical Biology and Medicine 48: 1535-1539

Gál K, Cseh Á, Szalay B, Rusai K, Vannay Á, Lukácsovits J, Heemann U, Szabó A, Losonczy G, Tamási L, Müller V (2011) Effect of cigarette smoke and dexamethasone on Hsp72 system of alveolar epithelial cells. Cell Stress and Chaperones 16: 369-378

Garcia-Canton C, Anadon A, Meredith C (2013) Genotoxicity evaluation of individual cigarette smoke toxicants using the in vitro γH2AX assay by High Content Screening. Toxicology letters 223: 81-87

Garcia-Canton C, Anadón A, Meredith C (2012) γH2AX as a novel endpoint to detect DNA damage: applications for the assessment of the in vitro genotoxicity of cigarette smoke. Toxicology in Vitro 26: 1075-1086

Garcia-Canton C, Errington G, Anadon A, Meredith C (2014) Characterisation of an aerosol exposure system to evaluate the genotoxicity of whole mainstream cigarette smoke using the in vitro gamma-H2AX assay by high content screening. BMC Pharmacology and Toxicology 15: 41

Gardner L, Corn PG (2008) Hypoxic regulation of mRNA expression. Cell Cycle 7: 1916-1924

Garside H, Marcoe KF, Chesnut-Speelman J, Foster AJ, Muthas D, Gerry Kenna J, Warrior U, Bowes J, Baumgartner J (2014) Evaluation of the use of imaging parameters for the detection of compound-induced hepatotoxicity in 384-well cultures of HepG2 cells and cryopreserved primary human hepatocytes. Toxicology in Vitro 28: 171-181

Gawaz M, Langer H, May AE (2005) Platelets in inflammation and atherogenesis. The Journal of Clinical Investigation 115: 3378-3384

Gebel S, Gerstmayer B, Bosio A, Haussmann H-J, Miert EV, Müller T (2004) Gene expression profiling in respiratory tissues from rats exposed to mainstream cigarette smoke. Carcinogenesis 25: 169-178

Getz GS, Reardon CA (2012) Animal Models of Atherosclerosis. Arteriosclerosis, Thrombosis, and Vascular Biology 32: 1104-1115

Ghio AJ, Dailey LA, Soukup JM, Stonehuerner J, Richards JH, Devlin RB (2013) Growth of human bronchial epithelial cells at an air-liquid interface alters the response to particle exposure. Particle and Fibre Toxicology 10: 1-8

Giannakou ME, Partridge L (2004) The interaction between FOXO and SIRT1: tipping the balance towards survival. Trends in Cell Biology 14: 408-412

Glick D, Barth S, Macleod KF (2010) Autophagy: cellular and molecular mechanisms. The Journal of Pathology 221: 3-12

Glover-Cutter KM, Lin S, Blackwell TK (2013) Integration of the Unfolded Protein and Oxidative Stress Responses through SKN-1/Nrf. PLoS Genet 9: e1003701

Gonzalez-Suarez I, Martin F, Marescotti D, Guedj E, Acali S, Johne S, Dulize R, Baumer K, Peric D, Goedertier D, Frentzel S, Ivanov NV, Mathis C, Hoeng J, Peitsch MC (2016) In Vitro Systems Toxicology Assessment of a Candidate Modified Risk Tobacco Product Shows Reduced Toxicity Compared to That of a Conventional Cigarette. Chemical Research in Toxicology 29: 3-18

Gonzalez-Suarez I, Sewer A, Walker P, Mathis C, Ellis S, Woodhouse H, Guedj E, Dulize R, Marescotti D, Acali S (2014) Systems biology approach for evaluating the biological impact of environmental toxicants in vitro. Chemical Research in Toxicology 27: 367-376

Gray TE, Guzman K, Davis CW, Abdullah LH, Nettesheim P (1996) Mucociliary differentiation of serially passaged normal human tracheobronchial epithelial cells. American Journal of Respiratory Cell and Molecular Biology 14: 104-112

Greer SN, Metcalf JL, Wang Y, Ohh M (2012) The updated biology of hypoxia-inducible factor. EMBO J 31: 2448-2460

Groneberg DA, Chung KF (2004) Models of chronic obstructive pulmonary disease. Respir Res 5: 18

Guarente L (2007) Sirtuins in Aging and Disease. Cold Spring Harbor Symposia on Quantitative Biology 72: 483-488

Halliwell B (2007) Oxidative stress and cancer: have we moved forward? Biochem J 401: 1-11

Halliwell B, Whiteman M (2004) Measuring reactive species and oxidative damage in vivo and in cell culture: how should you do it and what do the results mean? British Journal of Pharmacology 142: 231-255

Harding HP, Novoa I, Zhang Y, Zeng H, Wek R, Schapira M, Ron D (2000) Regulated Translation Initiation Controls Stress-Induced Gene Expression in Mammalian Cells. Molecular Cell 6: 1099-1108

Harding HP, Zhang Y, Zeng H, Novoa I, Lu PD, Calfon M, Sadri N, Yun C, Popko B, Paules R, Stojdl DF, Bell JC, Hettmann T, Leiden JM, Ron D (2003) An Integrated Stress Response Regulates Amino Acid Metabolism and Resistance to Oxidative Stress. Molecular Cell 11: 619-633

Harris JE, Thun MJ, Mondul AM, Calle EE (2004) Cigarette tar yields in relation to mortality from lung cancer in the cancer prevention study II prospective cohort, 1982-8. BMJ 328: 72

Harrison D, Griendling KK, Landmesser U, Hornig B, Drexler H (2003) Role of oxidative stress in atherosclerosis. The American journal of cardiology 91: 7-11

Helmersson J, Larsson A, Vessby B, Basu S (2005) Active smoking and a history of smoking are associated with enhanced prostaglandin F2α, interleukin-6 and F2-isoprostane formation in elderly men. Atherosclerosis 181: 201-207

Henderson B, Csordas A, Backovic A, Kind M, Bernhard D, Wick G (2008) Cigarette smoke is an endothelial stressor and leads to cell cycle arrest. Atherosclerosis 201: 298-305

Hengstermann A, Müller T (2008) Endoplasmic reticulum stress induced by aqueous extracts of cigarette smoke in 3T3 cells activates the unfolded-protein-response-dependent PERK pathway of cell survival. Free Radic Biol Med 44: 1097-1107

Hodge S, Matthews G, Mukaro V, Ahern J, Shivam A, Hodge G, Holmes M, Jersmann H, Reynolds PN (2011) Cigarette Smoke-Induced Changes to Alveolar Macrophage Phenotype and Function Are Improved by Treatment with Procysteine. American Journal of Respiratory Cell and Molecular Biology 44: 673-681

Hoeng J, Deehan R, Pratt D, Martin F, Sewer A, Thomson TM, Drubin DA, Waters CA, de Graaf D, Peitsch MC (2012) A network-based approach to quantifying the impact of biologically active substances. Drug Discovery Today 17: 413-418

Hogg JC, Chu F, Utokaparch S, Woods R, Elliott WM, Buzatu L, Cherniack RM, Rogers RM, Sciurba FC, Coxson HO, Pare PD (2004) The nature of small-airway obstruction in chronic obstructive pulmonary disease. N Engl J Med 350: 2645-2653

Hu W, Xie J, Zhao J, Xu Y, Yang S, Ni W (2009) Involvement of Bcl-2 Family in Apoptosis and Signal Pathways Induced by Cigarette Smoke Extract in the Human Airway Smooth Muscle Cells DNA and Cell Biology 28: 13-22

Hwang J-w, Chung S, Sundar IK, Yao H, Arunachalam G, McBurney MW, Rahman I (2010) Cigarette smoke-induced autophagy is regulated by SIRT1–PARP-1-dependent mechanism: Implication in pathogenesis of COPD. Archives of Biochemistry and Biophysics 500: 203-209

Hwang J-w, Yao H, Caito S, Sundar IK, Rahman I (2013) Redox regulation of SIRT1 in inflammation and cellular senescence. Free Radical Biology and Medicine 61: 95-110

Ioannidis I, Ye F, McNally B, Willette M, Flaño E (2013) Toll-like receptor expression and induction of type I and type III interferons in primary airway epithelial cells. Journal of virology 87: 3261-3270

Ishii T, Itoh K, Yamamoto M (2002) Roles of Nrf2 in activation of antioxidant enzyme genes via antioxidant responsive elements. Methods in Enzymology 348: 182-190

Iskandar A, Mathis C, Martin F, Leroy P, Sewer A, Majeed S, Kuehn D, Trivedi K, Grandolfo D, Cabanski M (2016) 3-D nasal cultures: Systems toxicological assessment of a candidate modified-risk tobacco product. ALTEX: [Epub ahead of print]

Jackson SP (2002) Sensing and repairing DNA double-strand breaks. Carcinogenesis 23: 687-696

Janssen LJ (2001) Isoprostanes: an overview and putative roles in pulmonary pathophysiology. American Journal of Physiology - Lung Cellular and Molecular Physiology 280: L1067-L1082

Jetten AM (1989) Multistep process of squamous differentiation in tracheobronchial epithelial cells in vitro: analogy with epidermal differentiation. Environmental health perspectives 80: 149

Jiang H-Y, Wek RC (2005) Phosphorylation of the α-Subunit of the Eukaryotic Initiation Factor-2 (eIF2α) Reduces Protein Synthesis and Enhances Apoptosis in Response to Proteasome Inhibition. Journal of Biological Chemistry 280: 14189-14202

Jin L, Yang H, Fu J, Xue X, Yao LI, Qiao LIN (2015) Association between oxidative DNA damage and the expression of 8-oxoguanine DNA glycosylase 1 in lung epithelial cells of neonatal rats exposed to hyperoxia. Molecular Medicine Reports 11: 4079-4086

Jorgensen E, Stinson A, Shan L, Yang J, Gietl D, Albino A (2008) Cigarette smoke induces endoplasmic reticulum stress and the unfolded protein response in normal and malignant human lung cells. BMC Cancer 8: 229

Jorgensen ED, Zhao H, Traganos F, Albino AP, Darzynkiewicz Z (2010a) DNA damage response induced by exposure of human lung adenocarcinoma cells to smoke from tobacco- and nicotine-free cigarettes. Cell Cycle 9: 2170-2176

Jorgensen ED, Zhao H, Traganos F, Albino AP, Darzynkiewicz Z (2010b) DNA damage response induced by exposure of human lung adenocarcinoma cells to smoke from tobacco-and nicotine-free cigarettes. Cell Cycle 9: 2170-2176

Jourdan KB, Evans TW, Curzen NP, Mitchell JA (1997) Evidence for a dilator function of 8-iso prostaglandin F2α in rat pulmonary artery. British Journal of Pharmacology 120: 1280-1285

Kastan MB (2008) DNA Damage Responses: Mechanisms and Roles in Human Disease: 2007 G.H.A. Clowes Memorial Award Lecture. Molecular Cancer Research 6: 517-524

Kaufman RJ (2002) Orchestrating the unfolded protein response in health and disease. The Journal of Clinical Investigation 110: 1389-1398

Keaney JF, Larson MG, Vasan RS, Wilson PW, Lipinska I, Corey D, Massaro JM, Sutherland P, Vita JA, Benjamin EJ (2003) Obesity and systemic oxidative stress clinical correlates of oxidative stress in the Framingham Study. Arteriosclerosis, Thrombosis, and Vascular Biology 23: 434-439

Kim CH, Han SI, Lee SY, Youk HS, Moon JY, Duong HQ, Park MJ, Joo YM, Park HG, Kim YJ, Yoo MA, Lim S-C, Kang HS (2007) Protein kinase C-ERK1/2 signal pathway switches glucose depletion-induced necrosis to apoptosis by regulating superoxide dismutases and suppressing reactive oxygen species production in A549 lung cancer cells. Journal of Cellular Physiology 211: 371-385

Kim CH, Ko AR, Lee SY, Jeon HM, Kim SM, Park HG, Han SI, Kang HS (2010) Hypoxia switches glucose depletion-induced necrosis to phosphoinositide 3-kinase/Akt-dependent apoptosis in A549 lung adenocarcinoma cells. International Journal of Oncology 36: 117-124

Kim HP, Wang X, Lee S-J, Huang M-H, Wan Y, Ryter SW, Choi AMK (2008) Autophagic proteins regulate cigarette smoke induced apoptosis: Protective role of heme oxygenase-1. Autophagy 4: 887-895

Kinoshita A, Wanibuchi H, Wei M, Yunoki T, Fukushima S (2007) Elevation of 8-hydroxydeoxyguanosine and cell proliferation via generation of oxidative stress by organic arsenicals contributes to their carcinogenicity in the rat liver and bladder. Toxicology and Applied Pharmacology 221: 295-305

Knight-Lozano CA, Young CG, Burow DL, Hu ZY, Uyeminami D, Pinkerton KE, Ischiropoulos H, Ballinger SW (2002) Cigarette smoke exposure and hypercholesterolemia increase mitochondrial damage in cardiovascular tissues. Circulation 105: 849-854

Kobayashi Y, Furukawa-Hibi Y, Chen C, Horio, Y. , Isobe K, Ikeda K, Motoyama N (2005) SIRT1 is critical regulator of FOXO-mediated transcription in response to oxidative stress. International Journal of Molecular Medicine 16: 237-243

Kode A, Rajendrasozhan S, Caito S, Yang S-R, Megson IL, Rahman I (2008) Resveratrol induces glutathione synthesis by activation of Nrf2 and protects against cigarette smoke-mediated oxidative stress in human lung epithelial cells. American Journal of Physiology-Lung Cellular and Molecular Physiology 294: L478-L488

Kogel U, Schlage WK, Martin F, Xiang Y, Ansari S, Leroy P, Vanscheeuwijck P, Gebel S, Buettner A, Wyss C (2014) A 28-day rat inhalation study with an integrated molecular toxicology endpoint demonstrates reduced exposure effects for a prototypic modified risk tobacco product compared with conventional cigarettes. Food and Chemical Toxicology 68: 204-217

Kohen R, Nyska A (2002) Invited Review: Oxidation of Biological Systems: Oxidative Stress Phenomena, Antioxidants, Redox Reactions, and Methods for Their Quantification. Toxicologic Pathology 30: 620-650

Koning H, Sayers I, Stewart CE, de Jong D, ten Hacken NH, Postma DS, van Oosterhout AJ, Nawijn MC, Koppelman GH (2012) Characterization of protocadherin-1 expression in primary bronchial epithelial cells: association with epithelial cell differentiation. The FASEB Journal 26: 439-448

Kregel KC (2002) Invited Review: Heat shock proteins: modifying factors in physiological stress responses and acquired thermotolerance. Journal of Applied Physiology 92: 2177-2186

Kreutmayer SB, Messner B, Knoflach M, Henderson B, Niederegger H, Böck G, Van der Zee R, Wick G, Bernhard D (2011) Dynamics of heat shock protein 60 in endothelial cells exposed to cigarette smoke extract. Journal of Molecular and Cellular Cardiology 51: 777-780

Kroemer G, Mariño G, Levine B (2010) Autophagy and the Integrated Stress Response. Molecular Cell 40: 280-293

Kültz D (2005) Molecular and evolutionary basis of the cellular stress response. Annual Review of Physiology 67: 225-257

Kültz D, Burg M (1998) Evolution of osmotic stress signaling via MAP kinase cascades. Journal of Experimental Biology 201: 3015-3021

Kunitomo M, Yamaguchi Y, Kagota S, Yoshikawa N, Nakamura K, Shinozuka K (2009) Biochemical evidence of atherosclerosis progression mediated by increased oxidative stress in apolipoprotein E-deficient spontaneously hyperlipidemic mice exposed to chronic cigarette smoke. Journal of pharmacological sciences 110: 354-361

Lau WKW, Chan SCH, Law ACK, Ip MSM, Mak JCW (2011) The role of MAPK and Nrf2 pathways in ketanserin-elicited attenuation of cigarette smoke-induced IL-8 production in human bronchial epithelial cells. Toxicological Sciences: kfr305

Leanderson P, Tagesson C (1992) Rapid and sensitive detection of hydroxyl radicals formed by activated neutrophils in the presence of chelated iron: hydroxylation of deoxyguanosine to 8-hydroxydeoxyguanosine. Agents and actions 36: 50-57

Lee J, Kim J, Ju P, Jung K, Lim H, Kang H (2010) CuZnSOD and MnSOD inhibit metabolic stress-induced necrosis and multicellular tumour spheroid growth. International Journal of Oncology 37: 195-202

Leong X-F, Ng C-Y, Jaarin K (2015) Animal Models in Cardiovascular Research: Hypertension and Atherosclerosis. BioMed Research International 2015: 528757

Libby P (2012) Inflammation in Atherosclerosis. Arteriosclerosis, Thrombosis, and Vascular Biology 32: 2045-2051

Libby P, Ridker PM, Maseri A (2002) Inflammation and atherosclerosis. Circulation 105: 1135-1143

Lin X-X, Yang X-F, Jiang J-X, Zhang S-J, Guan Y, Liu Y-N, Sun Y-H, Xie Q-M (2014) Cigarette smoke extract-induced BEAS-2B cell apoptosis and anti-oxidative Nrf-2 up-regulation are mediated by ROS-stimulated p38 activation. Toxicology mechanisms and methods 24: 575-583

Liu L, Cash TP, Jones RG, Keith B, Thompson CB, Simon MC (2006) Hypoxia-Induced Energy Stress Regulates mRNA Translation and Cell Growth. Molecular Cell 21: 521-531

Liu L, Wise DR, Diehl JA, Simon MC (2008a) Hypoxic Reactive Oxygen Species Regulate the Integrated Stress Response and Cell Survival. Journal of Biological Chemistry 283: 31153-31162

Liu TF, McCall CE (2013) Deacetylation by SIRT1 Reprograms Inflammation and Cancer. Genes & Cancer 4: 135-147

Liu X, Togo S, Al-Mugotir M, Kim H, Fang Q, Kobayashi T, Wang X, Mao L, Bitterman P, Rennard S (2008b) NF-kappaB mediates the survival of human bronchial epithelial cells exposed to cigarette smoke extract. Respir Res 9: 66-66

Lo Sasso G, Schlage WK, Boué S, Veljkovic E, Peitsch MC, Hoeng J (2016a) The Apoe−/− mouse model: a suitable model to study cardiovascular and respiratory diseases in the context of cigarette smoke exposure and harm reduction. Journal of Translational Medicine 14: 1-16

Lo Sasso G, Titz B, Nury C, Boué S, Phillips B, Belcastro V, Schneider T, Dijon S, Baumer K, Peric D, Dulize R, Elamin A, Guedj E, Buettner A, Leroy P, Kleinhans S, Vuillaume G, Veljkovic E, Ivanov NV, Martin F, Vanscheeuwijck P, Peitsch MC, Hoeng J (2016b) Effects of cigarette smoke, cessation and switching to a candidate modified risk tobacco product on the liver in Apoe−/− mice – a systems toxicology analysis. Inhalation toxicology 28: 226-240

Lopez-Souza N, Dolganov G, Dubin R, Sachs L, Sassina L, Sporer H, Yagi S, Schnurr D, Boushey H, Widdicombe J (2004) Resistance of differentiated human airway epithelium to infection by rhinovirus. American Journal of Physiology-Lung Cellular and Molecular Physiology 286: L373-L381

Lou J, Zhou G, Chu G, Jiang J, Huang F, Zheng S, Lu Y, Li X, He J (2010) Studying the cyto-genotoxic effects of 12 cigarette smoke condensates on human lymphoblastoid cell line in vitro. Mutation Research/Genetic Toxicology and Environmental Mutagenesis 696: 48-54

Lu B, Kerepesi L, Wisse L, Hitchman K, Meng QR (2007) Cytotoxicity and Gene Expression Profiles in Cell Cultures Exposed to Whole Smoke from Three Types of Cigarettes. Toxicological Sciences 98: 469-478

Luppi F, Aarbiou J, Van Wetering S, Rahman I, De Boer WI, Rabe KF, Hiemstra PS (2005) Effects of cigarette smoke condensate on proliferation and wound closure of bronchial epithelial cells in vitro: role of glutathione. Respir Res 6: 140

Lykkesfeldt J (2007) Malondialdehyde as biomarker of oxidative damage to lipids caused by smoking. Clinica Chimica Acta 380: 50-58

Lynch AM, Sasaki JC, Elespuru R, Jacobson Kram D, Thybaud V, De Boeck M, Aardema MJ, Aubrecht J, Benz RD, Dertinger SD (2011) New and emerging technologies for genetic toxicity testing. Environmental and Molecular Mutagenesis 52: 205-223

Madamanchi NR, Vendrov A, Runge MS (2005) Oxidative Stress and Vascular Disease. Arteriosclerosis, Thrombosis, and Vascular Biology 25: 29-38

Majmundar AJ, Wong WJ, Simon MC (2010) Hypoxia-Inducible Factors and the Response to Hypoxic Stress. Molecular Cell 40: 294-309

Malhotra D, Thimmulappa R, Vij N, Navas-Acien A, Sussan T, Merali S, Zhang L, Kelsen SG, Myers A, Wise R, Tuder R, Biswal S (2009) Heightened Endoplasmic Reticulum Stress in the Lungs of Patients with Chronic Obstructive Pulmonary Disease. American Journal of Respiratory and Critical Care Medicine 180: 1196-1207

March TH, Green FH, Hahn FF, Nikula KJ (2000) Animal models of emphysema and their relevance to studies of particle-induced disease. Inhalation toxicology 12 Suppl 4: 155-187

Martin F, Thomson T, Sewer A, Drubin D, Mathis C, Weisensee D, Pratt D, Hoeng J, Peitsch M (2012) Assessment of network perturbation amplitudes by applying high-throughput data to causal biological networks. BMC Systems Biology 6: 54

Martindale JL, Holbrook NJ (2002) Cellular response to oxidative stress: Signaling for suicide and survival*. Journal of Cellular Physiology 192: 1-15

Martinez-Anton A, Sokolowska M, Kern S, Davis AS, Alsaaty S, Taubenberger JK, Sun J, Cai R, Danner RL, Eberlein M (2013) Changes in microRNA and mRNA expression with differentiation of human bronchial epithelial cells. American Journal of Respiratory Cell and Molecular Biology 49: 384-395

Matés JM, Segura JA, Alonso FJ, Márquez J (2008) Intracellular redox status and oxidative stress: implications for cell proliferation, apoptosis, and carcinogenesis. Arch Toxicol 82: 273-299

Matthew EM, Hart LS, Astrinidis A, Navaraj A, Dolloff NG, Dicker DT, Henske EP, El-Deiry WS (2009) The p53 target Plk2 interacts with TSC proteins impacting mTOR signaling, tumor growth, and chemosensitivity under hypoxic conditions. Cell Cycle 8: 4168-4175

McBurney MW, Clark-Knowles KV, Caron AZ, Gray DA (2013) SIRT1 is a Highly Networked Protein That Mediates the Adaptation to Chronic Physiological Stress. Genes & Cancer 4: 125-134

McKarns S, Bombick D, Morton M, Doolittle D (2000) Gap junction intercellular communication and cytotoxicity in normal human cells after exposure to smoke condensates from cigarettes that burn or primarily heat tobacco. Toxicology in Vitro 14: 41-51

Messner B, Frotschnig S, Steinacher-Nigisch A, Winter B, Eichmair E, Gebetsberger J, Schwaiger S, Ploner C, Laufer G, Bernhard D (2012) Apoptosis and necrosis: two different outcomes of cigarette smoke condensate-induced endothelial cell death. Cell Death Dis 3: e424

Mestas J, Hughes CC (2004) Of mice and not men: differences between mouse and human immunology. Journal of immunology (Baltimore, Md : 1950) 172: 2731-2738

Michaud SÉ, Dussault S, Groleau J, Haddad P, Rivard A (2006) Cigarette smoke exposure impairs VEGF-induced endothelial cell migration: Role of NO and reactive oxygen species. Journal of Molecular and Cellular Cardiology 41: 275-284

Milara J, Ortiz JL, Juan G, Guijarro R, Almudever P, Martorell M, Morcillo EJ, Cortijo J (2010) Cigarette smoke exposure up-regulates endothelin receptor B in human pulmonary artery endothelial cells: molecular and functional consequences. British Journal of Pharmacology 161: 1599-1615

Milisav I. (2011a) Cellular Stress Responses In Wislet-Gendebien S (ed.), Advances in Regenerative Medicine. InTech.

Milisav I (2011b) Cellular stress responses. Advances in Regenerative Medicine: 215-232

Milne GL, Musiek ES, Morrow JD (2005) F2-Isoprostanes as markers of oxidative stress in vivo: An overview. Biomarkers 10: 10-23

Minamino T, Kitakaze M (2010) ER stress in cardiovascular disease. Journal of Molecular and Cellular Cardiology 48: 1105-1110

Minamino T, Komuro I, Kitakaze M (2010) Endoplasmic Reticulum Stress As a Therapeutic Target in Cardiovascular Disease. Circulation Research 107: 1071-1082

Minuz P, Andrioli G, Degan M, Gaino S, Ortolani R, Tommasoli R, Zuliani V, Lechi A, Lechi C (1998) The F2-Isoprostane 8-Epiprostaglandin F2α Increases Platelet Adhesion and Reduces the Antiadhesive and Antiaggregatory Effects of NO. Arteriosclerosis, Thrombosis, and Vascular Biology 18: 1248-1256

Mizushima N, Komatsu M (2011) Autophagy: Renovation of Cells and Tissues. Cell 147: 728-741

Morris BJ (2013) Seven sirtuins for seven deadly diseases ofaging. Free Radical Biology and Medicine 56: 133-171

Morrow JD, Frei B, Longmire AW, Gaziano JM, Lynch SM, Shyr Y, Strauss WE, Oates JA, Roberts LJ (1995) Increase in Circulating Products of Lipid Peroxidation (F2-Isoprostanes) in Smokers — Smoking as a Cause of Oxidative Damage. New England Journal of Medicine 332: 1198-1203

Morrow JD, Minton DA, Roberts 2nd LJ (1992) The F2-isoprostane, 8-epi-prostaglandin F2 alpha, a potent agonist of the vascular thromboxane/endoperoxide receptor, is a platelet thromboxane/endoperoxide receptor antagonist. Prostaglandins 44: 155-163

Mudau M, Genis A, Lochner A, Strijdom H (2012) Endothelial dysfunction: the early predictor of atherosclerosis. Cardiovascular Journal of Africa 23: 222-231

Müller T, Gebel S (1998) The cellular stress response induced by aqueous extracts of cigarette smoke is critically dependent on the intracellular glutathione concentration. Carcinogenesis 19: 797-801

Müller T, Gebel S (2006) Cigarette Smoke-Induced Redox Signaling and Gene Expression in In Vitro and In Vivo Models. In Cigarette Smoke and Oxidative Stress, Halliwell BB, Poulsen HE (eds), pp 75-112. Berlin: Springer-Verlag

Müller T, Hengstermann A (2012) Nrf2: Friend and Foe in Preventing Cigarette Smoking-Dependent Lung Disease. Chemical Research in Toxicology 25: 1805-1824

Munnia A, Bonassi S, Verna A, Quaglia R, Pelucco D, Ceppi M, Neri M, Buratti M, Taioli E, Garte S, Peluso M (2006) Bronchial malondialdehyde DNA adducts, tobacco smoking, and lung cancer. Free Radical Biology and Medicine 41: 1499-1505

Munnia A, Enrica Amasio M, Peluso M (2004) Exocyclic malondialdehyde and aromatic DNA adducts in larynx tissues. Free Radical Biology and Medicine 37: 850-858

Münzel T, Sinning C, Post F, Warnholtz A, Schulz E (2008) Pathophysiology, diagnosis and prognostic implications of endothelial dysfunction. Annals of Medicine 40: 180-196

Nakamura AJ, Rao VA, Pommier Y, Bonner WM (2010) The complexity of phosphorylated H2AX foci formation and DNA repair assembly at DNA double-strand breaks. Cell Cycle 9: 389-397

Nakashima Y, Plump AS, Raines EW, Breslow JL, Ross R (1994) ApoE-deficient mice develop lesions of all phases of atherosclerosis throughout the arterial tree. Arteriosclerosis, Thrombosis, and Vascular Biology 14: 133-140

Naugler WE, Karin M (2008) NF-κB and cancer - identifying targets and mechanisms. Current Opinion in Genetics & Development 18: 19-26

Nedeljkovic ZS, Gokce N, Loscalzo J (2003) Mechanisms of oxidative stress and vascular dysfunction. Postgraduate Medical Journal 79: 195-200

Neofytou E, Tzortzaki E, Chatziantoniou A, Siafakas N (2012) DNA Damage Due to Oxidative Stress in Chronic Obstructive Pulmonary Disease (COPD). International Journal of Molecular Sciences 13: 16853-16864

Neuhofer W (2010) Role of NFAT5 in inflammatory disorders associated with osmotic stress. Curr Genomics 11: 584-590

NRC (2007) Toxicity Testing in the 21st Century: A Vision and a Strategy: The National Academies Press.

Nyunoya T, Mebratu Y, Contreras A, Delgado M, Chand HS, Tesfaigzi Y (2013) Molecular Processes That Drive Cigarette Smoke-Induced Epithelial Cell Fate of the Lung. American Journal of Respiratory Cell and Molecular Biology

Nyunoya T, Monick MM, Klingelhutz A, Yarovinsky TO, Cagley JR, Hunninghake GW (2006) Cigarette Smoke Induces Cellular Senescence. American Journal of Respiratory Cell and Molecular Biology 35: 681-688

O'Brien PJ (2014) High-Content Analysis in Toxicology: Screening Substances for Human Toxicity Potential, Elucidating Subcellular Mechanisms and In Vivo Use as Translational Safety Biomarkers. Basic & Clinical Pharmacology & Toxicology 115: 4-17

OECD (2009a) Test No. 413: Subchronic Inhalation Toxicity: 90-day Study: OECD Publishing.

OECD (2009b) Test No. 453: Combined Chronic Toxicity/Carcinogenicity Studies: OECD Publishing.

Ohshima H, Sawa T, Akaike T (2006) 8-Nitroguanine, a Product of Nitrative DNA Damage Caused by Reactive Nitrogen Species: Formation, Occurrence, and Implications in Inflammation and Carcinogenesis. Antioxidants & Redox Signaling 8: 1033-1045

Orosz Z, Csiszar A, Labinskyy N, Smith K, Kaminski PM, Ferdinandy P, Wolin MS, Rivera A, Ungvari Z (2007) Cigarette smoke-induced proinflammatory alterations in the endothelial phenotype: role of NAD (P) H oxidase activation. American Journal of Physiology-Heart and Circulatory Physiology 292: H130-H139

Ortells MC, Morancho B, Drews-Elger K, Viollet B, Laderoute KR, López-Rodríguez C, Aramburu J (2012) Transcriptional regulation of gene expression during osmotic stress responses by the mammalian target of rapamycin. Nucleic Acids Research 40: 4368-4384

Owen JB, Butterfield DA (2010) Measurement of oxidized/reduced glutathione ratio. In Protein Misfolding and Cellular Stress in Disease and Aging, pp 269-277. Springer

Pace E, Ferraro M, Di Vincenzo S, Cipollina C, Gerbino S, Cigna D, Caputo V, Balsamo R, Lanata L, Gjomarkaj M (2013) Comparative cytoprotective effects of carbocysteine and fluticasone propionate in cigarette smoke extract-stimulated bronchial epithelial cells. Cell Stress & Chaperones 18: 733-743

Pace E, Ferraro M, Di Vincenzo S, Gerbino S, Bruno A, Lanata L, Gjomarkaj M (2014) Oxidative stress and innate immunity responses in cigarette smoke stimulated nasal epithelial cells. Toxicology in Vitro 28: 292-299

Paquette J, Tremblay P, Bernier V, Auger F, Laviolette M, Germain L, Boutet M, Boulet L, Goulet F (2003) Production of tissue-engineered three-dimensional human bronchial models. In Vitro Cellular & Developmental Biology-Animal 39: 213-220

Pastukh VM, Zhang L, Mykhaylo VR, Gorodnya O, Bardwell GC, Tuder RM, Gillespie MN (2011) Oxidative DNA damage in lung tissue from patients with COPD is clustered in functionally significant sequences. International Journal of Chronic Obstructive Pulmonary Disease 6: 209 - 217

Paul A, Ko KW, Li L, Yechoor V, McCrory MA, Szalai AJ, Chan L (2004) C-reactive protein accelerates the progression of atherosclerosis in apolipoprotein E–deficient mice. Circulation 109: 647-655

Paull TT, Rogakou EP, Yamazaki V, Kirchgessner CU, Gellert M, Bonner WM (2000) A critical role for histone H2AX in recruitment of repair factors to nuclear foci after DNA damage. Current Biology 10: 886-895

Peluffo G, Calcerrada P, Piacenza L, Pizzano N, Radi R (2009) Superoxide-mediated inactivation of nitric oxide and peroxynitrite formation by tobacco smoke in vascular endothelium: studies in cultured cells and smokers. American Journal of Physiology-Heart and Circulatory Physiology 296: H1781-H1792

Perfetti TA, Rodgman A (2011) The Complexity of Tobacco and Tobacco Smoke. Beitr Tabakforsch Int 24: 215-232

Phillips B, Esposito M, Verbeeck J, Boué S, Iskandar A, Vuillaume G, Leroy P, Krishnan S, Kogel U, Utan A (2015a) Toxicity of aerosols of nicotine and pyruvic acid (separate and combined) in Sprague–Dawley rats in a 28-day OECD 412 inhalation study and assessment of systems toxicology. Inhalation toxicology 27: 405-431

Phillips B, Veljkovic E, Boué S, Schlage WK, Vuillaume G, Martin F, Titz B, Leroy P, Buettner A, Elamin A, Oviedo A, Cabanski M, De León H, Guedj E, Schneider T, Talikka M, Ivanov NV, Vanscheeuwijck P, Peitsch MC, Hoeng J (2016) An 8-Month Systems Toxicology Inhalation/Cessation Study in Apoe−/− Mice to Investigate Cardiovascular and Respiratory Exposure Effects of a Candidate Modified Risk Tobacco Product, THS 2.2, Compared With Conventional Cigarettes. Toxicological Sciences 149: 411-432

Phillips B, Veljkovic E, Peck MJ, Buettner A, Elamin A, Guedj E, Vuillaume G, Ivanov NV, Martin F, Boué S (2015b) A 7-month cigarette smoke inhalation study in C57BL/6 mice demonstrates reduced lung inflammation and emphysema following smoking cessation or aerosol exposure from a prototypic modified risk tobacco product. Food and Chemical Toxicology 80: 328-345

Piconi L, Quagliaro L, Assaloni R, Da Ros R, Maier A, Zuodar G, Ceriello A (2006) Constant and intermittent high glucose enhances endothelial cell apoptosis through mitochondrial superoxide overproduction. Diabetes/Metabolism Research and Reviews 22: 198-203

Pilger A, Rüdiger HW (2006) 8-Hydroxy-2′-deoxyguanosine as a marker of oxidative DNA damage related to occupational and environmental exposures. Int Arch Occup Environ Health 80: 1-15

Pilz H, Oguogho A, Chehne F, Lupattelli G, Palumbo B, Sinzinger H (2000) Quitting Cigarette Smoking Results in a Fast Improvement of in vivo Oxidation Injury (Determined via Plasma, Serum and Urinary Isoprostane). Thrombosis Research 99: 209-221

Pirkkala L, Nykänen P, Sistonen L (2001) Roles of the heat shock transcription factors in regulation of the heat shock response and beyond. The FASEB Journal 15: 1118-1131

Plump AS, Smith JD, Hayek T, Aalto-Setälä K, Walsh A, Verstuyft JG, Rubin EM, Breslow JL (1992) Severe hypercholesterolemia and atherosclerosis in apolipoprotein E-deficient mice created by homologous recombination in ES cells. Cell 71: 343-353

Poussin C, Gallitz I, Schlage WK, Steffen Y, Stolle K, Lebrun S, Hoeng J, Peitsch MC, Lietz M (2014) Mechanism of an indirect effect of aqueous cigarette smoke extract on the adhesion of monocytic cells to endothelial cells in an in vitro assay revealed by transcriptomics analysis. Toxicology in Vitro 28: 896-908

Poussin C, Laurent A, Peitsch MC, Hoeng J, De Leon H (2015) Systems biology reveals cigarette smoke-induced concentration-dependent direct and indirect mechanisms that promote monocyte-endothelial cell adhesion. Toxicological Sciences: kfv137

Poussin C, Laurent A, Peitsch MC, Hoeng J, De Leon H (2016) Systems toxicology-based assessment of the candidate modified risk tobacco product THS2.2 for the adhesion of monocytic cells to human coronary arterial endothelial cells. Toxicology 339: 73-86

Pryor WA (1992) Biological effects of cigarette smoke, wood smoke, and the smoke from plastics: the use of electron spin resonance. Free Radic Biol Med 13: 659-676

Pryor WA (1997) Cigarette smoke radicals and the role of free radicals in chemical carcinogenicity. Environ Health Perspect 105: 875–882

Prytherch Z, Job C, Marshall H, Oreffo V, Foster M, BéruBé K (2011) Tissue -Specific Stem Cell Differentiation in an in vitro Airway Model. Macromolecular bioscience 11: 1467-1477

Rahman I, Li X, Donaldson K, Harrison D, MacNee W (1995) Glutathione homeostasis in alveolar epithelial cells in vitro and lung in vivo under oxidative stress. American Journal of Physiology-Lung Cellular and Molecular Physiology 269: L285-L292

Ravikumar P, Ye J, Zhang J, Pinch SN, Hu MC, Kuro-o M, Hsia CC, Moe OW (2014) α-Klotho protects against oxidative damage in pulmonary epithelia. American Journal of Physiology-Lung Cellular and Molecular Physiology 307: L566-L575

Raynes R, Brunquell J, Westerheide SD (2013) Stress Inducibility of SIRT1 and Its Role in Cytoprotection and Cancer. Genes & Cancer 4: 172-182

Reilly M, Delanty N, Lawson JA, FitzGerald GA (1996) Modulation of Oxidant Stress In Vivo in Chronic Cigarette Smokers. Circulation 94: 19-25

Roberts LJ, Morrow JD (2000) Measurement of F2-isoprostanes as an index of oxidative stress in vivo. Free Radical Biology and Medicine 28: 505-513

Rodgers JT, Lerin C, Haas W, Gygi SP, Spiegelman BM, Puigserver P (2005) Nutrient control of glucose homeostasis through a complex of PGC-1[alpha] and SIRT1. Nature 434: 113-118

Rodriguez-Porcel M, Lerman A, Best PJ, Krier JD, Napoli C, Lerman LO (2001) Hypercholesterolemia impairs myocardial perfusion and permeability: role of oxidative stress and endogenous scavenging activity. Journal of the American College of Cardiology 37: 608-615

Rogakou EP, Pilch DR, Orr AH, Ivanova VS, Bonner WM (1998) DNA double-stranded breaks induce histone H2AX phosphorylation on serine 139. Journal of Biological Chemistry 273: 5858-5868

Ross R (1999) Atherosclerosis - an inflammatory disease. N Engl J Med 340: 115-126

Ryter SW, Choi AMK (2013) Autophagy: An Integral Component of the Mammalian Stress Response. Journal of Biochemical and Pharmacological Research 1: 176-188

Saito H, Posas F (2012) Response to Hyperosmotic Stress. Genetics 192: 289-318

Salahuddin S, Prabhakaran D, Roy A (2012) Pathophysiological Mechanisms of Tobacco-Related CVD. Global Heart 7: 113-120

Salem AF, Al-Zoubi MS, Whitaker-Menezes D, Martinez-Outschoorn UE, Lamb R, Hulit J, Howell A, Gandara R, Sartini M, Galbiati F, Bevilacqua G, Sotgia F, Lisanti MP (2013) Cigarette smoke metabolically promotes cancer, via autophagy and premature aging in the host stromal microenvironment. Cell Cycle 12: 818-825

Sauve AA, Wolberger C, Schramm VL, Boeke JD (2006) The Biochemistry of Sirtuins. Annual Review of Biochemistry 75: 435-465

Scheffler S, Dieken H, Krischenowski O, Förster C, Branscheid D, Aufderheide M (2015) Evaluation of E-Cigarette Liquid Vapor and Mainstream Cigarette Smoke after Direct Exposure of Primary Human Bronchial Epithelial Cells. International Journal of Environmental Research and Public Health 12: 3915-3925

Schlage W, Westra J, Gebel S, Catlett N, Mathis C, Frushour B, Hengstermann A, Van Hooser A, Poussin C, Wong B, Lietz M, Park J, Drubin D, Veljkovic E, Peitsch M, Hoeng J, Deehan R (2011) A computable cellular stress network model for non-diseased pulmonary and cardiovascular tissue. BMC Systems Biology 5: 168

Schröder M, Kaufman RJ (2005) The mammalian unfolded protein response. Annual Review of Biochemistry 74: 739-789

Schroeter MR, Sawalich M, Humboldt T, Leifheit M, Meurrens K, Berges A, Xu H, Lebrun S, Wallerath T, Konstantinides S (2008) Cigarette smoke exposure promotes arterial thrombosis and vessel remodeling after vascular injury in apolipoprotein E-deficient mice. Journal of vascular research 45: 480-492

Schulz E, Anter E, Keaney Jr. JF (2004) Oxidative stress, antioxidants, and endothelial function. Current Medicinal Chemistry 11: 1093-1104

Schwartz L, Guais A, Pooya M, Abolhassani M (2009) Is inflammation a consequence of extracellular hyperosmolarity? Journal of Inflammation 6: 21

Selventa. (2010) Reverse Causal Reasoning Methods Whitepaper. Vol. 2011.

Semenza GL (2007) Hypoxia-Inducible Factor 1 (HIF-1) Pathway. Sci STKE 2007: cm8-

Services UDoHaH (2010) How tobacco smoke causes disease: the biology and behavioral basis for smoking-attributable disease: a report of the Surgeon General. Atlanta, GA: US Department of Health and Human Services, Centers for Disease Control and Prevention, National Center for Chronic Disease Prevention and Health Promotion, Office on Smoking and Health 2

Shen CX, Z. CH, Ge JB (2004a) The role of inflammatory stress in acute coronary syndrome. Chinese Medical Journal 117: 133-139

Shen H-M, Liu Z-g (2006) JNK signaling pathway is a key modulator in cell death mediated by reactive oxygen and nitrogen species. Free Radical Biology and Medicine 40: 928-939

Shen X, Zhang K, Kaufman RJ (2004b) The unfolded protein response—a stress signaling pathway of the endoplasmic reticulum. Journal of Chemical Neuroanatomy 28: 79-92

Shi Y, Cao J, Gao J, Zheng L, Goodwin A, An CH, Patel A, Lee JS, Duncan SR, Kaminski N, Pandit KV, Rosas IO, Choi AMK, Morse D (2012) Retinoic Acid–related Orphan Receptor-α Is Induced in the Setting of DNA Damage and Promotes Pulmonary Emphysema. American Journal of Respiratory and Critical Care Medicine 186: 412-419

Siebel A, Cubillos-Rojas M, Santos RC, Schneider T, Bonan CD, Bartrons R, Ventura F, Rodrigues de Oliveira J, Rosa JL (2013) Contribution of S6K1/MAPK Signaling Pathways in the Response to Oxidative Stress: Activation of RSK and MSK by Hydrogen Peroxide. PLoS ONE 8: e75523

Simmons SO, Fan C-Y, Ramabhadran R (2009) Cellular Stress Response Pathway System as a Sentinel Ensemble in Toxicological Screening. Toxicological Sciences 111: 202-225

Snajdar RM, Busuttil SJ, Averbook A, Graham DJ (2001) Inhibition of endothelial cell migration by cigarette smoke condensate. Journal of Surgical Research 96: 10-16

Somborac-Bačura A, van der Toorn M, Franciosi L, Slebos D-J, Žanić-Grubišić T, Bischoff R, van Oosterhout AJM (2013) Cigarette smoke induces endoplasmic reticulum stress response and proteasomal dysfunction in human alveolar epithelial cells. Experimental Physiology 98: 316-325

Starke RM, Ali MS, Jabbour PM, Tjoumakaris SI, Gonzalez F, Hasan DM, Rosenwasser RH, Owens GK, Koch WJ, Dumont AS (2013) Cigarette smoke modulates vascular smooth muscle phenotype: implications for carotid and cerebrovascular disease. PLoS ONE 8: e71954

Stockmann C, Fandrey J (2006) Hypoxia-induced erythropoietin production: a paradigm for oxygen-regulated gene expression. Clinical and Experimental Pharmacology and Physiology 33: 968-979

Stone P, Fisher A, Rainger G, Nash G (2002) Neutrophil capture by selectins on endothelial cells exposed to cigarette smoke. Biochemical and Biophysical Research Communications 295: 1150-1155

Storz P (2005) Reactive oxygen species in tumor progression. Frontiers in Bioscience 10: 1881-1896

Suzuki M, Aoshiba K, Nagai A (2006) Oxidative stress increases Fas ligand expression in endothelial cells. J Inflamm (Lond) 3: 11

Tabas I (2010) The Role of Endoplasmic Reticulum Stress in the Progression of Atherosclerosis. Circulation Research 107: 839-850

Tagawa Y, Hiramatsu N, Kasai A, Hayakawa K, Okamura M, Yao J, Kitamura M (2008) Induction of apoptosis by cigarette smoke via ROS-dependent endoplasmic reticulum stress and CCAAT/enhancer-binding protein-homologous protein (CHOP). Free Radical Biology and Medicine 45: 50-59

Takahashi K, Nammour TM, Fukunaga M, Ebert J, Morrow JD, Roberts LJ, 2nd, Hoover RL, Badr KF (1992) Glomerular actions of a free radical-generated novel prostaglandin, 8-epi-prostaglandin F2 alpha, in the rat. Evidence for interaction with thromboxane A2 receptors. The Journal of Clinical Investigation 90: 136-141

Takeuchi T, Morimoto K (1994) Crocidolite asbestos increased 8-hydroxydeoxyguanosine levels in cellular DNA of a human promyelocytic leukemia cell line, HL60. Carcinogenesis 15: 635-639

Tan X, Jin P, Feng L, Song J, Sun E, Liu W, Shu L, Jia X (2014) Protective effect of luteolin on cigarette smoke extract induced cellular toxicity and apoptosis in normal human bronchial epithelial cells via the Nrf2 pathway. Oncology reports 31: 1855-1862

Tanaka T, Huang X, Jorgensen E, Gietl D, Traganos F, Darzynkiewicz Z, Albino AP (2007) ATM activation accompanies histone H2AX phosphorylation in A549 cells upon exposure to tobacco smoke. BMC Cell Biology 8: 26-26

Tani S, Dimayuga PC, Anazawa T, Chyu K-Y, Li H, Shah PK, Cercek B (2004) Aberrant antibody responses to oxidized LDL and increased intimal thickening in apoE−/− mice exposed to cigarette smoke. Atherosclerosis 175: 7-14

Tanriverdi H, Evrengul H, Kuru O, Tanriverdi S, Seleci D, Enli Y, Kaftan HA, Kilic M (2006) Cigarette Smoking Induced Oxidative Stress may Impair Endothelial Function and Coronary Blood Flow in Angiographically Normal Coronary Arteries. Circulation Journal 70: 593-599

Taraseviciene-Stewart L, Scerbavicius R, Choe KH, Moore M, Sullivan A, Nicolls MR, Fontenot AP, Tuder RM, Voelkel NF (2005) An animal model of autoimmune emphysema. Am J Respir Crit Care Med 171: 734-742

Teske BF, Wek SA, Bunpo P, Cundiff JK, McClintick JN, Anthony TG, Wek RC (2011) The eIF2 kinase PERK and the integrated stress response facilitate activation of ATF6 during endoplasmic reticulum stress. Molecular Biology of the Cell 22: 4390-4405

Thomas SR, Witting PK, Drummond GR (2008) Redox Control of Endothelial Function and Dysfunction: Molecular Mechanisms and Therapeutic Opportunities Antioxidants & Redox Signaling 10: 1713-1766

Thomson TM, Sewer A, Martin F, Belcastro V, Frushour BP, Gebel S, Park J, Schlage WK, Talikka M, Vasilyev DM, Westra JW, Hoeng J, Peitsch MC (2013) Quantitative assessment of biological impact using transcriptomic data and mechanistic network models. Toxicology and Applied Pharmacology 272: 863-878

Thorne D, Wilson J, Kumaravel TS, Massey ED, McEwan M (2009) Measurement of oxidative DNA damage induced by mainstream cigarette smoke in cultured NCI-H292 human pulmonary carcinoma cells. Mutation Research/Genetic Toxicology and Environmental Mutagenesis 673: 3-8

Tietze F (1969) Enzymic method for quantitative determination of nanogram amounts of total and oxidized glutathione: Applications to mammalian blood and other tissues. Analytical Biochemistry 27: 502-522

Tsuji T, Aoshiba K, Nagai A (2006) Alveolar Cell Senescence in Patients with Pulmonary Emphysema. American Journal of Respiratory and Critical Care Medicine 174: 886-893

Valavanidis A, Vlachogianni T, Fiotakis K (2009) Tobacco Smoke: Involvement of Reactive Oxygen Species and Stable Free Radicals in Mechanisms of Oxidative Damage, Carcinogenesis and Synergistic Effects with Other Respirable Particles. International Journal of Environmental Research and Public Health 6: 445-462

van der Toorn M, Frentzel S, Goedertier D, Peitsch M, Hoeng J, De Leon H (2015) A prototypic modified risk tobacco product exhibits reduced effects on chemotaxis and transendothelial migration of monocytes compared with a reference cigarette. Food and Chemical Toxicology 80: 277-286

van der Toorn M, Smit-de Vries MP, Slebos D-J, de Bruin HG, Abello N, van Oosterhout AJ, Bischoff R, Kauffman HF (2007) Cigarette smoke irreversibly modifies glutathione in airway epithelial cells. American Journal of Physiology-Lung Cellular and Molecular Physiology 293: L1156-L1162

Vasilios P, Ioannis P (2008) Adaptative mechanisms during chronic hypoxia in COPD. ΠΝΕΥΜΩ 21: 134

Versari D, Daghini E, Virdis A, Ghiadoni L, Taddei S (2009) Endothelial Dysfunction as a Target for Prevention of Cardiovascular Disease. Diabetes Care 32: S314-S321

Visioli F, Galli C, Plasmati E, Viappiani S, Hernandez A, Colombo C, Sala A (2000) Olive Phenol Hydroxytyrosol Prevents Passive Smoking–Induced Oxidative Stress. Circulation 102: 2169-2171

Von Holt K, Lebrun S, Stinn W, Conroy L, Wallerath T, Schleef R (2009) Progression of atherosclerosis in the Apo E−/− model: 12-Month exposure to cigarette mainstream smoke combined with high-cholesterol/fat diet. Atherosclerosis 205: 135-143

Wakai K, Inoue M, Mizoue T, Tanaka K, Tsuji I, Nagata C, Tsugane S, Japan ftRGftDaEoCPSi (2006) Tobacco Smoking and Lung Cancer Risk: An Evaluation Based on a Systematic Review of Epidemiological Evidence Among the Japanese Population. Japanese Journal of Clinical Oncology 36: 309-324

Walter P, Ron D (2011) The Unfolded Protein Response: From Stress Pathway to Homeostatic Regulation. Science 334: 1081-1086

Wang G, Yang Z-Q, Zhang K (2010) Endoplasmic reticulum stress response in cancer: molecular mechanism and therapeutic potential. Am J Transl Res 2: 65-74

Wang S, Kaufman RJ (2012) The impact of the unfolded protein response on human disease. The Journal of Cell Biology 197: 857-867

Wolz L, Krause G, Scherer G (2001) The comet assay with MCL-5 cells as an indicator of genotoxic treatment with chemicals and cigarette smoke condensates. Alternatives to laboratory animals: ATLA 30: 331-339

Wu Y-L, Lin A-H, Chen C-H, Huang W-C, Wang H-Y, Liu M-H, Lee T-S, Kou YR (2014) Glucosamine attenuates cigarette smoke-induced lung inflammation by inhibiting ROS-sensitive inflammatory signaling. Free Radical Biology and Medicine 69: 208-218

Xiang M, Xu Y-j, Liu X-s, Zeng D-x (2010) Cigarette smoke extract promotes human pulmonary artery smooth muscle cells proliferation through protein kinase C alpha-dependent induction of cyclin D1. Chinese Medical Journal 123: 3663-3670

Xu C-B, Zheng J-P, Zhang W, Zhang Y, Edvinsson L (2008) Lipid-soluble smoke particles upregulate vascular smooth muscle ETB receptors via activation of mitogen-activating protein kinases and NF-kappaB pathways. Toxicological Sciences 106: 546-555

Xu CB, Lei Y, Chen Q, Pehrson C, Larsson L, Edvinsson L (2010) Cigarette smoke extracts promote vascular smooth muscle cell proliferation and enhances contractile responses in the vasculature and airway. Basic & Clinical Pharmacology & Toxicology 107: 940-948

Yamada S, Zhang XQ, Kadono T, Matsuoka N, Rollins D, Badger T, Rodesch CK, Barry WH (2009) Direct toxic effects of aqueous extract of cigarette smoke on cardiac myocytes at clinically relevant concentrations. Toxicology and Applied Pharmacology 236: 71-77

Yamaguchi Y, Haginaka J, Morimoto S, Fujioka Y, Kunitomo M (2005) Facilitated nitration and oxidation of LDL in cigarette smokers. European Journal of Clinical Investigation 35: 186-193

Yang IA, Relan V, Wright CM, Davidson MR, Sriram KB, Savarimuthu Francis SM, Clarke BE, Duhig EE, Bowman RV, Fong KM (2011) Common pathogenic mechanisms and pathways in the development of COPD and lung cancer. Expert opinion on therapeutic targets 15: 439-456

Yang Q, Hergenhahn M, Weninger A, Bartsch H (1999) Cigarette smoke induces direct DNA damage in the human B-lymphoid cell line Raji. Carcinogenesis 20: 1769-1775

Yang S-R, Chida AS, Bauter MR, Shafiq N, Seweryniak K, Maggirwar SB, Kilty I, Rahman I (2006) Cigarette smoke induces proinflammatory cytokine release by activation of NF-κB and posttranslational modifications of histone deacetylase in macrophages. American Journal of Physiology - Lung Cellular and Molecular Physiology 291: L46-L57

Yang S-R, Wright J, Bauter M, Seweryniak K, Kode A, Rahman I (2007) Sirtuin regulates cigarette smoke-induced proinflammatory mediator release via RelA/p65 NF-κB in macrophages in vitro and in rat lungs in vivo: implications for chronic inflammation and aging. American Journal of Physiology - Lung Cellular and Molecular Physiology 292: L567-L576

Yauk CL, Williams A, Buick JK, Chen G, Maertens RM, Halappanavar S, White PA (2012) Genetic toxicology and toxicogenomic analysis of three cigarette smoke condensates in vitro reveals few differences among full-flavor, blonde, and light products. Environmental and Molecular Mutagenesis 53: 281-296

Yoshida T, Tuder RM (2007) Pathobiology of cigarette smoke-induced chronic obstructive pulmonary disease. Physiol Rev 87: 1047-1082

Zainol M, Stoute J, Almeida GM, Rapp A, Bowman KJ, Jones GD (2009) Introducing a true internal standard for the Comet assay to minimize intra-and inter-experiment variability in measures of DNA damage and repair. Nucleic Acids Research: gkp826

Zanetti F, Sewer A, Mathis C, Iskandar AR, Kostadinova R, Schlage WK, Leroy P, Majeed S, Guedj E, Trivedi K, Martin F, Elamin A, Merg C, Ivanov NV, Frentzel S, Peitsch MC, Hoeng J (2016) Systems toxicology assessment of the biological impact of a candidate Modified Risk Tobacco Product on human organotypic oral epithelial cultures. Chemical Research in Toxicology: [Epub ahead of print]

Zeng H, Kong X, Peng H, Chen Y, Cai S, Luo H, Chen P (2012) Apoptosis and Bcl-2 family proteins, taken to chronic obstructive pulmonary disease. Eur Rev Med Pharmacol Sci 16

Zhang H, Cai B (2003) The impact of tobacco on lung health in China. Respirology 8: 17-21

Zhang SH, Reddick RL, Piedrahita JA, Maeda N (1992) Spontaneous hypercholesterolemia and arterial lesions in mice lacking apolipoprotein E. Science 258: 468-471

Zhang Y, Chen S-Y, Hsu T, Santella RM (2002) Immunohistochemical detection of malondialdehyde–DNA adducts in human oral mucosa cells. Carcinogenesis 23: 207-211

Zhao H, Albino AP, Jorgensen E, Traganos F, Darzynkiewicz Z (2009) DNA damage response induced by tobacco smoke in normal human bronchial epithelial and A549 pulmonary adenocarcinoma cells assessed by laser scanning cytometry. Cytometry Part A 75A: 840-847

Zhou S-j, Li M, Zeng D-x, Zhu Z-m, Hu X-W, Li Y-h, Wang R, Sun G-y (2015) Expression variations of connective tissue growth factor in pulmonary arteries from smokers with and without chronic obstructive pulmonary disease. Scientific reports 5